THESIS ON INFORMATICS AND SYSTEM ENGINEERING C84

# The Piezo-Electric Impedance Spectroscopy: Solutions and Applications

TÕNIS SAAR

TUT
PRESS

TALLINN UNIVERSITY OF TECHNOLOGY
Faculty of Information Technology
Thomas Johann Seebeck Department of Electronics

**Dissertation was accepted for the defence of the degree of Doctor of Philosophy in Engineering on April 29, 2013.**

Supervisor: Dr. Olev Märtens
Thomas Johann Seebeck Department of Electronics,
Faculty of Information Technology, Tallinn University of Technology

Opponents: Professor Alvo Aabloo
University of Tartu, Estonia

Dr. Serge dos Santos
ENI Val de Loire University, Blois, France

Defence of the thesis: June 13, 2013

Declaration:
*Hereby I declare that this doctoral thesis, my original investigation and achievement, submitted for the doctoral degree at Tallinn University of Technology has not been submitted for any academic degree.*

/Tõnis Saar/


ISSN1406-4731
ISBN 978-9949-23-470-7 (publication)
ISBN 978-9949-23-471-4 (PDF)

INFORMAATIKA JA SÜSTEEMITEHNIKA C84

# Piesoelektriline impedants-spektroskoopia: lahendused ja rakendused

TÕNIS SAAR

TTÜ
KIRJASTUS

# CONTENTS

# LIST OF PUBLICATIONS


1. O. Märtens, T. Saar and M. Reidla, “Study of Various Excitation and Reference Signals for Pulsed Correlation-based Ultrasound Signal Processing,” *Electronics and Electrical Engineering*, Vol. 105, No. 9, pp. 89–92, 2010.
2. O. Märtens and T. Saar, “Fast Impedance Spectroscopy of Piezosensors for Structural Health Monitoring,” *Electronics and Electrical Engineering*, Vol. 103, No. 7, pp. 31–34, 2010.
3. T. Saar, O. Martens, M. Reidla and A. Ronk, “Chirp-based impedance spectroscopy of piezo-sensors,” in *Electronics Conference (BEC), 2010. 12th Biennial Baltic*, 2010, pp. 339–342.
4. T. Saar, “Robust Piezo Impedance Magnitude Measurement Method,” *Electronics and Electrical Engineering*, Vol. 113, No. 7, pp. 107–110, 2011.
5. O. Märtens, M. Reidla and T. Saar, “Simple DSP interface for impedance spectroscopy of piezo-sensors,” in *Electronics Conference (BEC), 2010. 12th Biennial Baltic*, 2010, pp. 343–344.
6. O. Martens, T. Saar and M. Reidla, “TMS320F28335-based piezosensor monitor-node,” in *Education and Research Conference (EDERC), 2010. 4th European*, 2010, pp. 62–65.
7. O. Märtens, M. Min, R. Land, P. Annus, T. Saar and M. Reidla, “Method and device for frequency response measurement,” US Patent Application, US2012/0007583, 2012.
8. O. Märtens, M. Min, R. Land, P. Annus, T. Saar and M. Reidla, „Meetod ja seade sageduskarakteristiku mõõtmiseks,” Estonian patent EE 05616 B1, 2012.

# INTRODUCTION

The thesis describes methods and solutions for PZT (lead zirconate titanate) transducer electromechanical impedance measurements, which could be used in SHM (structural health monitoring) applications for piezo sensor diagnostics or other related applications.

The lifespan of a SHM asset (airplanes, bridges, buildings and wind turbines) is usually very long and due to this integrity of the monitoring system has to be ensured. Structures can have tens or hundreds of PZTs embedded or bonded to the host structure. The bond between a PZT transducer and the host structure may degrade over time because of environmental conditions and this may cause faulty measurement results. In order to evaluate SHM measurement results, sensor/actuator bond has to be monitored regularly. EMI (electromechanical impedance) is one possible solution for sensor monitoring. In real SHM applications there is also always a possibility of the PZT transducer structural damage. Cracks in PZT ceramics may cause false measurement results. These topics have been previously covered by [1] and [2].

EMI can be also used for local structural damage detection. Host structure parameters like stiffness and damping influence directly energy conversion from mechanical to electrical and vice versa [3]. Defect types like composite delamination, steel bolt joint loosening and cracking can be detected using electromechanical impedance spectroscopy [4], [5], [6].

A large number of sensing nodes requires impedance measurement hardware to be low cost and low maintenance. Use of the PZT sensor monitoring hardware enables to lower overall SHM maintenance costs and reduce failure rate. More generally decreasing the price of SHM technology increases overall price efficiency. For example, the use of SHM encourages development of larger and more energy efficient offshore wind turbines. In very harsh offshore environmental conditions turbines still require regular maintenance. Use of SHM solutions minimizes the need for on-site inspections. Minimizing maintenance costs also increases the price efficiency of energy production.

This thesis was motivated by the lack of suitable solutions for on-site PZT transducer impedance measurement. Existing solutions are either based on bulky commercial impedance analyzers or Analog Devices AD5933(4) [7] IC (integrated circuit) with limited frequency (up to 100 kHz). New impedance measurement solutions with extended frequency range and short measurement time could improve existing PZT sensor impedance measurement techniques. The solutions and methods proposed in this thesis try to fill the gap between solutions existing today.

The goal of this research is to propose and test novel solutions for EMI spectroscopy measurements, more specifically solutions for PZT sensor impedance measurements in the field of structural health monitoring. New solutions should be suitable for on-site measurements and must take into account specific requirements like overall dimensions, power consumption and measurement time. Moreover, measurement results should be comparable with results using commercial

impedance analyzers. This enables to compare laboratory and on-site measurements and tests of the materials and structures.

Industries creating large, complex and long lifespan structures are always trying to create more efficient and cheaper products. Ability to create monitoring systems which outlasts structure itself enables clients to save on maintenance costs. By developing structures with lower maintenance costs companies will have more competitive products on the global market. Author of this thesis has participated in two research projects as a contracted researcher for the competence center ELIKO. Both projects involved research bodies and private companies from specific fields.

*Eurostars SESS (The Smart Embedded Sensor System)* [8] was a wind industry oriented project in the time period 2009-2011. The main focus of this project was to develop a structural health monitoring solution for wind turbine blades. While wind turbine sizes grow almost yearly, their blades need regular checkups. The most traditional way of doing blade inspection is manual inspection. The maintenance personnel has to crawl inside and outside of the blade to find any defects. The project consortia tried to develop a low cost real-time monitoring system, specialized for turbine blades. Ultrasonic technique was selected as the most optimal solution. The PZT elements were used for ultrasonic wave generation and measurement. An array of piezo sensors was used to monitor a number of critical joints inside a turbine blade. Software and hardware solutions together with innovative signal processing techniques were developed. PZT element EMI measurement method was tested and evaluated for sensor diagnostics. As a result of this research different hardware and software solutions were created for EMI measurement. Parts of this research are also covered in this thesis.

*Smart Composites – Designs and Manufacturing* **(**2012–2014) is a research project with the goal to develop smart composite materials/structures with structural health and performance monitoring capabilities.

The sub-measure goals of the project are:

- development of methodologies for the design of a new smart composite,
- development of new manufacturing techniques for fabrication of a smart composite,
- prototyping of the smart composites,
- evaluation and validation of the smart composites (monitoring capabilities; mechanical, thermal, etc. properties),
- practical introduction of a smart composite in industry.

In the frame of this project ultrasonic SHM methods were studied. The feasibility of embedding PZT elements together with electronics into composite material was considered. Among other methods, EMI based method was also tested and evaluated not only for sensor/transducer diagnostics, but also for structural fault detection. Parts of this research are covered in this thesis.

The results described in this thesis were presented in eight publications: three journal papers, three conference papers, one patent and one patent application. Conferences where works were presented were as follows: Electronics Conference 2010 (Kaunas, Lithuania), Baltic Electronics Conference 2010 (Tallinn, Estonia), Electronics Conference 2011 (Kaunas, Lithuania), Education and Research

Conference (EDERC) 2010 (Nice, France). Three papers were published in the journal *Electronics and Electrical Engineering* published by the Kaunas University of Technology, Lithuania. There is also one patent, issued by the Estonian Patent Office and one patent application to the US Patent Office.

Additionally, all works presented in this thesis were demonstrated on (or as) a prototype hardware during research phase of the two above-mentioned projects.

# ABBREVIATIONS

| | |
|---|---|
| AC | alternating current |
| AE | acoustic emission |
| CF | crest factor |
| DC | direct current |
| DDS | direct digital synthesis |
| DFT | discrete Fourier transform |
| DMA | direct memory access |
| DSP | digital signal processor |
| DSC | digital signal controller |
| DUT | device under test |
| EMI | electromechanical impedance |
| FFT | fast Fourier transform |
| FPGA | field-programmable gate array |
| IC | integrated circuit |
| MAC | multiply accumulate |
| MCU | micro controller unit |
| NDE | non-destructive evaluation |
| PWAS | piezoelectric wafer active sensors |
| PZT | lead zirconate titanate |
| RAM | random access memory |
| RMS | root mean square |
| SHM | structural health monitoring |
| SNR | signal to noise ratio |
| SUT | sample under test |
| TOF | time-of-flight |
| XINTF | external interface |

# 1. ELECTROMECHANICAL IMPEDANCE IN STRUCTURAL HEALTH MONITORING

## 1.1 SHM in General

Structural health monitoring is usually defined as damage detection strategy for aerospace, civil and mechanical infrastructure. Damage is defined as changes in a system discrete state that affects its current or future performance [1], [9]. It is assumed that two different states exist: damaged and undamaged. Damage may lead to failure. Failure is a state where a system does not operate in an acceptable way. Not all damages will grow into failure or even influence the system functionality. The goal of the SHM is to detect and monitor damage growth and predict system failure [10]. This technology is widely used on bridges [11], offshore platforms, trusses and aerospace structures [9], [12].

SHM requires regular measurements of system parameters. It enables to monitor system performance over time. From this measured data, damage sensitive features are extracted and based on statistical analysis it is determined whether damage is present or not. The sensors could be based on active ultrasonic, eddy current, radiography or acoustic emission technology. The measurements could also be initiated by request after extreme stress loadings. For example, after earthquakes the structural health of buildings is monitored to assure their safety. Furthermore, real-time monitoring could be used.

SHM is combined closely with four other disciplines: non-destructive evaluation (NDE), condition monitoring, damage control and statistical process control. NDE uses off-line damage severity check. There has to be knowledge about damage location beforehand. Usually it is conducted by maintenance staff on site by hand. Condition monitoring is similar to SHM but deals with reciprocating and rotating systems. It is usually implemented in power generation and manufacturing fields. Damage prognosis is used to predict systems' operational lifespan after damage. Statistical process control describes statistical methods for monitoring systems. [1]

Overall SHM should address the following questions [13]:

- damage existence
- damage location
- damage severity
- remaining lifespan

## 1.2 Acoustic Methods in SHM

Properties of elastic waves in structures make it good candidates for SHM measuring methods. Acoustic methods were used already in the 19th century. For example, train engineers used to tap train wheels with hammer to detect defects. Certain audible sounds would indicate the presence of damage in the wheels. Elastic

waves traveling through host structure can be early indicators of damage. Parameters like attenuation, dispersion and time of flight can be used for feature extraction in SHM applications.

Elastic waves are disturbances, created by extracting/contracting forces in elastic medium. In general form, elastic waves are described by wave equations:

$$\frac{\partial^2 \phi}{\partial x^2} + \frac{\partial^2 \phi}{\partial y^2} + \frac{\omega^2}{c_L^2} = 0\,, \tag{1.1}$$

$$\frac{\partial^2 \psi}{\partial x^2} + \frac{\partial^2 \psi}{\partial y^2} + \frac{\omega^2}{c_T^2} = 0\,, \tag{1.2}$$

where $\phi$ and $\psi$ are two potential functions and $c_L$ and $c_T$ longitudinal and transversal wave speeds. General solutions of eq. (1.1), (1.2) can be written as follows:

$$\phi = [A_1 \sin(py) + A_2 \cos(py)]e^{i(kx-\omega t)}\,, \tag{1.3}$$

$$\psi = [B_1 \sin(py) + B_2 \cos(qy)]e^{i(kx-\omega t)}, \tag{1.4}$$

$$p = \sqrt{\frac{\omega^2}{c_L^2} - k^2}\,, \tag{1.5}$$

$$q = \sqrt{\frac{\omega^2}{c_T^2} - k^2}\,, \tag{1.6}$$

$$k = \frac{2\pi}{L}, \tag{1.7}$$

where $k$ is the Lamb wave number and $L$ is the wavelength; $x$ is the co-ordinate in wave propagation direction and $y$ is co-ordinate in the plate thickness direction [14].

In plate-like structures ultrasonic guided waves exist as Lamb and shear horizontal waves. Guided Lamb waves can travel large distances in thin structures. Lamb waves can travel also through curved plate like structures. These properties make it suitable for SHM where structures have often spherical shapes (airplane wings, wind turbine blades, pipes) [15].

The Lamb dispersion equations can be expressed as:

$$\frac{\tan\left(\frac{qd}{2}\right)}{\tan\left(\frac{pd}{2}\right)} = -\frac{4k^2pq}{(q^2-k^2)^2}, \tag{1.8}$$

$$\frac{\tan\left(\frac{qd}{2}\right)}{\tan\left(\frac{pd}{2}\right)} = -\frac{(q^2-k^2)^2}{4k^2pq}, \tag{1.9}$$

where *d* is the plate thickness. These equations describe symmetrical and anti-symmetrical Lamb waves [14].

Two main methods in acoustic testing are the passive (acoustic emission – AE) and active methods (Figure 1). In the active method, the structure under test is studied using acoustic excitation signals either in pulse-echo or pitch-catch mode. The passive mode uses no artificial excitation, instead acoustic signals generated inside the structure are measured.

The acoustic emission method utilizes ultrasonic acoustic sensors to measure elastic waves traveling through a host structure. When materials inside a host structure go from one state to another they generate elastic waves. These waves have usually specific wavelength and amplitude. By measuring these waves, events of damage can be detected. Waves are measured using transducers which are bonded to the host structure. To locate damage at least three transducers have to be used. Common materials used in acoustic emission measurements are steel, wood, concrete, carbon fiber and glass fiber. AE measurements have to be conducted continuously as waves are generated only when previous stress levels inside material are exceeded. This method does not enable to evaluate damage extent [13]. The most common acoustic emission parameters are the event rate (cumulative events), count rate (cumulative counts), duration (cumulative duration), rise time (cumulative rise time), energy (cumulative energy) and AE signal amplitude [16].

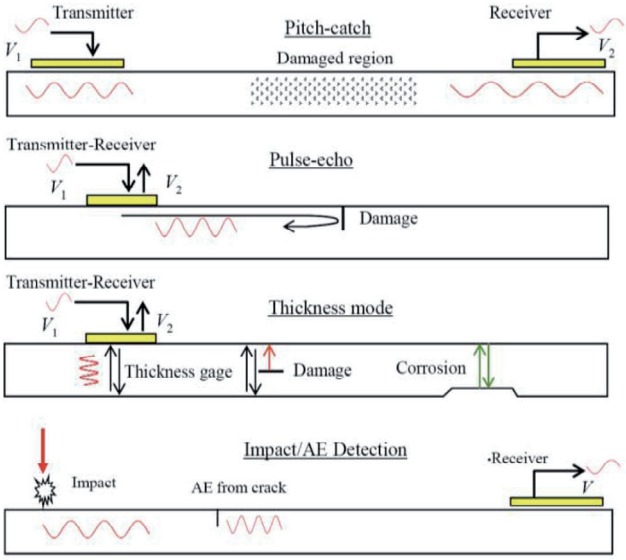


**Figure 1. Differences between active and passive methods [17]**

The active method is based on the Lamb wave transmission from transmitter to receiver through a host structure. A change in the wave indicates a defect. In the thickness mode and with pulse-echo cases, the transmitter and receiver are integrated into one unit. In the pitch-catch mode, the receiver and transmitter are separated by some specific distance. Compared to the AE method, active methods enable to measure damage extent. Also if active methods are used, there is no need to measure continuously (in real-time). Active measurements are conducted periodically or after excessive stress loadings. It is also easier to detect damage locations using active methods. Based on this data it is possible to predict the remaining lifespan of the system, whereas if the AE system is used it is not possible.

Different materials have different wave transmission properties like attenuation, dispersion and wave velocity. Isotropic and anisotropic materials have totally different wave propagation properties. Usually anisotropic materials such as carbon and glass fiber have very high wave attenuation properties. This reduces the size of the region which could be covered with a single transmitter/receiver, compared to the isotropic materials (such as metals). The measurement area for a single actuator/sensor is 0.4 m for composite materials and up to 2 m for simple metal beams [18].

## 1.3 PZT Sensors/Actuators

Lead zirconate titanate is a ceramic material which is used for acoustic sensors and actuators. Because of the piezoelectric effect, PZT transducer enables to convert electrical energy to mechanical and vice versa. Following equations describe relation between electric field and mechanical strain:

$$S_{ij} = s_{ijkl}^{E} T_{kl} + d_{kij} E_k \,, \tag{1.10}$$

$$D_j = d_{jkl} T_{kl} + \varepsilon_{jk}^{T} E_k \,, \tag{1.11}$$

where $S_{ij}$ is the mechanical strain, $T_{kl}$ the mechanical stress, $s_{ijkl}^{E}$ the mechanical compliance at zero electric field, $E_k$ the electrical field, $D_j$ the electrical displacement and $d_{jkl}$ is the piezoelectric coupling effect, $\varepsilon_{jk}^{T}$ is the dielectric permittivity measured at zero mechanical stress [15].

Piezoelectric effect was discovered by P. Curie and J. Curie in 1880 [19]. One of the first descriptions of a PZT vibration sensor was given by Harry O. Wood in 1921 [20]. There are other materials known to have piezoelectric effect but, PZT is the most cost-effective and widely used. PZT consists of lead and titanium powder which is combined with binder material to form a specific shape. In 2012 [21], virus-based piezoelectric material was described. The production of virus-based material enables to replace toxic compounds used for the PZT transducer manufacturing. It was demonstrated that new phage-based piezoelectric generator can produce 400 mV of potential and up to 6 nA of current. If mass produced, virus-based piezoelectric materials offer environmentally friendly solutions for energy generation and structural health monitoring.

PZT transducers are widely used in SHM for acoustic wave generation and measurement [22]. Two main types are bulk and multilayer sensors/actuators. Multilayer structure is combined by layering several bulk PZT layers on top of each other. This enables to use lower excitation voltages in actuators. Usually PZT sensors are either embedded in or mounted on the surface of host structure. Depending on the material of the host structure, excitation frequencies usually go up to 500 kHz. Frequencies above that have very small measurement area and tend to indicate the bond quality (condition of the bonding between PZT transducer and host structure) or condition of the PZT element itself [18].

## 1.4 Electromechanical Impedance – EMI

Piezo EMI is based on the coupling effect between a bonded PZT sensor and the host structure. Electrical admittance is a combined function of the mechanical impedance of the PZT actuator $Z(\omega)$ and of the host structure $Z_a(\omega)$ [23], [24]:

$$Y(\omega) = i\omega a \left( \bar{\varepsilon}_{33}^{T} - \frac{Z(\omega)}{Z(\omega) + Z_a(\omega)} d_{3x}^2 \hat{Y}_{xx}^{E} \right), \tag{1.12}$$

where *a* is the geometry constant, $d_{3x}^2$ the piezoelectric coupling constant, $\hat{Y}_{xx}^{E}$ the Young modulus and $\bar{\varepsilon}_{33}^{T}$ the complex dielectric constant of the PZT at zero stress [18]. If mechanical conditions of the PZT transducer stay constant over time, electrical admittance (and impedance) can indicate condition of the host structure. Changes caused by excessive loading, corrosion [25], etc. are measureable through

electrical admittance. Besides, EMI is influenced by the bond quality between transducer and the host structure and by overall condition of the piezo sensor.

## 1.5 Electrical Impedance

EMI is characterized through the electrical impedance. Electrical impedance indicates the ratio between voltage and current (generally both AC and DC). It is described in the complex form [26]:

$$\dot{Z} = R + jX = Re\dot{Z} + jIm\dot{Z} \,. \tag{1.13}$$

The magnitude and phase of the impedance can be calculated using following equations:

$$\left|\dot{Z}\right| = \sqrt{Re\dot{Z}^2 + Im\dot{Z}^2}\,, \tag{1.14}$$

$$\varphi = \arctan\left(\frac{Im\dot{Z}}{Re\dot{Z}}\right). \tag{1.15}$$

Fig. 2 describes visually the impedance real part (R) on the horizontal and imaginary part (X) on vertical axis.

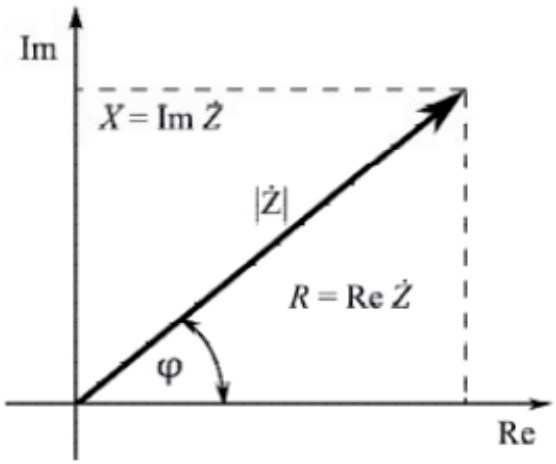


**Figure 2. The complex impedance vector [27]**

In the most basic form, electrical impedance is measured by applying sinusoidal excitation signal to a DUT and by measuring the current response. To characterize a circuit with unknown capacitive and inductive components sine waves with different frequencies has to be applied. A greater number of frequencies will give a more accurate impedance plot.

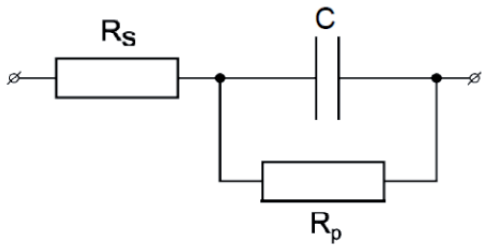


**Figure 3. Simplified equivalent circuit of a PZT transducer [28]**

A piezo sensor simplified electrical schematic is given on Figure 3. Below resonant frequencies, a PZT transducer acts as a capacitor.

# 2. RELATED WORK

## 2.1 Laboratory Solutions

Previously there have been many publications covering aspects of the mechanical parameters of a host structure influencing the EMI spectra. In contrast to this thesis laboratory grade measurement equipment are usually used and proposed. Paper "A low-cost variant of electro-mechanical impedance (EMI) technique for structural health monitoring" [29] described method for PZT transducer EMI measurement. The method is meant to replace expensive (20,000 – 40,000 $) impedance analyzers by combining the off-the-shelf Agilent 33220A signal generator and Agilent 54622D mixed signal oscilloscope (Figure 4). The overall cost of hardware was 5000 $. Like with impedance analyzers the excitation signal frequency was changed incrementally.

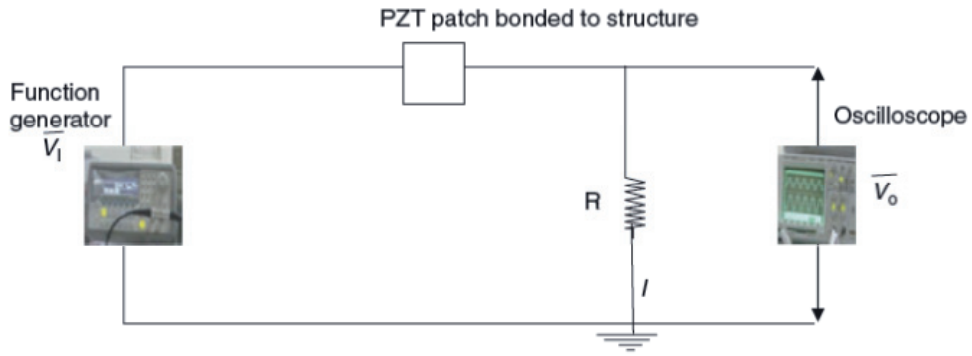


**Figure 4. Proposed measurement scheme [29]**

In the same vein, the paper "A low-cost and field portable electromechanical (e/m) impedance analyzer for active structural health monitoring" [30] proposed a DAQ card based EMI measurement solution.

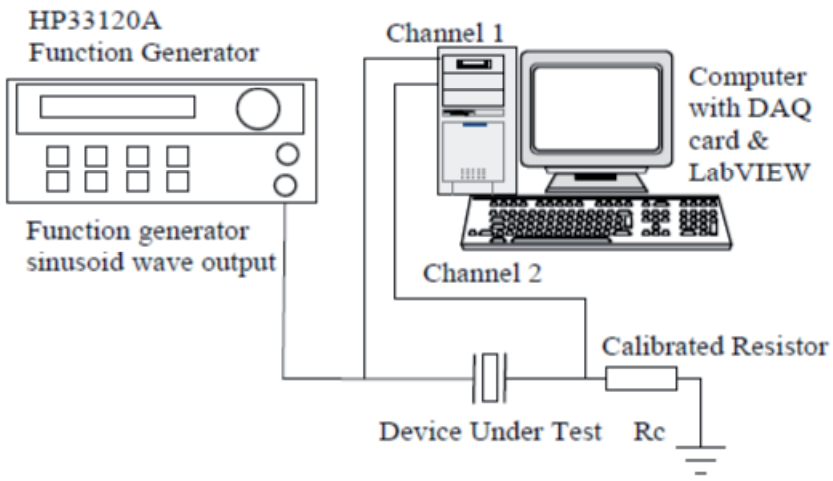


**Figure 5. Conceptual diagram representation of the proposed solution [30]**

The authors describe experiments with two different excitation signals: frequency sweep and linear chirp. Proposed frequency sweep signal was constructed in frequency domain and had very flat amplitude spectrum, compared to a chirp signal, which had some ripples in high frequency end. HP33120A function generator was used for signal generation and a two-channel 8-bit 10 MHz DAQ card was used for sampling (Figure 5). Measurements and calculations were done on a PC computer with the Labview software.

Similarly to the solutions described above laboratory grade hardware was used in this study to test and develop impedance measurement methods (and solutions). Many different measurement methods were evaluated and tested using PC and external data acquisition (DAQ) hardware, described below the heading: Experimental setup.

## 2.2 Embedded Solutions

Both methods, proposed by [29] and [30] are very efficient for laboratory conditions, but for on-site measurement more compact solutions are needed. For on-site EMI measurement the paper "A low-cost electromechanical impedance-based SHM architecture for multiplexed piezoceramic actuators" [31] proposed a digital signal processor (DSP) based solution for the multiplexed sensor/actuator EMI measurement in 0 – 400 kHz range. Solution is based on a TMDSEZS2808 eZdsp Starter Kit (Texas Instruments) and an external DDS AD9834 (Analog Devices). Three external multiplexers (ADG526) were used for signal switching. Current was measured on sixteen precision shunt resistors (100 Ω). An impedance analyzer by HP (HP4194A) was used as a reference tool to evaluate the measurement results (Figure 6). Root-mean-square deviation (RMSD) was calculated between measurements obtained using the DSP-based solution and the HP impedance analyzer.

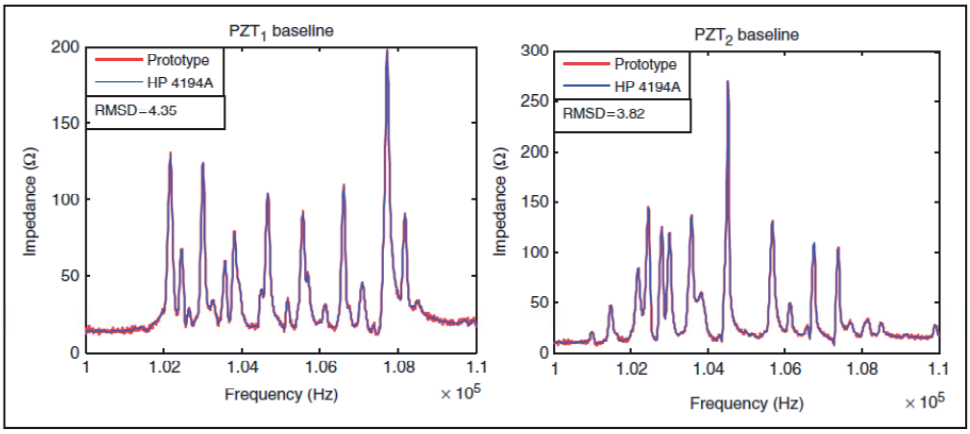


**Figure 6. Experimental results by Neto *et al*. Comparison of measurement results from proposed solution vs HP impedance analyzer [31]**

Article [5] describes impedance measurement hardware based on an Cortex M3 32 bit CPU in combination with an AD5932 DDS IC. The excitation signal is linear chirp signal from 1 kHz to 400 kHz. The signal length is 2.05 s. In real SHM applications shorter measurement times would be preferred. This is the main reason, why short excitation signals (up to 100 ms) are proposed in this thesis. Simple MCU PIC16F877A based solution was described in [32]. Although this solution is very low cost, it is limited only up to 50 kHz frequencies. Similarly [33] use AD5933 IC for impedance measurement in a frequency range up to 70 kHz. For structural health monitoring frequencies up to 600 kHz have to be measured [5]. This is one of the main requirements also considered in this thesis.

The paper [34] demonstrates a more complex Ti 6416T DSP and Xilinx XC50E Virtex FPGA based impedance measurement node. It is running on 1 GHz clock rate and is capable to measure impedance up to 1 MHz. Although having very high performance, it is expensive to implement in sufficient numbers needed in SHM applications. By the approach provided in this thesis measurement hardware should be low power and low cost. Solutions provided in this thesis try to provide low-power and low-cost results but by sustaining a wide measurement frequency and short measurement time.

## 2.3 Structures under Test

EMI measurement technique has been tested on many different structures for detection of the different defect types. The authors of the publication [29] tested EMI method on steel structure. As a host structure 1.2 m long galvanized steel pipe was used. Piezo sensor (10 x 5 x 0.3 mm) was glued to a pipe using an epoxy adhesive. In series with actuator was a 20 Ohm resistor which enabled to calculate current passing PZT sensor over signal sweep. Experimental measurements were conducted over 80 kHz–100 kHz range. By drilling holes into the pipe structural defects were simulated. Drilling additional holes into the pipe enabled to simulate progression the severity of the damage. Progressing damage was detected on the

admittance curve. Shifting resonance peaks and appearance of new peaks indicates progressing of the damage. Xu and Giurgiutiu [30] used for a test specimen a free PZT and an aluminum panel with bonded PZTs. Test results were compared against results from HP 4194A impedance analyzer in 150 kHz–600 kHz range. It is claimed that "*Both the novel impedance analyzer and HP4194 impedance analyzer can detect the presence of DB1 disbond on the test panel*". Disbond is indicated by new sharp resonant peaks in impedance spectrum plot. In paper [31] two different specimens were used as host structure. For the first case aluminum beam 500 x 25 x 4 mm with inserted rivet was used. Measurements were carried out with rivet attached and without. Measurements for both cases were conducted and compared. Measured frequency range was 100–110 kHz. The second experiment was conducted on aircraft panel. Damage was simulated by extracting rivet from panel. Two impedance plots were compared in the 100–110 kHz frequency range. In both experimental cases damage could be indicated in changes of the impedance plot. Article "SHM of CFRP-structures with impedance spectroscopy and Lamb waves" [3] investigates CFRP (Carbon Fibre Reinforced Polymer) material with embedded PZT transducers. Authors compare impedance spectroscopy and lamb wave applications on impact damage detection. In this case magnitude of the impedance has overall lower values over frequency range, probably caused by an impact damage to the PZT contacts [3].

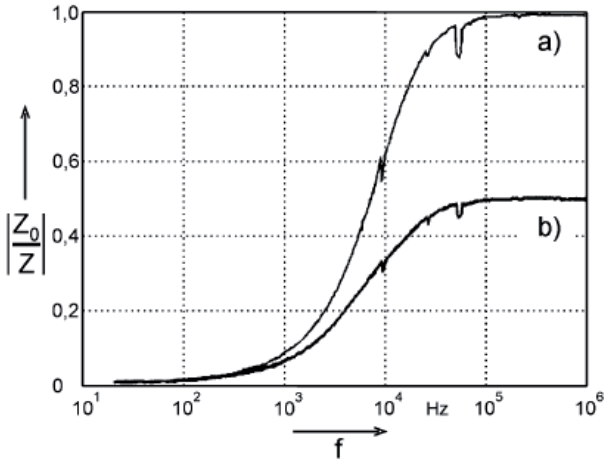


**Figure 7. Admittance plot before (a) and after (b) impact damage [3]**

Self-diagnostics for the PZT have been proposed in [35], [3] and [36]. In article [35] author proposes method for PWAS self-test procedure. It is based on EMI technique by comparing impedance imaginary impedance spectrum. On the Figure 8 two cases of the PWAS can be seen. Resonant peak at ~267 kHz indicates disbond between PZT and the host structure. Small resonance peaks on bonded PWAS plot indicate structural resonances of the host structure. Disbonded PWAS has relatively smooth plot except a single resonant peak at ~ 267 kHz. It is claimed

that "*For a partially disbonded PWAS, a mixture of PWAS and structure vibration was recorded*".

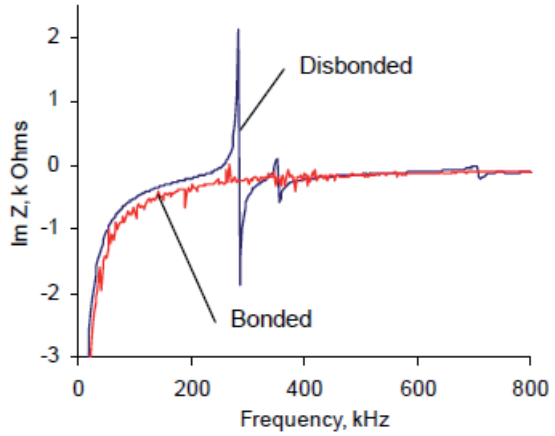


**Figure 8. Bonded vs disbonded sensor [35]**

Paper [3] also describes the effects of degrading electrical connection between PZT and measurement system. Changes in electrical connectivity could be misinterpreted as structural damage of the host structure or PZT itself (Figure 9).

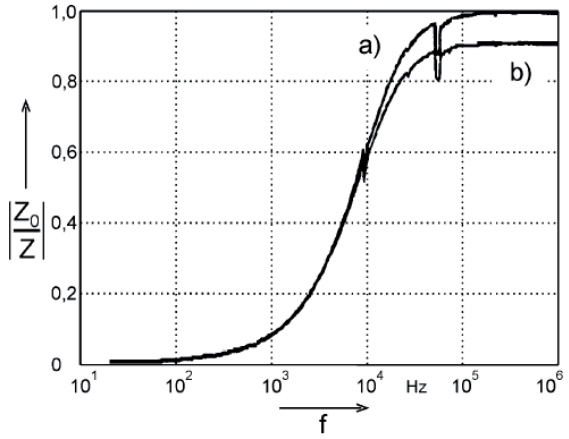


**Figure 9. Aging effect of electric contacts (a) reference measurement (b) measurement after 3 months [3]**

The authors in [36] proposed an admittance measurement based PZT self-diagnostics model. Effects like sensor degradations and coupling quality are described in admittance range up to 50 kHz.

Similarly to publications described above, real structures were used for testing in this thesis. In contrast to most previous works, embedded hardware was used for impedance measurement in an extended (up to 600 kHz) frequency range.

# 3. EXPERIMENTAL SETUP

To simulate PZT sensors in real conditions a measurement setup has been prepared. Fiber glass plate with 500 x 500 x 4 mm dimensions has three PZT transducers bonded to it by use of the special adhesive (Figure 10 and Figure 11). This set of sensors simulate sensor configuration on a real SHM monitoring set. Fiber glass plate was chosen to mimic structure of a wind turbine blade or a ship hull. As the wave properties in a composite differ substantially, compared to metal structures, composite plate was chosen for the experiments. Composite material is the most common material used for the wind turbine blades, for small ships and airplanes.

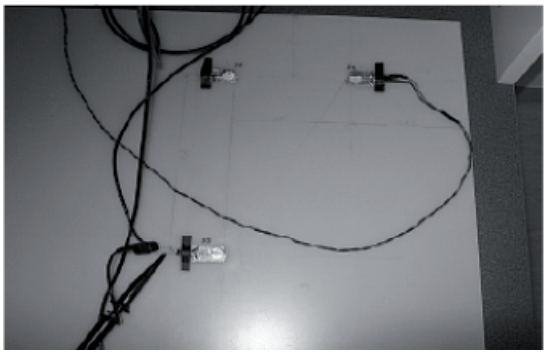

**Figure 10. Fiber glass plate with PZTs**

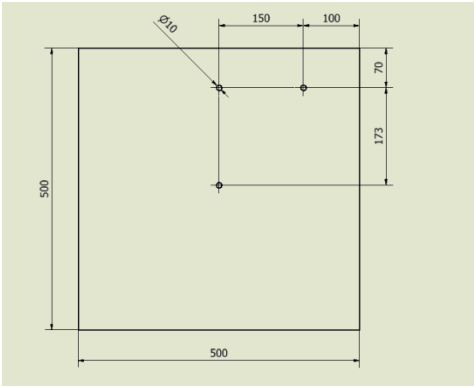


**Figure 11. Drawing of the fiber glass plate (500 x 500 x 4 mm) with the PZT elements**

PZT sensors had a 10 mm diameter and 0.5 mm thickness (Figure 12). Sensor elements were bulk type piezos. Copper tape was used to connect electrical wires to PZTs. Three bonded PZTs were marked as S1, S2 and S3. Additional free PZT was marked as Sx.

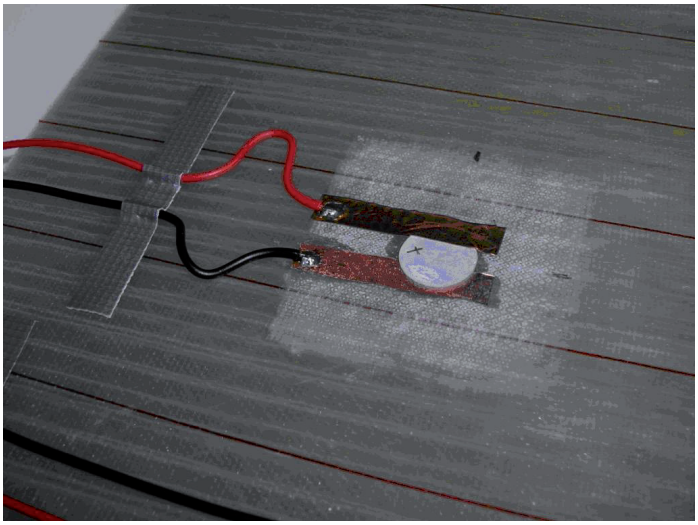

**Figure 12. Example of the PZT fixture on the plate structure with copper electrodes**

Transducers were connected to the amplifier which supplies ±30V excitation signal voltage (Figure 13). For the signal generation and sampling a National Instruments USB6259 USB high-speed multifunction data acquisition (DAQ) module has been used. Ni USB6259 has 16 bit 1.25 MS/s single-channel or 1 MS/s aggregated analog-digital converter (ADC) [37]. For the excitation signal generation DAQ has 4 analog output channels with 16 bit and 2.8 MS/s. DAQ enables to generate different excitation signals using PC-based Matlab software. One transducer was connected to DAQ input and other to the output. Between transducers and DAQ external amplifiers were used.

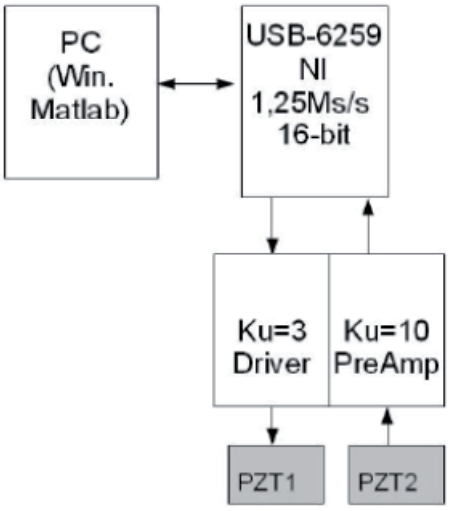


**Figure 13. Principal layout of measurement system [38]**

The described test setup enables to test the pitch-catch and pulse-echo methods on this test structure. A Matlab-based software was written to test the pitch-catch acoustic wave transmission between the transducers. An excitation signal (Figure 14) at 200 kHz was generated and a response signal (Figure 15) from another transducer was measured. All transducers were measured to make sure correct physical connection between PZT and host plate has been established.

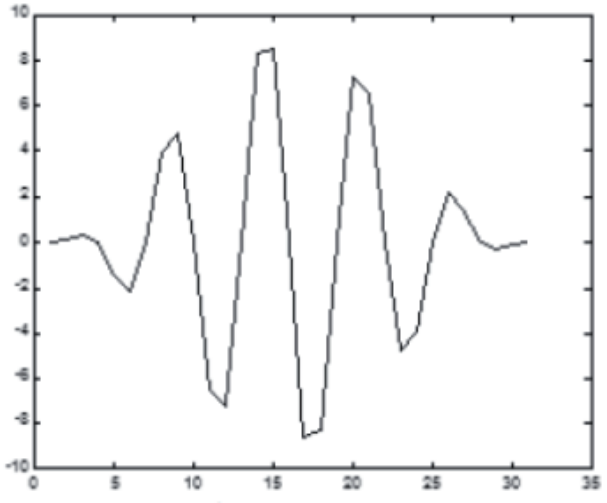


**Figure 14. Example of the pitch-catch excitation signal: 5 period 200 kHz signal in Hanning window (voltage [V] vs. time [ms])**

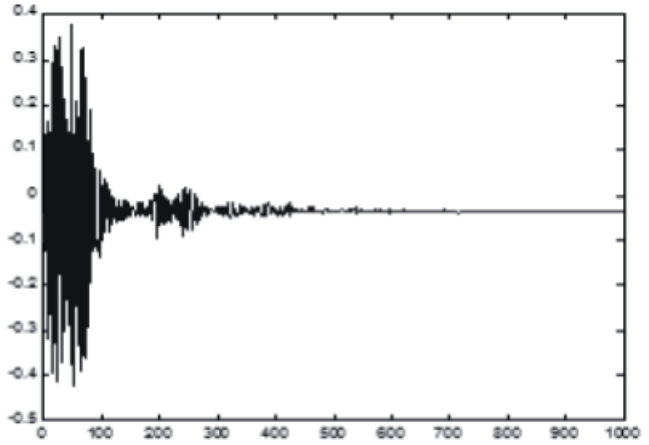


**Figure 15. Measured voltage response of the pitch-catch excitation (voltage [V] vs. time [ms]) [38]**

Energy of the measured response signal can indicate defects in the region between two transducers [39], but also the quality of the connection between PZT and host structure can affect energy transmitted from one transducer to another. To acquire more accurate TOF (time of flight) measurement the response signal was correlated with the original one and the quadrature excitation signal (Figure 16). This results with smoother response signal with distinctive peaks. Integral of this signal enables

to evaluate overall energy transmitted to the host structure. In cases where PZT bond quality is low – also less energy is transmitted to the host structure.

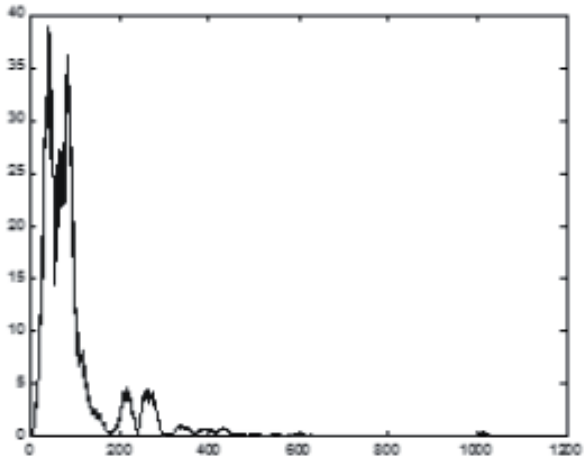


**Figure 16. Windowed burst of excitation- sum of cross-correlations (absolute values) with response signal and its quadrature component (correlation coefficient vs time [ms]) [38]**

In current research work the commercial impedance analyzer Wayne Kerr 6500K has been used as a reference electrical impedance measurement device. EMI spectra of two PZTs in two different conditions have been measured using this device. First measurement was done on a free (Sx) and second on a bonded PZT (S1) (Figure 17 and Figure 18). Wayne Kerr 6500B is a commercial impedance analyzer used by research institutes and companies. It can characterize components from 20 Hz to 120 MHz and it has a basic measurement accuracy of 0.05% [40]. Excitation signal level can be selected up to 1 V voltage. 20 KHz to 600 kHz frequency range was chosen as a reference measurement range.

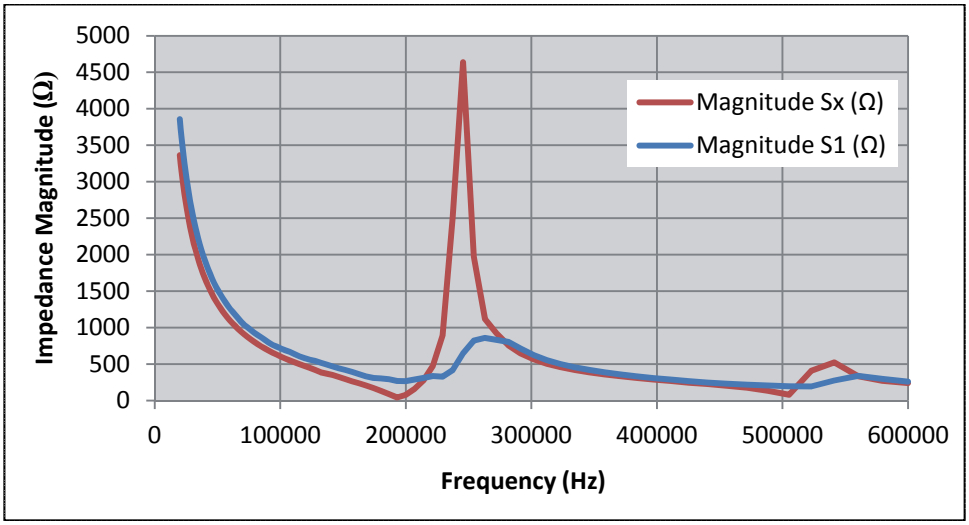


**Figure 17. EMI magnitude spectra of a bonded and a free PZT**

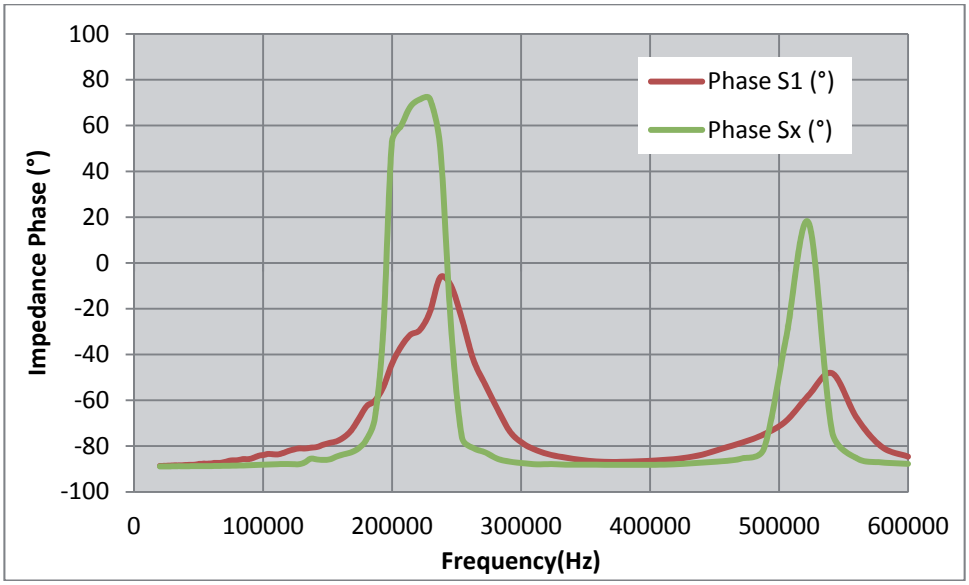


**Figure 18. EMI phase spectra of a bonded and a free PZT**

As can be clearly seen from EMI plots, the bonded vs. free PZT have very different magnitude and phase graph shapes. It is clear from those graphs that two states of transducers can easily be distinguished. Both EMI magnitude and phase peaks can be used as indicators of the PZT state.

For EMI measurements a schematics with a shunt resistor (R1) has been constructed (Figure 19). Voltage measurement point V1 was used for the voltage response measurement, while voltage from V2 was used for the current response calculation. Synchronous sampling of voltages V1 and V2 enables to calculate the electrical impedance Zx in a complex form.

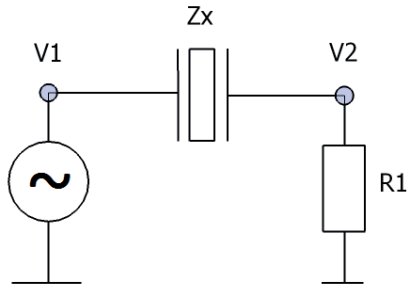


**Figure 19. The PZT measurement schematic with shunt resistor R1**

# 4. METHODS

The easiest way to measure impedance is to excite DUT on predefined number of frequencies with static frequency sine wave signal and measure the current and voltage responses. Then, using these response signals, EMI plot can be calculated. Disadvantage of this method is time and energy consumption. Often in real SHM applications environmental conditions (loading, temperature, etc.) of the host structure are time variant and shorter measurement time enables to measure more accurate result. Use of a wide band sweep excitation signal enables to reduce measurement time, but also requires more complex computation. The following chapter gives an overview of the proposed impedance calculation methods.

## 4.1 Excitation Signals

Theoretically any linear, time invariant system can be described by their response to the Dirac delta function excitation:

$$\delta(t) = \begin{cases} +\infty & , t = 0 \\ 0 & , t \neq 0 \end{cases} , \tag{1.16}$$

while integral of Dirac delta function is equal to 1

$$\int_{-\infty}^{\infty} \delta(t)dt = 1 . \tag{1.17}$$

While Dirac delta function has ideal properties in theory, which in real electronics it is very hard to achieve.

Excitation signals can be divided generally into two groups: spectrally dense and sparse signals. Spectrally sparse excitation signals have energy distributed between small numbers of frequency components. It is useful in cases where frequency response is smooth and spectrum description, using small number of frequency bins is sufficient. Most well-known sparse excitation signal is the multi sine wave signal. It is a sum of sine wave signal with predefined frequency. It can be expressed with following equation:

$$S_{exc}(t) = \sum_{i=1}^{i=k} A_i * \sin(2\pi f_i + \Phi_i) , \tag{1.18}$$

where: $S_{exc}$ is the multi sine wave signal, $A_i$ is the amplitude of a sine component, $f_i$ is the i-th frequency, $\Phi_i$ is the phase shift of i-th component.

Spectrally dense wideband excitation signals have energy distributed over large number of frequency points. It describes frequency response of a DUT in more detail compared to sparse excitation signals [27]. Most commonly known dense excitation signal is a chirp signal.

The most common wide band excitation signals in EMI measurement are usually periodic random noise, multi-sine or chirp. Based on our experimental measurements chirp excitation signal is one of the best suited signals for the PZT EMI measurement [41]. Successful measurement results are also claimed by others [34] [42] [5]. Moreover, chirp excitation signal is widely used in the measurement of the living tissue(s) and cell impedance because of its time and frequency scalability [43].

The following equation describes sine-wave chirp with amplitude $A$:

$$V_{ch}(t) = A \sin\left[2\pi\left(f_0 t + \frac{\beta t^{n+1}}{n+1}\right)\right], \tag{1.19}$$

where $\beta = B_{exc}/T_{ch}$ is the frequency change rate, $T_{ch}$ the signal duration and $B_{exc} = f_{in} - f_0$ the frequency range.

In some cases binary chirp is used as an excitation signal. Binary version of the chirp signal enables to use simplified hardware for the signal generation. In this case signal is described as $A \cdot \mathrm{sgn}(V_{ch}(t))$ and can only have values $\pm A$ (Figure 20).

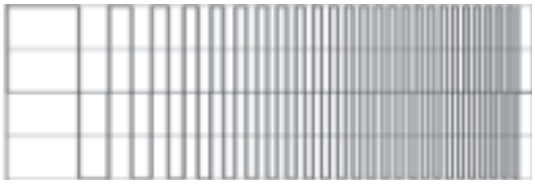

**Figure 20. Example of binary chirp signal [43]**

**Figure 21. Example of ternary chirp signal [43]**

Another version of chirp signal has three different signal values $+A$, 0, $-A$ (Figure 21).

## 4.2 Signal Processing

Electrical impedance can be described using the following mathematical formula:

$$Z(j\omega) = Re\big(Z(j\omega)\big) + jIm\big(Z(j\omega)\big) = |Z(\omega)|e^{(j\,\Phi_z(\omega))}, \tag{1.20}$$

$$\omega = 2\pi f \tag{1.21}$$

and magnitude and phase of the impedance can be expressed as:

$$|Z(\omega)| = \sqrt{(Re(Z(j\omega))^2 + (Im(Z(j\omega))^2}\,, \tag{1.22}$$

$$\Phi(\omega) = \arctan\left[\frac{Im(Z(j\omega)}{Re(Z(j\omega)}\right]. \tag{1.23}$$

One of the most common ways to calculate impedance is to apply Fourier transform to voltage and current passing PZT. EMI can be expressed as a relation between Fourier transforms of voltage and current responses:

$$Z(j\omega) = \frac{F\left(V_z(t)\right)}{F\left(I_{exec}(t)\right)}\,. \tag{1.24}$$

Although commonly used in signal processing, Fourier transform is computationally very intensive. This makes it relatively hard to implement in cases, where only low computational capability is available (low cost, low power processors and DSPs).

Alternatively, EMI can be calculated by correlating response signal with the direct original signal and with the quadrature version of the original signal. Results have to be passed through low pass filter for smoothing:

$$A\sin(\omega t + \varphi_u) * \sin(\omega t) = \frac{A}{2}\cos(\varphi_u) - \frac{A}{2}\cos(2\omega t + \varphi_u)\,. \tag{1.25}$$

## 4.3 Simplified Impedance Measurement Method

Implementation of the Fourier transform can be computationally expensive. Use of the linear chirp excitation signal enables to avoid Fourier transform calculation in certain cases. As in linear chirp signal frequency components are spread equally across signal length, so it is easy to convert response signal from the time domain into a frequency domain. This approach can be also used with the nonlinear chirp excitation signal.

Eq. 1.24 can be expressed as magnitude of impedance in the following equation:

$$|Z(j\omega)| = \frac{|F(V_z(t))|}{|F(I_{exec}(t))|}\,. \tag{1.26}$$

So the magnitude of the impedance is the ratio of the voltage and current responses for the specified frequency. Use of the linear chirp excitation signal enables to avoid Fourier transform calculation for voltage and current response signals. These signals can be converted to frequency domain directly [44].

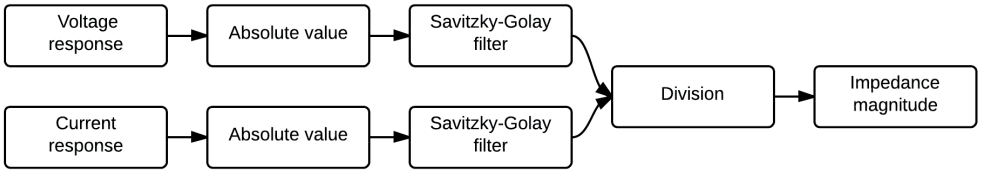


**Figure 22. Principal layout scheme of the magnitude of the impedance calculation method**

Figure 22 describes the method for magnitude of the impedance calculation. Firstly linear chirp signal will be used for DUT excitation. Thee voltage and current responses from DUT will be saved (Figure 23, Figure 25). Further absolute values for both signals will be calculated. After that Savitzky-Golay smoothing filter will be applied (Figure 24, Figure 26) [45]. Savitzky-Golay filter is a polynomial filter. It is effective for wide band signal filtering because of ability to retain signal maximum values.

By dividing two smoothed (voltage and current) magnitude signals similarly to equation (1.26) magnitude of the impedance plot will be resulted (Figure 27). Resolution of this calculated magnitude plot will be defined by length of the Savitzky-Golay filter window. For example, in the case where wide band linear chirp signal is spread over 1 MHz frequency and the measured signal length is 200 kSamples long, use of filter window 1000 samples long will result frequency resolution 5 kHz.

Measurement experiments have been carried out with the proposed method. PZT element bonded to the plate structure was used as test specimen. Linear chirp signal with ±20 V peak values was used for excitation. Response voltage and current signals were saved in a PC for further processing. Matlab based software was used for magnitude of the impedance calculation. Different excitation signal lengths were tested. Best relation between measurement time and signal to noise ratio was achieved using excitation signals with 100 ms duration.

Experimental results show good correlation between the proposed method and results obtained by the commercial impedance analyzer.

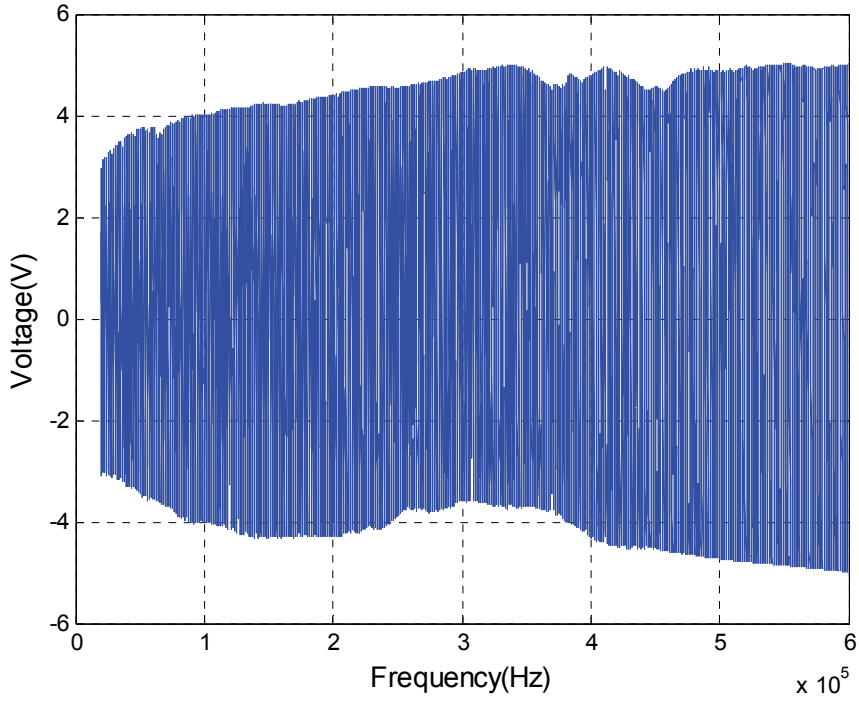


**Figure 23. Measured voltage response**

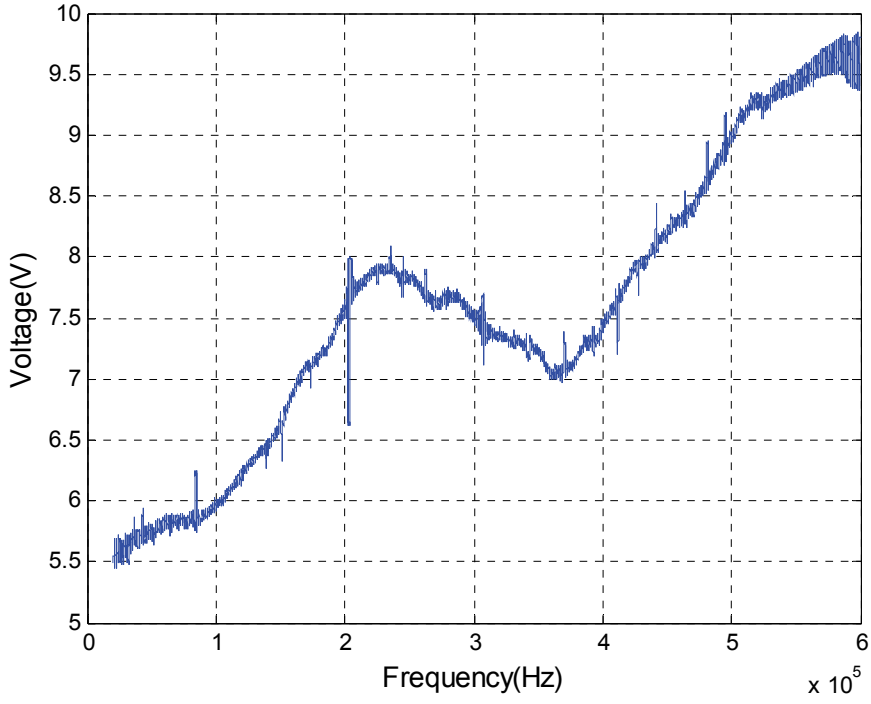


**Figure 24. Smoothed voltage magnitude (with corrected magnitude)**

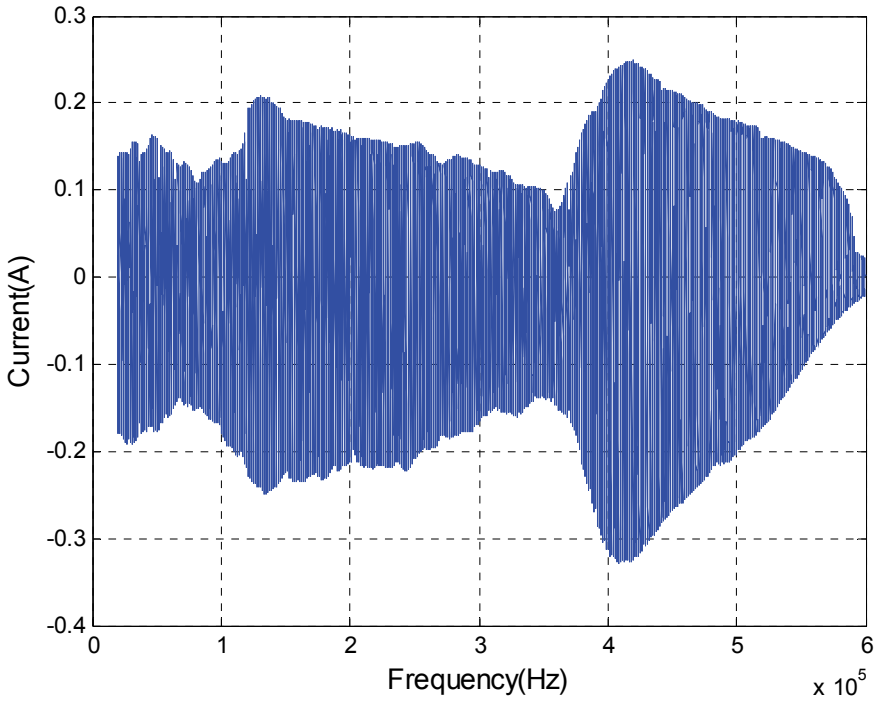


**Figure 25. Calculated current response**

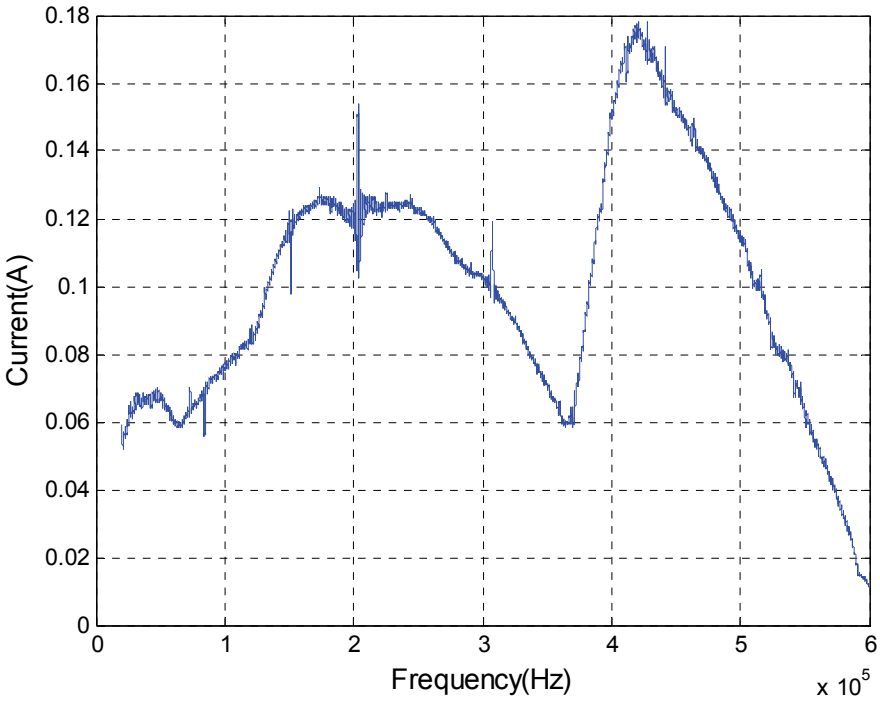


**Figure 26. Smoothed current magnitude**

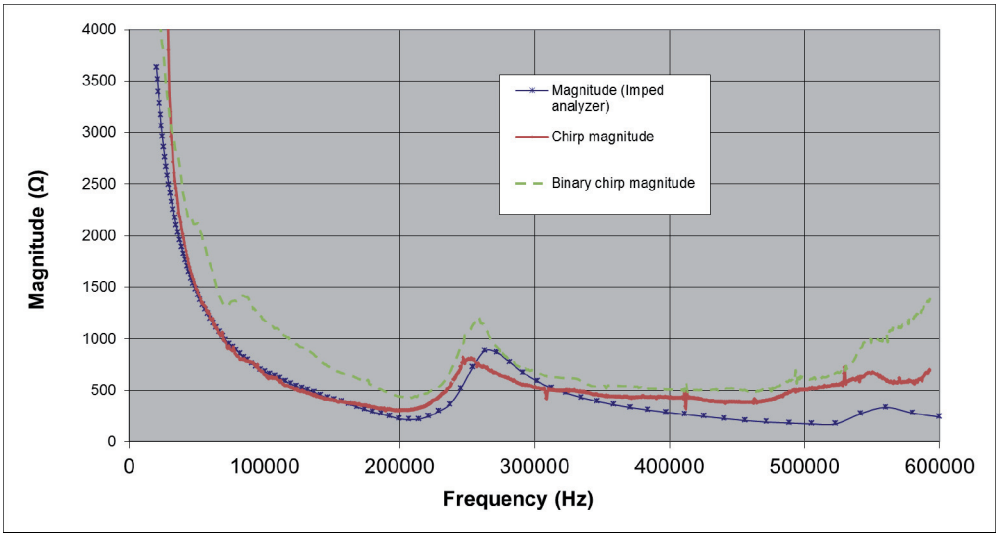


**Figure 27. Calculated PZT magnitude of the impedance**

Two types of the excitation signals were used: chirp and binary chirp. Use of the binary chirp signal caused ripples in the magnitude of the impedance plot. These deviations could be caused by higher energy level in higher harmonics compared to an ordinary chirp signal. The proposed simple EMI magnitude measurement and calculation method can be used for applications where only EMI magnitude is needed.

## 4.4 Short Sliding Window Based Correlation Method

A novel frequency response measurement method has been proposed by our patent application [46]. Method is based on the correlation between response signals from DUT and with excitation (and quadrature) signal (Figure 28). For excitation, a signal with fast changing frequency in the time domain is proposed. Signal frequency is defined by time domain function. In most common cases linear, logarithmic and exponential chirp signal could be considered. In some specific cases arbitrary excitation signal could be considered, for example with varying signal resolution over frequency range. The excitation signal is introduced to the test object. Response signals consist of two parts, current and voltage response. Response signals from the object are saved and correlated with two reference signals in short time domain windows. One of the reference signals could be the original excitation signal in its original form. The second reference signal could be quadrature signal of the original excitation signal. Quadrature signal can be obtained by applying Hilbert transform on original excitation signal. Correlation will be calculated in a relatively short-time domain window. Depending on the application requirements window size and overlap could be uniform or frequency dependent. Parts of the frequency range, which contain more valuable information, may be scanned with a higher resolution

compared to parts which have lower value. In addition sliding window can be divided into even smaller parts to improve calculation performance.

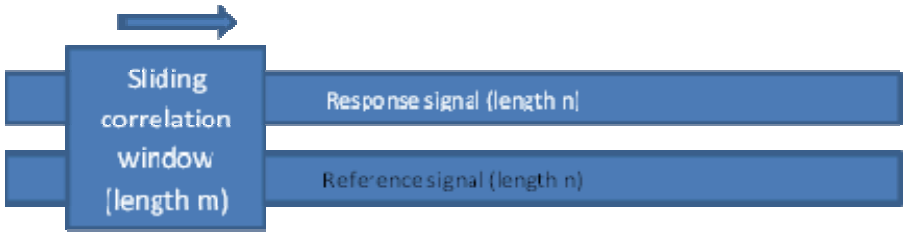


**Figure 28. Principal layout of response and reference signal correlation**

Calculation procedure using proposed technique enables to use very low computational power. All calculations can be implemented using MAC operations which are very effective for example on DSP platforms. A small number of calculations and use of efficient MAC calculations enable to utilize lower- cost and lower power platforms for impedance calculations.

Experimental measurements were conducted on bonded PZT element. Excitation signal was 0.1 s long linear chirp in 20 kHz – 600 kHz range. For the excitation signal generation Agilent 33220A function/arbitrary waveform Generator was used. Response signals were sampled with 2 Ms/s sampling rate using Agilent U2500A Series USB Modular Simultaneous Sampling Multifunction DAQ. For the impedance calculation window size of 350 samples was used. Proposed method is very sensitive to window size. To produce the most accurate result, the exact window size had to be found experimentally. Some window sizes produced very noisy results. The exact cause for this is still unclear.

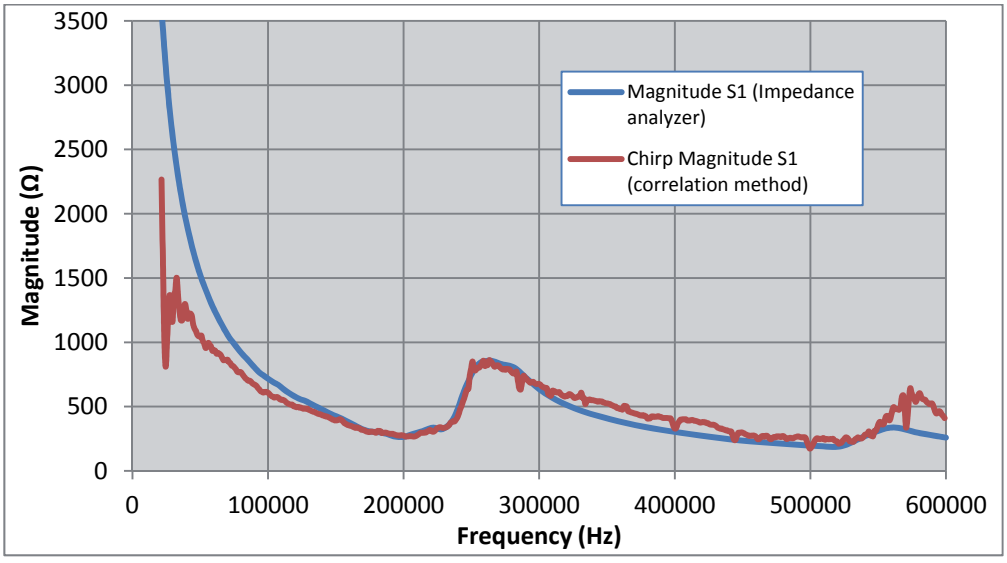


**Figure 29. Magnitude of the impedance of a bonded PZT**

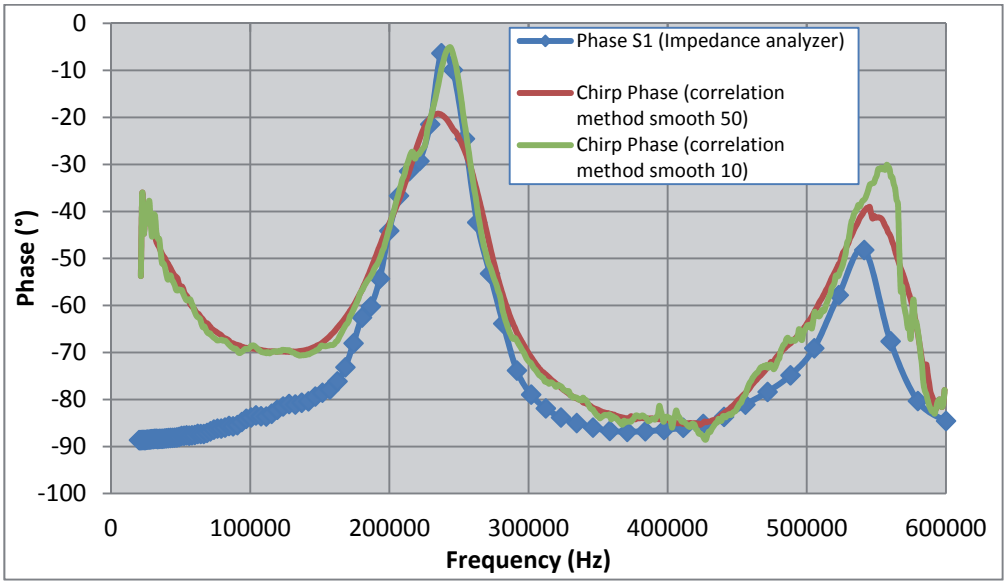


**Figure 30. Phase of the impedance of bonded PZT**

Figure 29 and Figure 30 demonstrate the experimental results of the proposed method. For the phase of the impedance measurements additional smoothing function was applied. Different window sizes were tested to find the most optimal one.

# 5. HARDWARE

The most common hardware for EMI measurements in lab condition is industrial impedance analyzer, for example HP 4192 impedance analyzer or similar. While these devices are very handy in lab conditions, on-site measurement conditions require totally different approach. Parameters like size, cost, weight and power consumption make use of industrial impedance analyzers in real SHM applications impossible.

## 5.1 Integrated Solution by Analog Devices

Analog Devices has developed integrated solution for impedance measurement (Figure 31). With small dimensions and low energy consumption it is widely used for this specific application. AD5933 by Analog Devices is a 12 MSPS, 12 bit network analyzer IC. It has integrated signal generator, DSP and ADC. Signal generator has programmable interface and maximum frequency of 100 KHz. Impedance can be measured in 1 MΩ to 10 MΩ range. For impedance calculation DFT has been used on DSP core.

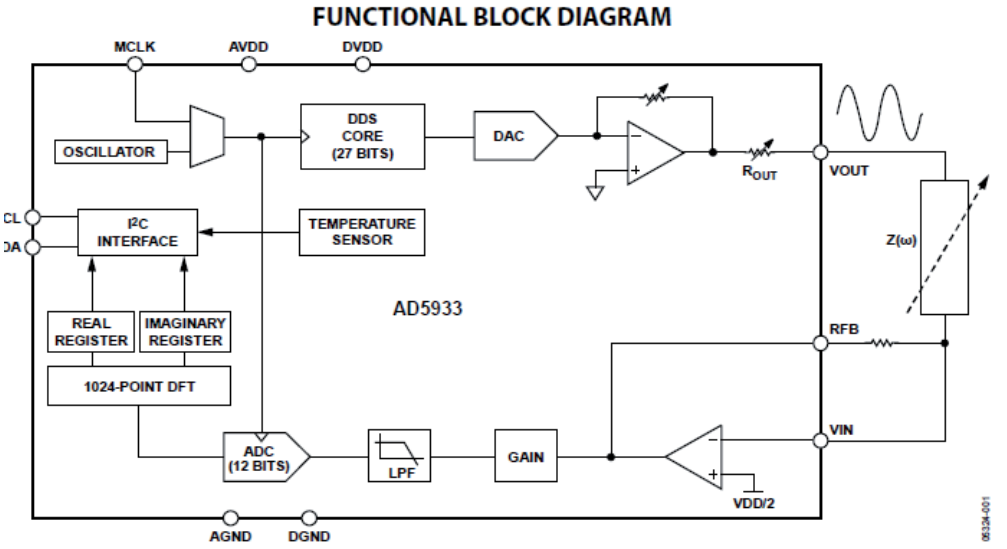


**Figure 31. Functional block diagram of AD5933 [7]**

While commonly used, AD5933 has only frequency range up to 100 kHz which in many applications is not sufficient enough. Limited frequency and dynamic range can limit usefulness of the AD5933.

Some publications claim unsuccessful results by phase of the impedance measurement using a AD5933 IC. ”The real and imaginary parts of impedance can

be calculated, however, the AD5933 does not record the phase data with enough precision near the limits of its measurement range to make the transformation meaningful" [47]. "From the results, the AD5933 was able to accurately measure the magnitude of the impedance, but not the phase. Therefore, calculating the real part of the impedance that is typically used for the impedance method would not be useful" [48].

Based on the limitations mentioned above current thesis tries to find alternatives to AD5933. Wider frequency range and more accurate EMI results could improve current existing solutions.

## 5.2 Ti MSP430-based Solution

Texas Instruments MSP430 is ultra-low power 16-bit RISC mixed-signal MCU. It is widely used in battery powered applications because of low power consumption. In shutdown mode current consumption can go as low as 100 nA@2.2V and it takes only 1 µs to wake up from the low power mode. These properties make MSP430 very suitable processing platform for a SHM monitoring node. Low power requirements on monitoring node enable to use energy harvesting. Use of the energy harvesting can lower installation and maintenance costs of a SHM system.

The proposed MSP430 based system consists of MCU, DDS, external amplifier and analog front end (Figure 32). MCU's internal 16 bit sigma/delta A/D converter was used for analog signal sampling. Analog Devices AD5932 DDS IC was used for excitation signal generation. MCU and DDS were connected using synchronous I2C data connection.

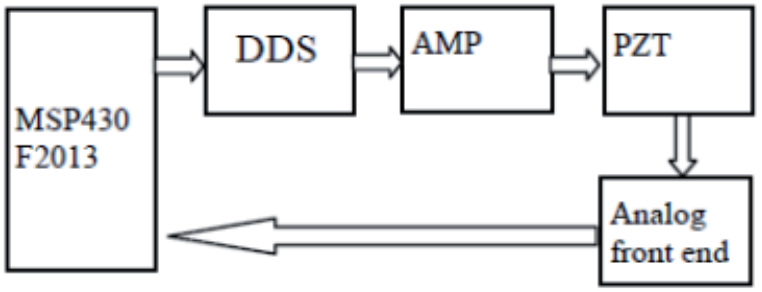


**Figure 32. Principal layout of proposed system [49]**

Analog front end was used for signal smoothing. It consisted of a full period rectifier and a low pass filter (Figure 33, Figure 34). Rectifier design was based on the National Semiconductor LM318 operational amplifiers. Use of an analog front end enables to use lower sampling rate compared to the conventional Nyquist criteria.

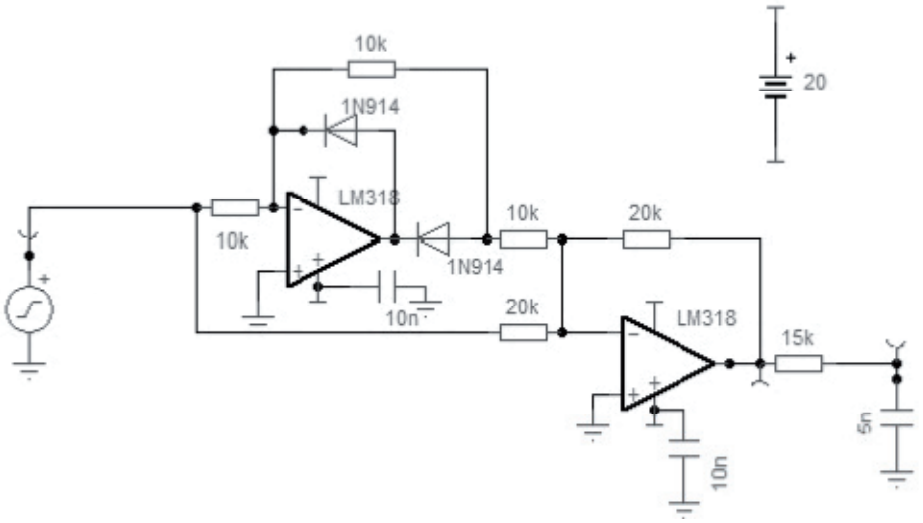


**Figure 33. Schematic of analog front end [49]**

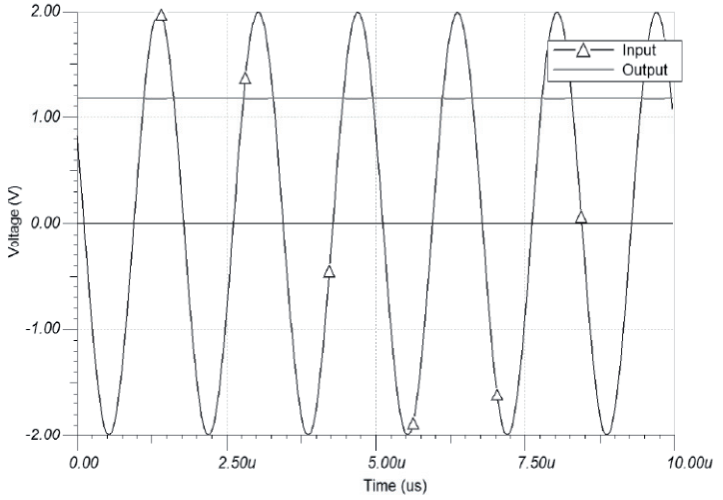


**Figure 34. Ti TINA software simulation of the full period rectifier at 600 kHz [49]**

The linear chirp signal from 20 kHz to 600 kHz was used for PZT excitation. Both EMI magnitude of bonded and free PZT were measured and compared against results obtained using commercial impedance analyzer (Figure 35).

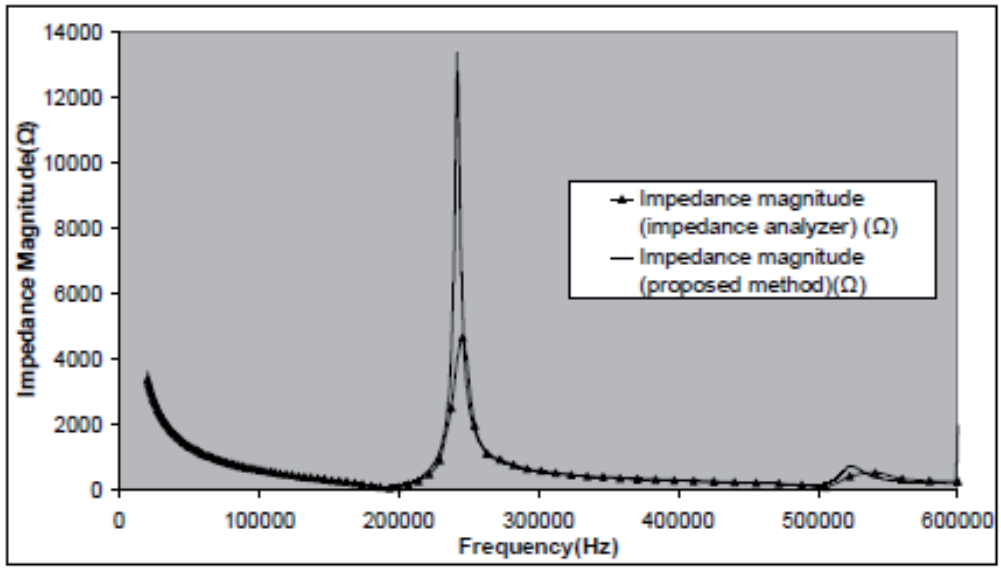


**Figure 35. EMI magnitude of a free PZT measured using MPSB430-based solution [49]**

Proposed solution has very low price and low energy consumption. Overall total power consumption was below 3.5 W of which MCU consumes at maximum power 1.3 mW. Because of low power consumption MSP430 based solution could be implemented in applications where energy harvesting is possible [50].

## 5.3 TI TMS320F28335-based Solution

TMS320F28335 is Texas Instruments 32 bit high performance DSC. It has 150 MHz clock rate and single precision floating point unit. An integrated 12 bit AD converter and a high-resolution enhanced 16 bit high-resolution PWM make it suitable platform for ultrasonic signal generation and sampling. Maximum power consumption is less than 900 mW at 150 MHz and supply voltage 3.3 V.

Proposed solution uses external 3$^{rd}$ order analog active low-pass filter for smoothing of the PWM excitation signal (Figure 36, Figure 37) [51]. ADC and DAC both were used with 2MHz sampling rate. This enables sufficient oversampling rate for signal up to 600 kHz and more. For sampling of the response signals an integrated 12 bit ADC was used. Although controller has 256K × 16 of embedded flash memory and 34K x 16 SARAM, it is not sufficient enough for long excitation and response signals. DSC was combined with external static RAM (Cypress Semiconductor Corporation CY7C1061AV33). The CY7C1061AV33 is a CMOS Static RAM consisting 1Mx16 bits. Combination of external RAM with DSC enables to use longer excitation and response signals. Controller and RAM are connected through XINTF interface. XINTF is an asynchronous bus which consists of 20 address, 32 data lines and three chip select lines.

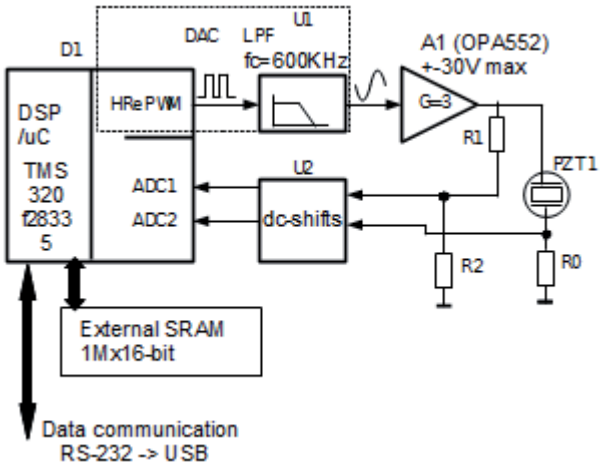


**Figure 36. Principal layout of proposed F28335 solution**

For PZT excitation signal generation operational amplifier together with voltage step up converter was used. Excitation signal had unipolar 60 V peak-to-peak voltage. Supply voltage was 12 V. Maximum combined (DSC, SRAM and amplifier) current consumption during excitation phase was below 400 mA.

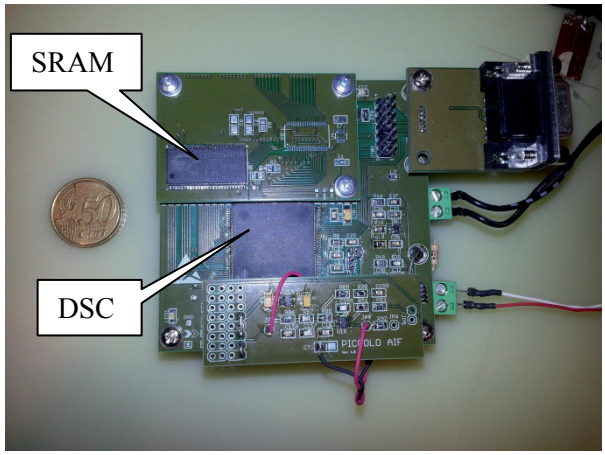


**Figure 37. Assembled monitor node**

For piezo excitation linear chirp signal was used. Because of the XINTF 16 bit limitation, excitation signal was limited to 65536 samples. With 2 MS/s AD conversion rate this enabled to use excitation signals up to 32 ms long.

For EMI signal processing method described in patent [46] was used. F28335 enables to calculate dual 16 bit MAC operations simultaneously which makes this platform very efficient for these applications. At 150 MHz clock rate DSC performs impedance calculations well beyond data rate of the XINTF interface.

Similarly to other methods, test measurements on the PZT elements were conducted and the results were compared against a results obtained using

commercial impedance analyzer. Figure 38-41 display experimental measurement results on the bonded and on the free piezo.

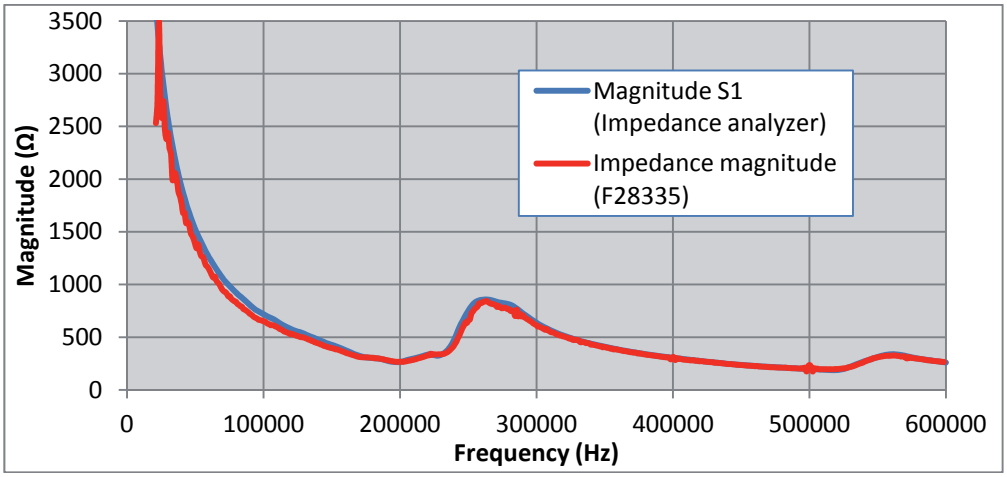


**Figure 38. Magnitude of the impedance of a bonded PZT (S1)**

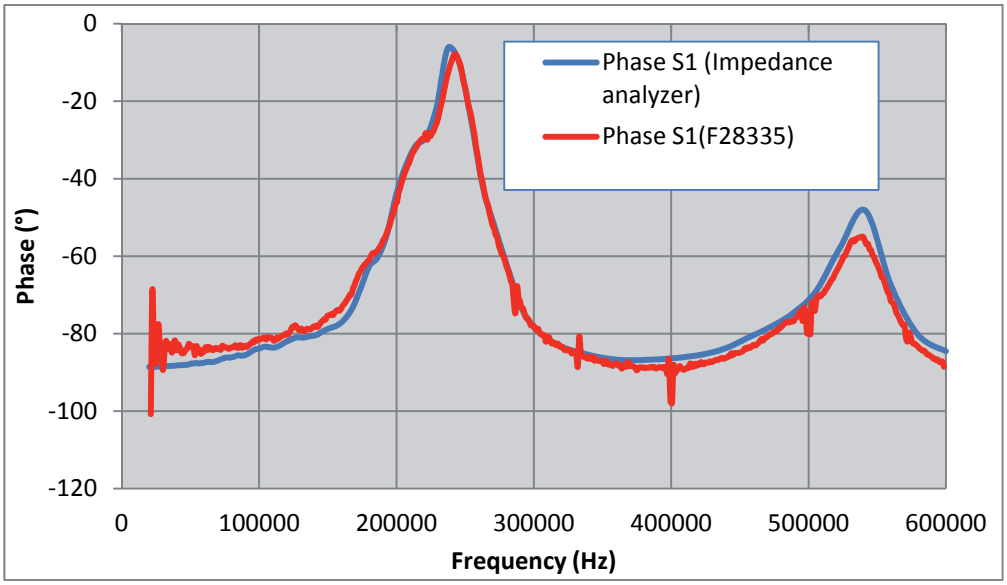


**Figure 39. Phase of the impedance of a bonded PZT**

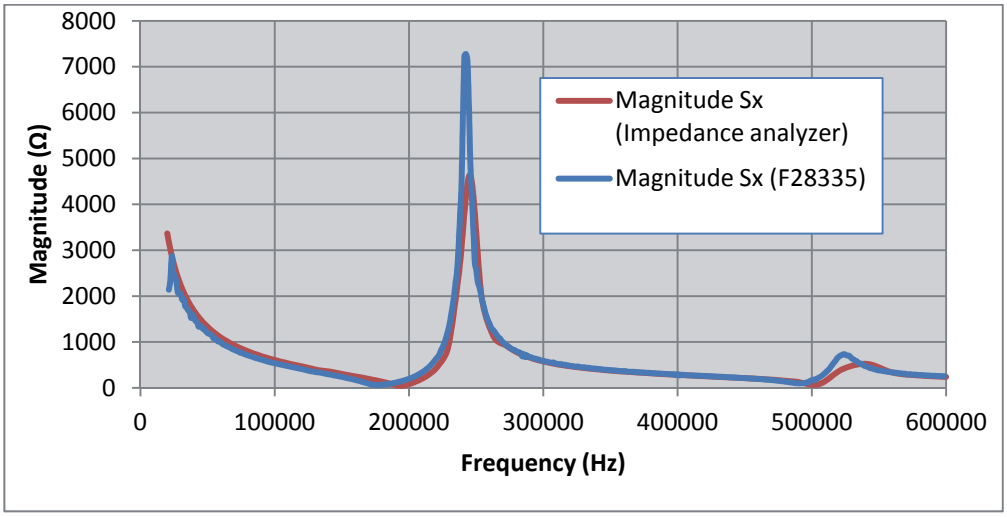


**Figure 40. Magnitude of the impedance of a free PZT**

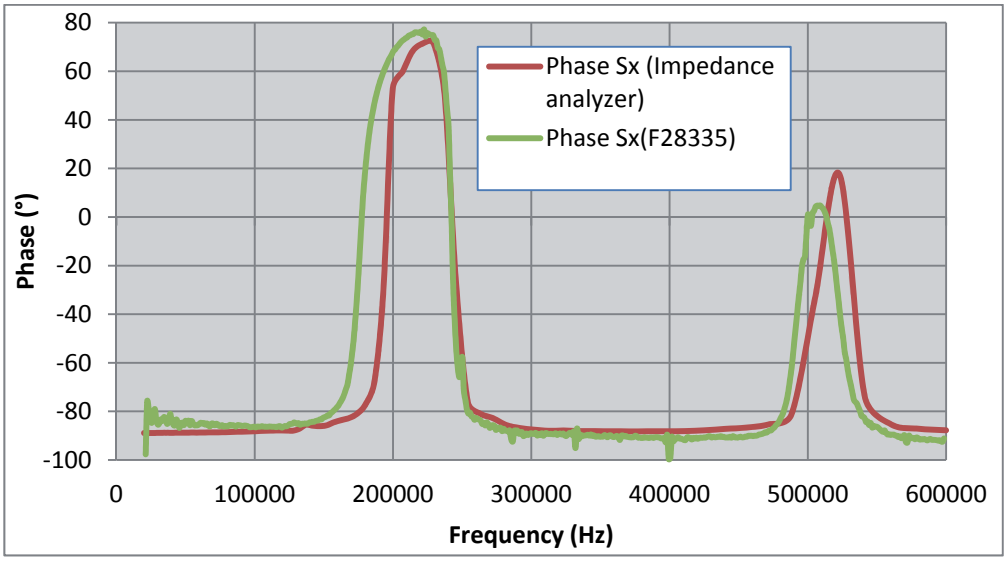


**Figure 41. Phase of the impedance of a free PZT**

The described solution may also be used for pitch-catch measurements. Twelve ADC channels on F28335 enable to connect up to 6 PZTs for combined EMI and pitch-catch measurements.

# 6. EXAMPLE APPLICATIONS

In addition to sensor bond diagnostics EMI can be used also in many other applications. In this section two separate possible applications are studied and experiments are conducted. For impedance the spectra measurement F28335 based solution (described in chapter 5) was used.

## 6.1 EMI Spectroscopy for Composite Delamination Detection

Delamination is one of the most common failure modes in composite materials. In this mode different layers of the material separate from each other. It may be caused by excessive impact load, static or fatigue loading. This failure mode may critically compromise structural integrity of the host structure. Previously [5] [53] [4] have described methods for composite delamination measurement using EMI.

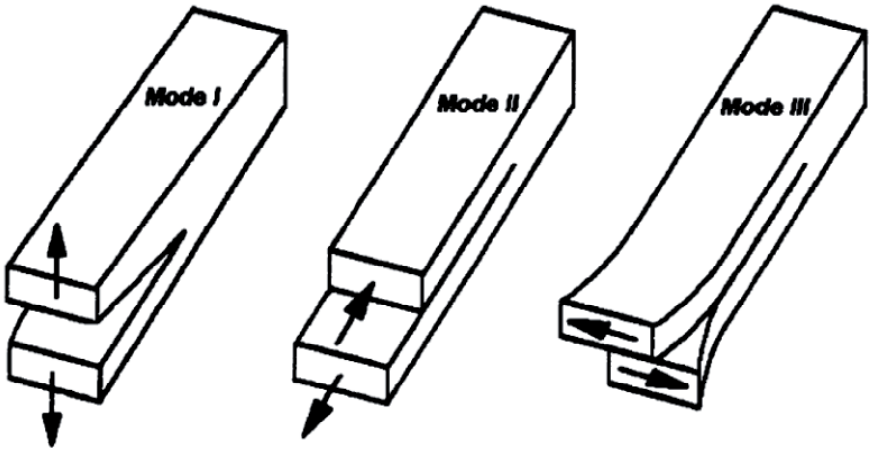


**Figure 42. Basic delamination modes [54]**

For this case study, a composite specimen with delamination mode 1 failure was used (Figure 42). It is the most common delamination mode in composite materials [54]. PZT transducers with 7 mm diameter were used for the measurement. Three transducers were bonded to test structure (Figure 43, Figure 44). Two of the sensors (SL1 and SL2) were on laminate sections without delamination. Third transducer (Sdl) was in the middle of delaminated section. The distance between sensors was 250 mm.

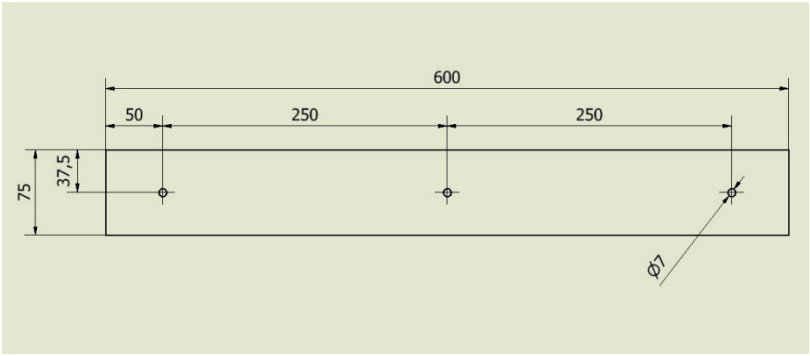


**Figure 43. Drawing of a test specimen (in millimeters)**

The composite specimen was a sandwich material with enhanced weather protection design. Main load carrying layers were biaxial fabrics with layer weight 600 g/m2. These layers are protected from moisture attack on both sides with chopped stranded mats layers. The specimen outer side is protected with gel coat and three extra layers of chopped stranded mat. Transducers were mounted on to the surface of gel coat. The sandwich core was Airex C70.55 with layer thickness of 15 mm. Sandwich total thickness was 22.5mm.

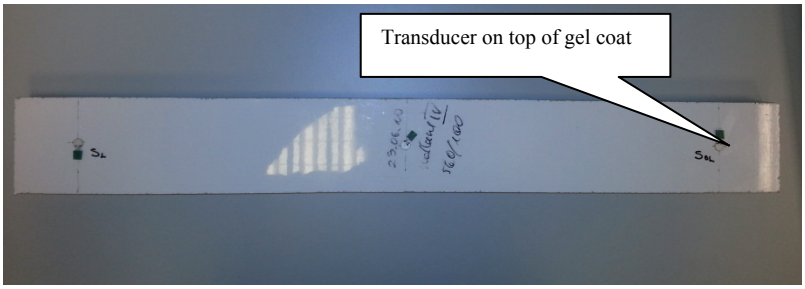


**Figure 44. Photo of a test specimen with PZT transducers**

The delamination type in the test specimen was mode 1 (Figure 42). Length of the delamination was about 100 mm (Figure 45). To further test PZT bond quality pitch-catch measurements were conducted between sensors to ensure correct bonding of PZT and host structure.

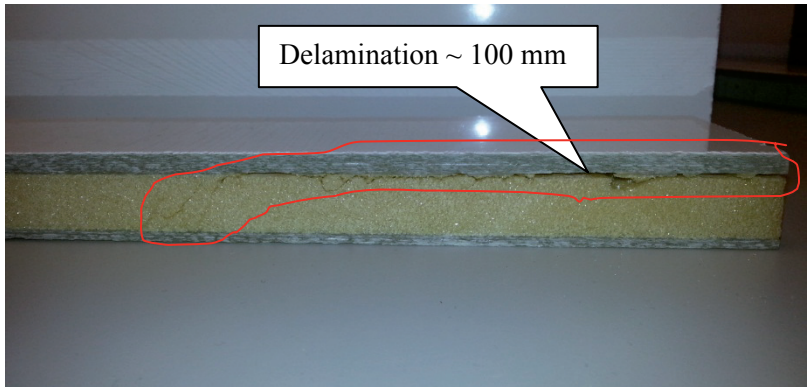


**Figure 45. Delaminated section of the test structure**

Electromechanical impedance of the three transducers was measured to compare results between the delaminated and structurally intact sections.

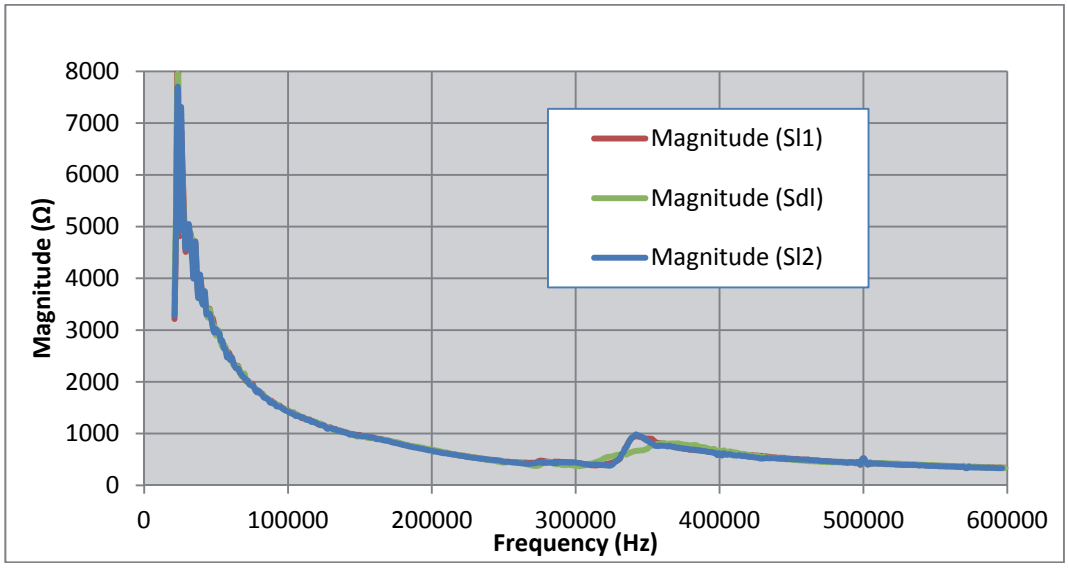


**Figure 46. Magnitude of the impedance plots of the PZTs**

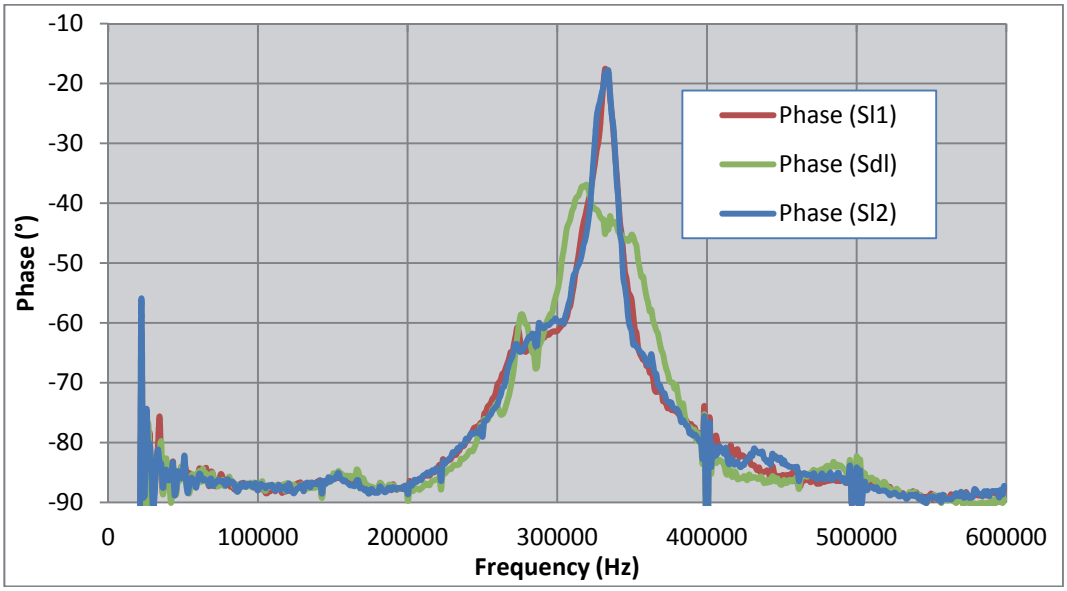


**Figure 47. Phase of the impedance plots of the PZTs**

As can be clearly seen from the figures (Figure 46 and Figure 47) the transducer (Sdl) on delaminated area had significantly different EMI plot. Differences are concentrated in regions between 200 kHz and 400 kHz.

## 6.2 PZT Transducer Structural Diagnostics

In this case study, the structural integrity of a PZT was experimentally studied. Previous studies [55], [55] have shown good correlations between the PZT condition and EMI spectra. A 10 mm diameter PZT was broken in half to simulate mechanical damage to the transducer (Figure 48). The defected transducer (S4) was bonded to a 500x500 mm plate structure.

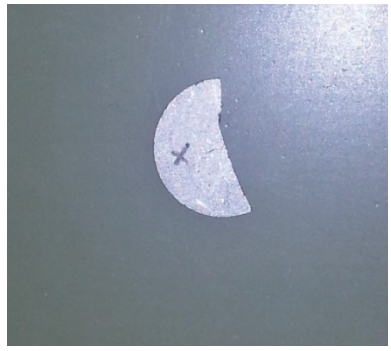

**Figure 48. Damaged PZT transducer**

Electromechanical impedance of an undamaged and damaged PZT was measured and compared in the 20 kHz–600 kHz frequency range.

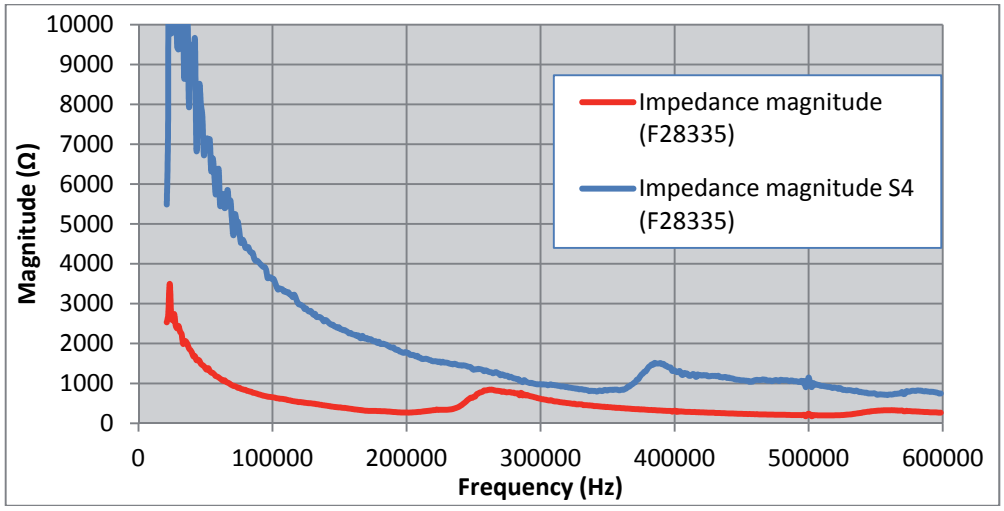


**Figure 49. Magnitude of the impedance of a undamaged and damaged PZT (S4)**

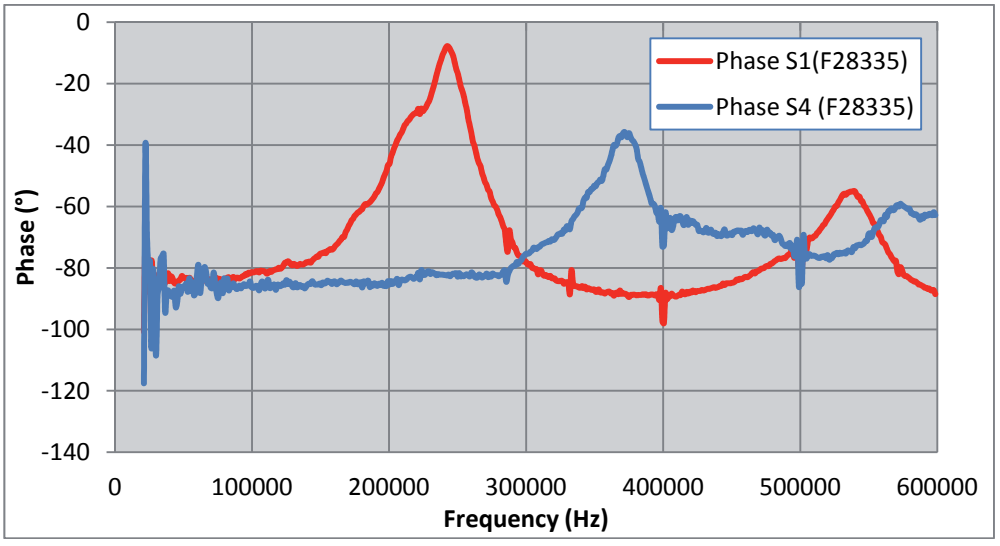


**Figure 50. Phase of the impedance of a undamaged and damaged PZT (S4)**

EMI spectra measurements indicate that structurally damaged PZT has a totally different impedance plot compared to a structurally intact one (Figure 49, Figure 50). Magnitude and phase of the impedance peaks have shifted over 100 kHz. This frequency shift could be used as an indicator for transducer structural damage. These results comply with claims in [55].

# 7. SUMMARY OF PUBLICATIONS

The following section gives an overview of the publications related to this thesis.

## 7.1 Study of Various Excitation and Reference Signals for Pulsed Correlation-based Ultrasound Signal Processing (Paper Summary)

In this paper methods for pitch-catch measurements were studied. In the test setup described in Chapter 3 different waveform signals were studied and tested. Effects of window functions signals were tested and the results compared. In addition to this, binary excitation signals were tested and compared. Use of binary signals would enable to simplify signal generation electronics. For improving time resolution accuracy of TOF data chirp-based excitation signals were proposed in 180 kHz–220 kHz range.

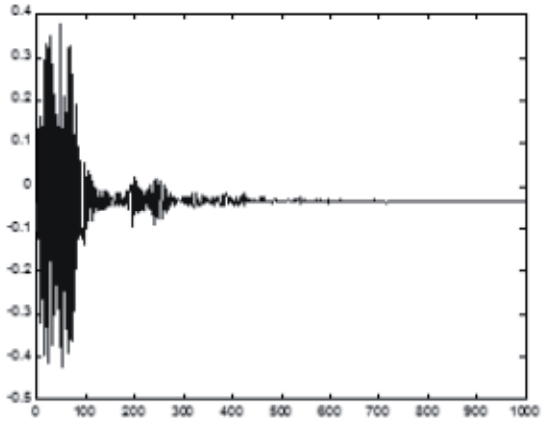


**Figure 51. Measured voltage response of pitch-catch method (voltage [V] vs time [ms])**

For the improvement of the measured signal correlation method, a new improved method was proposed. The new method is based on the response signal correlation with the original excitation and with quadrature of the original excitation signal. Computed results will be added as a sum of absolute values. Similarly to the Hilbert transform, it will simplify signal detection from noisy measurement results.

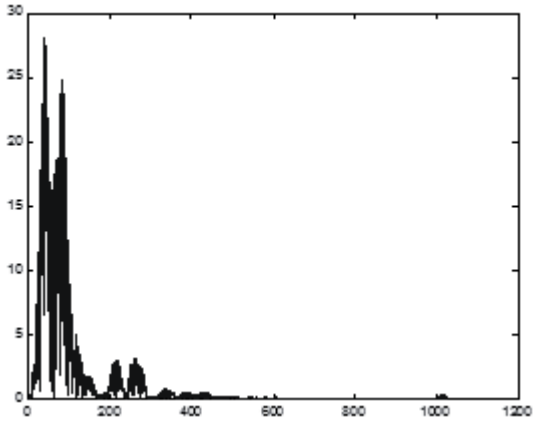


**Figure 52. Result of cross-correlation with excitation and qudrature signal (time [ms] vs correlation)**

This paper was published in the journal *Electronics and Electrical Engineering* 2010, No. 9 (105). The main contributions by the author to this study were the design of the test setup, experimental measurements and analysis of the results.

## 7.2 Fast Impedance Spectroscopy of Piezo Sensors for Structural Health Monitoring (Paper Summary)

In this paper, different piezo EMI measurement methods were compared. The goal of this paper was to compare different EMI measurement methods. Traditionally EMI is measured with different frequencies one by one. The use of wide band excitation signal enables to reduce the measurement time significantly. In this experiment, different wide and narrow band excitation signals were tested. Measurement setup was based on National Instruments USB-6259 data acquisition box (DAQ) and a PC. Matlab (PC) based software was used for excitation signal generation, sampling and FFT or DCT calculation. DAQ had 16 bit 1.25 MS/s analog AD input. ± 30 V was used for excitation signal voltage.

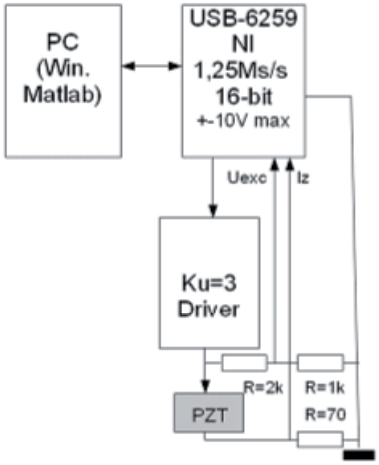


**Figure 53. Impedance measurement schematics**

The device under test (DUT) was a piezo sensor with a host structure. A bulk piezo sensor with an 8 mm diameter was bonded to a 500 x 500 mm fiberglass plate.
Three measurement methods were chosen: frequency scanning, multi-frequency and chirp. First method used measurement of frequencies one-by-one. One measurement point took 0.5 s. Complex DFT was calculated of reference sine- and cosine-waves.

The second method used was based on multi-frequency excitation signal and DFT or FFT analysis. A 5 kHz and 1.25 kHz frequency step was used in a 5 kHz to 300 kHz frequency range.

The third method used linear chirp excitation signal combined with FFT. Different pulse lengths from 0.8 ms to 80 ms were tested.

It is concluded that all tested methods have a great potential in SHM applications by making measurement solutions cheaper.

This paper was published in the journal *Electronics and Electrical Engineering* 2010. No.7(103). The main contributions by the author to this study were the design of the test setup, experimental measurements using chirp excitation signal and analysis of the results.

## 7.3 Chirp-based Impedance Spectroscopy of Piezo Sensors (Paper Summary)

This paper describes methods for impedance spectroscopy of piezo sensors. Methods were proposed with novel time domain analysis without complex spectral analysis calculations. The overall goal of proposed and evaluated methods was to find simple signal processing solutions without FFT or DFT calculations. As the FFT and DFT transforms are computationally very expensive, simpler alternatives were studied in this paper. Simpler methods enable to use low power and low-cost processing units.

The described measurement setup consisted of NI-6259 USB DAQ box and custom analog front end. Calculations were done on PC-based Matlab software.

Two alternative methods were proposed. The first method used linear chirp excitation signal from 20 kHz to 600 kHz. The signal length was 80 ms. Voltage and current response of the DUT were sampled at a 1.25 MS/s sample rate. For voltage and current signal smoothing Savitzky-Golay's second order polynomial filter was used. Compared to a regular FIR filter it has the ability to obtain signal maximum values. The filter window was 250 samples. Experimental measurements were made on the piezo sensor without a host structure. The calculated magnitude of the impedance was compared against measurements made using the Wayne-Kerr commercial impedance analyzer.

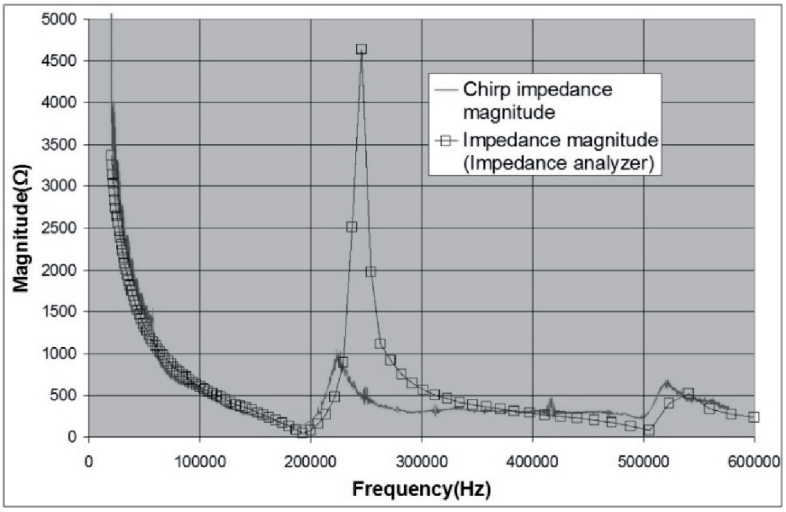


**Figure 54. Results of the magnitude of the impedance using the chirp method (compared with commercial impedance analyzer)**

The results of this study were presented in 2010, at the 12th Biennial Baltic Electronics Conference (BEC2010 Tallinn, Estonia, October 4–6, 2010). The main contribution to this research by the author was the study of the chirp-based impedance magnitude measurement method. Experimental measurements on PZTs were conducted and the results evaluated.

## 7.4 Robust Piezo Impedance Magnitude Measurement Method (Paper Summary)

In this article, very minimalistic piezo transducer impedance magnitude measurement solutions are proposed. The overall goal of this publication is to offer a low-cost and low-power piezo impedance magnitude measurement method in the 20 kHz–600 kHz range. A linear chirp signal was used for excitation. The Texas Instruments MSP430F2013 MCU was chosen for signal processing and sampling. Small dimensions and low power consumption make it ideal for SHM applications. As the chosen MCU has a low sampling rate, a front end analog interface was used.

A full period rectifier combined with a low pass filter was used for signal smoothing.

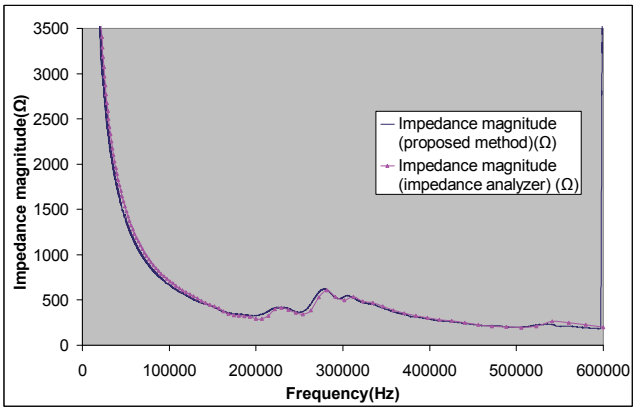


**Figure 55. Impedance magnitude results (MSP430-based solution vs commercial impedance analyzer)**

Results were compared against the measurements made by the commercial impedance analyzer by Wayne-Kerr. Experimental measurements were carried out on a free and bonded piezo. Both results indicated a great similarity between the commercial impedance analyzer and the proposed solution.

It is concluded that a simple MCU combined with a simple analog front end is a very effective impedance magnitude measurement method. Both low cost and low power use make it useful for SHM applications.

This paper was published in the journal *Electronics and Electrical Engineering* 2011, No.7(1113). The author of this thesis is the sole author of the paper.

## 7.5 Simple DSP Interface for Impedance Spectroscopy of Piezo Sensors (Summary)

The paper describes a simple DSP hard- and software solution for piezo sensor impedance spectroscopy. The solution is based on the Texas Instruments Delfino series DSP. The overall goal of this study was to find a DSP-based impedance spectroscopy solution while using a minimal number of external components. The paper describes the use of DSP integrated ADC and DAC components effectively. For excitation, a signal generation external active low pass filter is needed to convert the PWM signal to the analog domain. Both ADC and PWM had a sampling frequency of 2 MHz. The use of 3 ADC channels enables to utilize the proposed solution for the pitch-catch measurement, making it a more universal SHM measurement node solution.

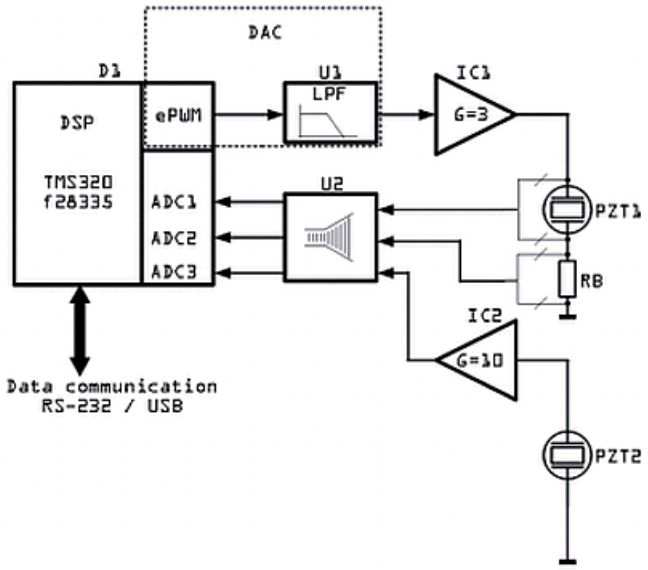


**Figure 56. Hardware layout of the F28335-based hardware solution**

It is concluded that an integrated single chip solution for piezo impedance spectroscopy is possible. The development of DSP peripherals enables to reduce overall external components needed for impedance measurement systems.

Results of this study were presented in 2010, at the 12th Biennial Baltic Electronics Conference (BEC2010 Tallinn, Estonia, October 4–6, 2010). The main contribution to this research by the author was the testing and evaluation of the measurement results.

## 7.6 TMS320F28335-based Piezo Sensor Monitor-Node (Summary)

In this publication, the use of TMS320F28355 DSP is analyzed for piezo impedance spectroscopy. The goal of this paper was to investigate DSP solutions with minimal external interfaces which would maximize the use of internal ADC and DAC components.

The paper describes experimental measurements on free and bonded piezo sensors. The results were compared against commercial impedance analyzer results by Wayne-Kerr 6500B.

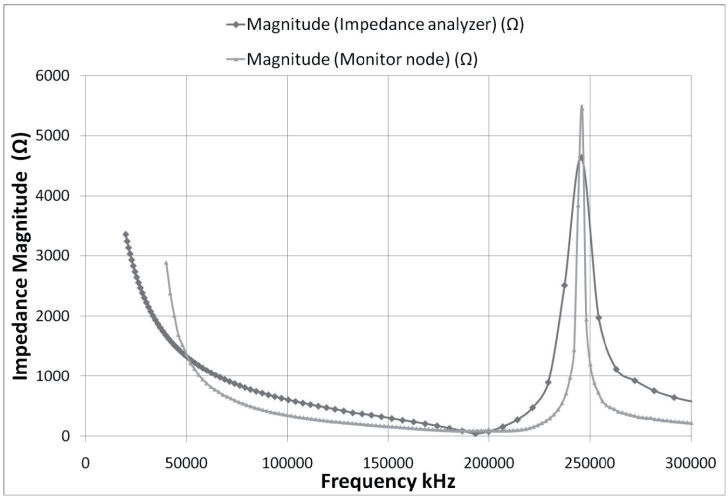


**Figure 57. Magnitude of the impedance results (F28335-based solution vs commercial impedance analyzer)**

It is concluded that the developed solution is effective for impedance measurements up to 400 kHz and could be extended up to 1 MHz with relative ease.

The results of this study were presented in 2010, at the 4th European DSP Education and Research Conference (EDERC). The main contribution to this research by the author was the development of software, experimental measurements and analysis of the results.

## 7.7 Method and Device for Frequency Response Measurement (Summary)

The patent proposes a method for frequency response measurement. FFT and DFT are computationally very expensive transforms. Avoiding those transforms enables to use simpler (cheaper) processing units. The solution describes the use of a wide-band linear chirp signal for DUT excitation. The response signal is correlated with two reference signals. The first reference signal could be exact excitation signal and the second one the quadrature of the first reference signal. Correlation is done in a sliding window. The window could have a fixed size or be dynamic in the time domain. This enables to get a different accuracy in different parts of the time domain signal. By calculating the correlation between those signals, a real and imaginary part of response signal could be extracted.

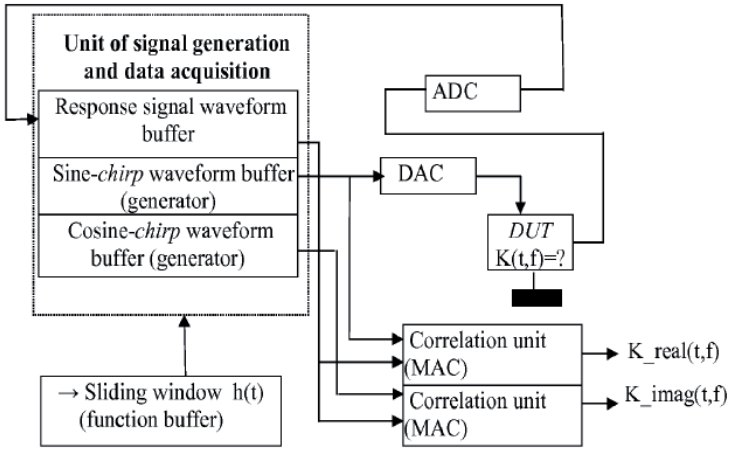


**Figure 58. Principal layout of the solution**

As only MAC calculations are used in this method it is very effective on DSP platforms which are optimized for MAC calculations.

The results of this research were published as a US patent application and as an Estonian patent. The main contribution to this research by the author was experimental measurements, result analysis, Matlab scripts for measurements and analysis.

# 8. RESULTS

## 8.1 Conclusions

New methods for EMI measurement have been investigated and proposed in this thesis. State of the art methods for EMI signal processing have been tested and simulated using actual PZT transducers in different conditions. Experimental hardware solutions have been developed and tested. Tests include comparison of experimental results with industry standard commercial impedance analyzers.

As a result of this thesis, two principally different impedance measurement methods were proposed. The two methods were both implemented on PC-based and embedded hardware.

PC-based based implementations were written in Matlab code and using USB DAQ box for excitation signal generation and response signal measurement. Measurements were conducted on a PZT element and compared against measurements made by the commercial impedance analyzer.

Embedded hardware based implementations were developed keeping in mind real-life SHM applications. Low power consumption and low price were considered to be the priorities dictated by real life scenarios. Two solutions based on TI MSP430 MCU and MS320F28335 DSP were proposed. The first solution was very simple and robust for very low-power applications. The second one was for more advanced and higher performance applications. Both hardware solutions were tested and evaluated. Measurement results of a PZT element were compared against the commercial impedance analyzer.

All goals set for this theses were met. New solutions were proposed and tested.

The results of this thesis could be summarized as follows:

- The magnitude and phase of the EMI peaks can be used as indicators of the PZT transducer state.
- The magnitude and phase of the EMI can be the indicator of a host structure condition.
- The proposed 30 ms is a sufficient length and 20 kHz - 600 kHz is a sufficient frequency range for PZT transducer EMI linear chirp excitation signal to distinguish different states.
- The TI MSP430-based solution is a sufficient EMI magnitude measurement in the 20 kHz–600 kHz range.
- The TI F28335-based measurement node is sufficient for PZT transducer pitch-catch and EMI measurements in the 20 kHz–600 kHz range.
- The proposed sliding window correlation method is a feasible alternative to FFT calculation.

- Additionally it was confirmed experimentally that PZT transducer EMI spectra can be used for composite delamination and PZT transducer structural damage detection.

## 8.2 Future Work

Future work could involve improving EMI measurement results using binary signals. In [27] effective impedance measurement results have been demonstrated, using wide-band binary signals in the biological tissue. Binary signals enable to use more simplified electronics for signal generation but require more complex excitation signals or later signal processing.

Further more experimental measurement results are needed using actual composite structures to see different defect modes influencing electromechanical impedance spectra. In this thesis, only simple structures and defect modes were covered. In future studies, more complex structures and progression of the defects should be covered.

Additionally damage metric could be developed, similarly to [56]. This enables to classify the damage severity and type into different classes. Damage metric could either be simple linear or more complex neural network based. Also damage prognosis, similarly to descriptions in [57] could be in the focus for future studies.

# REFERENCES


[1] Charles Farrar and Keith Worden, "An introduction to structural health monitoring," *Philosphical Transactions of The Royal Society*, vol. 365, no. 1851, pp. 303-315, 2006.

[2] Giola Santoni-Bottai and Victor Giurgiutiu, "Damage detection at cryogenic temperatures in composites using piezoelectric wafer active sensors," *Structural Health Monitoring*, vol. 11, no. 5, pp. 510-525, 2012.

[3] Jürgen Pohl and Gerhard Mook, "SHM of CFRP-structures with impedance spectroscopy and Lamb waves," *International Journal of Mechanics and Materials in Design* , vol. 6, no. 1, pp. 53-62, 2010.

[4] Christophe Bois and Christian Hochard, "Monitoring of Laminated Composites Delamination Based on Electro-Mechanical Impedance Measurement," *Journal of Intelligent Material Systems and Structures*, vol. 15, no. 1, pp. 59-67, January 2004.

[5] Hamza Boukabache et al., "System-on-Chip Integration of a New Electromechanical Impedance Calculation Method for Aircraft Structure Health Monitoring," *Sensors*, vol. 12, no. 10, pp. 13617–13635, 2012.

[6] Suresh Bhalla, Panduranga A. Vittal, and Milan Veljkovic, "Piezo-impedance transducers for residual fatigue life assessment of bolted steel joints," *Structural Health Monitoring*, vol. 11, no. 6, pp. 733-750, 2012.

[7] Analog Devices, AD5933 Data Sheet, 2011.

[8] Competence Center ELIKO. (2011) The Smart Embedded Sensor System (SESS). [Online]. http://www.eliko.ee/sess/

[9] Hoon Sohn et al., *A Review of Structural Health Monitoring Literature: 1996–2001.*: Los Alamos National Laboratory, 2004.

[10] Li Hui and Ou Jinping, "Structural Health Monitoring: From Sensing Technology Stepping to Health Diagnosis," in *The Twelfth East Asia-Pacific Conference on Structural Engineering and Construction*, vol. 14, 2011, pp. 753-760.

[11] Andre Orcesi and Dan Frangopol, "Optimization of bridge maintenance strategies based on structural health," *Structural Safety*, vol. 33, pp. 26-41, 2011.

[12] Scott Doebling, Charles Farrar, Michael Prime, and Daniel Shevitz, "Damage Identification and Health Monitoring of Structural and Mechanical Systems from Changes in Their Vibration Characteristics:A Literature Review," Los Alamos National Lab., NM (United States), Technical Report 1996.

[13] Anders Rytter, "Vibrational Based Inspection of Civil Engineering Structures," *Fracture and Dynamics*, 1993, Ph.D.-Thesis defended publicly at the

University of Aalborg, April 20, 1993.

[14] Roman T. Underwood, "Damage Detection Analysis Using Lamb Waves in Restricted Geometry for Aerospace Applications," Department of the Air Force Air University, Wright-Patterson Air Force Base, Ohio, Master thesis 2008.

[15] Victor Giurgiutiu, Lingyu Yu, and Dustin Thomas, "Embedded Ultrasonic Structural Radar with Piezoelectric Wafer Active Sensors for Damage Detection in Cylindrical Shell Structures," in *45th AIAA/ASME/ASCE/AHS/ASC Structures, Structural Dynamics & Materials Conference and 12th AIAA/ASME/AHS Adaptive Structures Forum*, Palm Springs, 2004.

[16] Pawel Gebski, Leszek Golaski, and Kanji Ono, "Acoustic emission monitoring of fatigue of glass-fiber wound pipes under biaxial loading," *Journal of Acoustic Emission*, vol. 19, pp. 285-314, 2001.

[17] Victor Giurgiutiu, "Piezoelectric Wafer Active Sensors for Structural Health Monitoring of Composite Structures Using Tuned Guided Waves," *Journal of Engineering Materials and Technology*, vol. 133, no. 4, pp. 041012-1-041012-6 , 2011.

[18] Gyuhae Park, Hoon Sohn, and Charles R Farrar, "Overview of piezoelectric impedance-based health monitoring and path forward ," *The Shock and Vibration Digest*, vol. 35, no. 6, pp. 451-463, 2003.

[19] Jan Achenbach, "Structural health monitoring – What is the prescription?," *Mechanics Research Communications*, vol. 36, no. 2, 2009.

[20] Harry O. Wood, "On a piezo-electrical accelerograph," *Bulletin of the Seismological Society of America*, pp. 51-57, 1921.

[21] Byung Yang Lee et al., "Virus-based piezoelectric energy generation," *Nature Nanotechnology*, vol. 7, pp. 351-356, 2012.

[22] A. Sen, A. Seal, N. Das, R. Mazumdar, and H. S. Maiti, "Technological Challenges of Making PZT Based Piezoelectric Wafers," in *Proceedings of ISSS 2005 lnternational Conference on Smart Materials Structures and Systems*, Bangalore, India, 2005.

[23] C. Liang, F. P. Sun, and C. A. Rogers, "Coupled Electro-Mechanical Analysis of Adaptive Material Systems — Determination of the Actuator Power Consumption and System Energy Transfer," *Journal of Intelligent Material Systems and Structures*, vol. 5, pp. 12-20, 1994.

[24] Seunghee Park, Chung-Bang Yun, Yongrae Roh, and Jong-Jae Lee, "Health monitoring of steel structures using impedance of thickness modes at PZT patches," *Smart Structures and Systems*, vol. 1, no. 4, pp. 339-353, 2005.

[25] Lingyu Yu, Victor Giurgiutiu, Jingjiang Wang, and Yong-June Shin, "Corrosion detection with piezoelectric wafer active sensors using pitch-catch waves and cross-time-frequency analysis," *Structural Health Monitoring*, vol. 11, no. 1, pp. 83-93, 2012.

[26] Evgenij Barsoukov and J. Ross Macdonald, *Impedance Spectroscopy Theory, Experiment, and Applications Second Edition*. New Jersey: John Wiley & Sons, Inc, 2005.

[27] Jaan Ojarand, "Wideband Excitation Signals for Fast Impedance Spectroscopy of Biological Objects," Tallinn University of Technology, Tallinn, PhD thesis 2012.

[28] L. Skarbek, T. Wandowski, S. Opoka, P. Malinowski, and W. Ostachowicz, "Electromechanical Impedance Technique and Scanning Vibrometry for Structure Characterization," in *6th European Workshop on Structural Health Monitoring - Tu.2.C.4*, Dresden, Germany, 2012.

[29] R. Panigrahi, S. Bhalla, and A. Gupta, "A low-cost variant of electro-mechanical impedance (emi) technique for structural health monitoring," *Experimental Techniques*, vol. 34, no. 2, pp. 25-29, 2009.

[30] Buli Xu and Victor Giurgiutiu, "A Low-Cost and Field Portable Electromechanical (E/M) Impedance Analyzer for Active Structural Health Monitoring," in *5th International Workshop on Structural HealthMonitoring*, Stanford, 2005.

[31] Roberto M. Finzi Neto, Valder Steffen Jr, Domingos A Rade, Carlos A. Gallo, and Lizeth V. Palomino, "A low-cost electromechanical impedance-based SHM architecture for multiplexed piezoceramic actuators," *Structural Health Monitoring*, vol. 10, no. 4, pp. 391-402, 2010.

[32] Nicolas E. Cortez, Jozue V. Filho, and Fabricio G. Baptista, "A new microcontrolled structural health monitoring system based on the electromechanical impedance principle," *Structural Health Monitoring*, vol. 12, no. 1, pp. 14-22, 2013.

[33] S. Park, C.-B. Yun, and D. J. Inman, "Structural health monitoring using electro-mechanical impedance sensors," *Fatigue & Fracture of Engineering Materials & Structures*, vol. 31, no. 8, pp. 714-724, 2008.

[34] Buli Xu and Victor Giurgiutiu, "Development of DSP-based Electromechanical (E/M) Impedance Analyzer for Active Structural Health Monitoring," in *SPIE's 13th International Symposium on Smart Structures and Materials and 11th International Symposium on NDE for Health Monitoring and Diagnostics, Health Monitoring and Smart NDE of Structural and Biological Systems Conference*, 2006.

[35] Victor Giurgiutiu, "Lamb Wave Generation with Piezoelectric Wafer Active Sensors for Structural Health Monitoring," in *SPIE's 10th Annual International Symposium on Smart Structures and Materials and 8th Annual International Symposium on NDE for Health Monitoring and Diagnostics*, 2002.

[36] Seunghee Park, Gyuhae Park, Chung-Bang Yun, and Charles R. Farrar, "Sensor Self-diagnosis Using a Modified Impedance Model for Active Sensing-based Structural Health Monitoring," *Structural Health Monitoring*, vol. 8, no. 1, pp. 71-82, 2009.

[37] National Instruments, NI 625x Specifications, 2007.

[38] O. Märtens, T. Saar, and M. Reidla, "Study of Various Excitation and Reference Signals for Pulsed Correlation-based Ultrasound Signal Processing," *Electronics and Electrical Engineering*, vol. 105, no. 9, pp. 89-92, 2010.

[39] Jeong-Beom Ihn and Fu-Kuo Chang, "Pitch-catch Active Sensing Methods in Structural Health Monitoring for Aircraft Structures," *Structural Health Monitoring*, vol. 7, no. 1, pp. 5-19, 2008.

[40] Wayne Kerr Electronics, Precision Impedance Analyzers, 2008.

[41] O. Märtens and T. Saar, "Fast Impedance Spectroscopy of Piezosensors for Structural Health Monitoring," *Electronics and Electrical Engineering*, vol. 103, no. 7, pp. 31-34, 2010.

[42] Fabricio Guimaraes Baptista, Jozue Vieira Filho, and Daniel J Inman, "Influence of Excitation Signal on Impedance-based Structural," *Journal of Intelligent Material Systems and Structures*, vol. 21, pp. 1409-1416, November 2010.

[43] T. Paavle and M. Min, "Discrete-Level Broadband Excitation Signals: Binary/Ternary Chirps," *Electronics and Electrical Engineering*, vol. 6, no. 122, pp. 23-26, 2012.

[44] T. Saar, O. Martens, M. Reidla, and A. Ronk, "Chirp-based impedance spectroscopy of piezo-sensors," in *Proceedings of the 12th Biennal Baltic Electronics Conference*, Tallinn, 2010, pp. 339-342.

[45] Abraham Savitzky and Marcel J. E. Golay, "Smoothing and Differentiation of Data by Simplified Least Squares Procedures," *Analyctical Chemistry*, vol. 36, no. 8, pp. 1627–1639, 1964.

[46] Olev Märtens et al., "Method and Device for Frequency Response Measurement," Patent Application US2012/0007583, 2012.

[47] Daniel M. Peairs, "High Frequency Modeling and Experimental Analysis for Implementation of Impedance-based Structural Health Monitoring," Virginia Polytechnic Institute and State University, Blacksburg, Virginia, PhD thesis 2006.

[48] Corey Wilson Pitchford, Benjamin L. Grisso, and Daniel J. Inman, "Impedance-Based Structural Health Monitoring of Wind Turbine Blades," in *Proc. SPIE 6532, Health Monitoring of Structural and Biological Systems 2007*, 2007.

[49] T. Saar, "Robust Piezo Impedance Magnitude Measurement Method," *Electronics and Electrical Engineering*, vol. 113, no. 7, pp. 107-110, July 2011.

[50] Reza Abbaspour, "A Practical Approach to Powering Wireless SensorNodes by Harvesting Energy From Heat Flow in Room Temperature," in *2010 International Congress on Ultra Modern Telecommunications and Control Systems and Workshops (ICUMT)*, 2010.

[51] O. Märtens, M. Reidla, and T. Saar, "Simple DSP interface for impedance spectroscopy of piezo-senors," in *Electronics Conference (BEC), 2010 12th Biennial Baltic*, Tallinn, 2010, pp. 343-348.

[52] O. Märtens, T. Saar, and M. Reidla, "TMS320F28335-Based Piezosensor Monitor-Node," in *EDERC2010 European DSP in Education and Research Conference PROCEEDINGS*, Nice, 2010, pp. 62-65.

[53] Wei Yan, "Delamination detection in laminated composite beams using electro-mechanical impedance signatures," in *Piezoelectricity, Acoustic Waves, and Device Applications, 2008. SPAWDA 2008. Symposium on*, 2008.

[54] Wei Ding, "Delamination Analysis of Composite Laminates," University of Toronto, Toronto, PhD thesis 1999.

[55] Gyuhae Park, Charles R. Farrar, Francesco Lanza di Scalea, and Stefano Coccia, "Performance Assessment and Validation of Piezoelectric Active-Sensors in Structural Health Monitoring," *Smart Materials and Structures*, vol. 15, no. 6, 2006.

[56] Fanny Bouteiller, Benjamin L. Grisso, Daniel M. Peairs, and Daniel J. Inman, "Broken rail track detection using smart materials," in *Proc. SPIE 6178, Nonintrusive Inspection, Structures Monitoring, and Smart Systems for Homeland Security*, San Diego, 2006.

[57] Charles Farrar and Nick Lieven, "Damage prognosis: the future of structural health monitoring," *Philosophical Transactions of The Royal Society*, vol. 365, pp. 623-632, 2007.

# ACKNOWLEDGEMENTS

I would like to thank my colleagues in the Competence Center ELIKO and Tallinn University of Technology, department of Thomas Johann Seebeck, Department of Electronics, especially my supervisor leading researcher Dr. Olev Märtens. Also special thanks to Marko Reidla and Dr. Raul Land for the help in conducting experimental measurements.

Additionally I would like to thank partners NOLIAC Ltd. and DTU (Risoe, Denmark), Innowacja Polska and EC Electronics (Poland) from the Eurostars-SESS project. Special thanks to Malcolm McGugan from DTU for providing us with SHM know-how and Charles Mangeot for providing us the PZT sensors for the experiments.

Also thanks to Smart Composite project partners, especially junior researcher Henrik Herranen and senior researcher Jüri Majak from the Department of Machinery.

My sincere thanks go to Professor Emeritus Enn Velmre for his help in reviewing the thesis.

I am truly thankful for support from my mother, father and my friends.

This work has been supported by the Estonian Information Technology Foundation, Estonian Science Foundation (ETF grant 8905) and Enterprise Estonia through the Competence Center ELIKO.

# ABSTRACT

This thesis describes methods and hardware for piezo electromechanical impedance measurement. PZT transducers are widely used in structural health monitoring applications. Piezo effect turns alternating current into mechanical waves. These waves in specific frequency range can be used for host structure health monitoring. The host structure could be a bridge, an airplane wing or a blade of a wind turbine. Methods like pitch-catch or pitch echo are commonly known and widely used in monitoring applications. In one simple example, electromechanical impedance (EMI) can be used to evaluate bond quality between PZT and host structure. Additionally to this, EMI can be used to detect the host structure and PZT transducer structural defects. In this thesis, the host structure delamination and PZT structural defects are experimentally studied

In lab conditions, EMI is usually measured using commercial impedance analyzers. These are very expensive and bulky pieces of hardware. The use of this kind of devices on the site would be very complicated. In order to measure EMI in real SHM applications, the measurement system should be small, light and have low energy consumption. In this thesis, two embedded low-power, low-cost hardware solutions are proposed.

One of the most important parameters in SHM is the measurement time. Impedance spectrum is measured in specific frequency range, by measuring determined frequency points one-by-one. This is a very time-consuming but simple method, but often in real SHM applications measurement conditions change less than in seconds. These changes could be caused by alternating loading, temperature or other parameters. To avoid inaccurate measurement caused by fast changing conditions, measurement time should be as short as possible. Use of wide band excitation signal may shorten EMI measurement time. In this study, short wide-band excitation signals are studied and tested. Two impedance calculations methods are proposed and the results demonstrated.

In the first chapter, the motivation and goals of this thesis are described. Shortly, an overview of SHM and sensorics is given. Different structural health monitoring methods like passive and active acoustic methods are described.

In the second chapter, previous publications most relevant to this thesis are described. Previous methods are explained and compared to the approach used in this thesis.

In the third section, experimental hardware setup for PZT EMI measurement is described. This setup is prepared to simulate the actual working conditions of a PZT transducer together with a host structure. In this setup, experimental measurements are conducted.

In the fourth section, different methods for impedance measurement are described. Different excitation signals and impedance calculations methods are analyzed. Two impedance calculation methods are proposed. These methods are described in detail and the experimental measurement results are demonstrated.

In the fifth chapter, different hardware solutions for impedance measurement and calculation are described. Two new hardware solutions are proposed. These solutions are described in detail and the measurement results are demonstrated. Impedance plots are compared against the commercial impedance analyzer from Wayne Kerr.

In the sixth chapter, two specific applications in SHM are studied. In the first case, a structure with delamination defect is studied using EMI methods. The goal of this study is to find an indicator of delamination using PZT EMI spectroscopy. In the second case, the structural integrity of a PZT transducer is monitored. Based on the PZT EMI spectrum plot, indicators of structural defects are extracted.

In the seventh chapter, an overview of publications related to this thesis is given. Overall three journal articles, three conference publications and one invention specification are listed. Each publication is described in detail and the parts provided by author of this thesis are described.

In the final chapter, the results of this thesis are described. The proposed methods and solutions are summarized. In addition to this, a potential list of future research activities is described.

# KOKKUVÕTE

Käesolev väitekiri kirjeldab meetodeid ja lahendusi piesotäituri/tajuri elektromehaanilise impedantsi mõõtmiseks. Piesotäiturid ja -tajurid on laialt levinud struktuuride konditsiooni monitooringu rakendustes. Piesoefekt muundab elektrilised võnked mehaanilisteks ja vastupidi. Neid laineid saab kindlatel sagedustel kasutada erinevate struktuuride seisundi monitoorimiseks. Vaatluse all olevaks struktuuriks võib olla näiteks lennuki tiib, silla kandevkonstruktsioon või tuuleturbiini laba. Lihtsaima näitena võib pieso-elektromehaanilist impedantsi kasutada tajurite/täiturite diagnostikaks. Lisaks sellele saab impedantsi kasutada ka struktuuride endi diagnostikaks. Selles töös kirjeldatakse kahte näidisjuhtumit impedantsi kasutusvõimalustest. Esimesel juhul kirjeldatakse komposiitstruktuuri delaminatsiooni tuvastamist, teisel juhul täituri diagnostikat.

Laboritingimustes mõõdetakse elektromehaanilist impedantsi tööstuslike impedantsanalüsaatorite abil. Need seadmed on äärmiselt kallid ja mõeldud statsionaarseteks mõõtmisteks. Reaalsetes tingimustes mõõtmiseks peab kasutatav mõõtesüsteem olema piisavalt väike, odav ja väikese energiatarbega. Selles töös pakutakse välja lahendusi, mis vastavad nendele tingimustele.

Üks peamisi parameetreid konditsiooni monitooringu juures on mõõteaeg. Traditsiooniliselt mõõdetakse impedantsi kindlas sagedusvahemikus sageduspunkti haaval. Selline mõõteviis on väga ajakulukas, kuid lihtsalt teostatav. Paraku on reaalsetes oludes vajalik mõõteaeg alla sekundi. Muutuvad keskkonna parameetrid nagu koormus, temperatuur jne võivad muuta mõõtetulemust. Selle vältimiseks peab mõõteaeg olema võimalikult lühike. Laiaribaliste ergutussignaalide kasutamine võimaldab teostada impedantsi mõõtmisi oluliselt lühema ajaga. Antud töös uuritakse ning testitakse lühikesi ja laiaribalisi ergutussignaale. Sellistel ergutussignaalidel baseeruvad ka kaks esitatud mõõtemeetodit.

Esimeses peatükis kirjeldatakse töö eesmärke. Kirjeldatud on lühiülevaade olemasolevatest mõõtemeetoditest, nagu näiteks passiivne ja aktiivne akustiline meetod.

Teises peatükis kirjeldatakse eelnevaid töid samas valdkonnas. Ülevaade kirjeldab teiste autorite töid ja võrdleb neid antud töös pakutud lahendustega.

Kolmandas peatükis kirjeldatakse eksperimentaalset riistvara, mida kasutati piesoimpedantsi mõõtmiseks. Antud riistvara koosneb mõõteosast ja mõõdetavast piesotäiturist koos tugistruktuuriga. Selles seadmes on teostatud eksperimentaalsed mõõtmised simuleerimaks reaalseid rakendustingimusi.

Neljandas peatükis kirjeldatakse piesoimpedantsi mõõtmiseks ja arvutamiseks võimalikke meetodeid. Lisaks kirjeldatakse erinevaid ergutussignaale. Pakutakse välja kaks uut mõõtemeetodit. Detailselt kirjeldatakse nende sisu ja lisaks demonstreeritakse eksperimentaalseid mõõtetulemusi.

Viiendas peatükis kirjeldatakse impedantsi mõõtmiseks vajalikku riistvaralisi lahendusi. Esitletakse kahte riistvaralist mõõtelahendust. Lahendusi on

detailselt kirjeldatud ning lisaks on teostatud eksperimentaalsed mõõtmised. Mõõtetulemusi on võrreldud tööstusliku impedantsanalüsaatoriga.

Kuuendas peatükis kirjeldatakse kahte konkreetset rakendust. Esimesel juhul kasutatakse piesoimpedantsi komposiitmaterjalis delaminatsiooni defekti tuvastamiseks. Teisel juhul kirjeldatakse piesotäituri diagnostikat impedantsi abil.

Seitsmes peatükk annab ülevaate publikatsioonidest. Igast publikatsioonist antakse sisuline ülevaade. Kokku on loetletud 3 ajakirja, 3 konverentsi artiklit ja ühte patendikirjeldust kahes riigis.

Viimases peatükis võetakse kokku pakutud lahendused ja saavutused. Lisaks loetletakse võimalike tulevaste tegevuste nimekiri.

# APPENDICES

## Appendix I

O. Märtens, T. Saar and M. Reidla, “Study of Various Excitation and Reference Signals for Pulsed Correlation-based Ultrasound Signal Processing,” Electronics and Electrical Engineering, Vol. 105, No. 9, pp. 89–92, 2010.

*ELECTRONICS AND ELECTRICAL ENGINEERING*
*ISSN 1392 – 1215* *2010. No. 9(105)*
*ELEKTRONIKA IR ELEKTROTECHNIKA*

*T 121* *SIGNAL TECHNOLOGY*
*SIGNALŲ TECHNOLOGIJA*

# Study of Various Excitation and Reference Signals for Pulsed Correlation-based Ultrasound Signal Processing

**O. Märtens, T. Saar, M. Reidla**
*Tallinn University of Technology, Department of Electronics,*
*Competence Center ELIKO,*
*Ehitajate tee 5, 19086, Tallinn,phone: +372 6 202167, e-mails: olev@elin.ttu.ee*

## Introduction

Ultrasound lamb-waves (generated and received for example, by piezo-transducers -PZTs) can be efficiently used for health monitoring of composite structures (SHM) [1], including (among other applications) monitoring of the wind turbine blades, which is based on changes in wave attenuations, time-frequency analysis, wave reflections and "time of flight" (TOF) information. Pulse-echo and pitch-echo methods are main alternatives of implementation of the pulsed Lamb-waves based diagnostics [2]. Also beam-forming (ultrasonic radar) can be a useful approach [2–5].

Typically excitation signal is 3-5 periods ("burst") of windowed sinewave of ultrasound frequency and received signal is found by cross-correlation processing [1-5] (by convolution or dot-product calculation in digital case, as a function of the time delay) of the received signal, by using of the reference (expected) waveform (generated signal itself, in a most typical case). Further more, reconstruction of the envelope of the received burst from the correlation signal, for example by using of the Hilbert transfer [3,4,5,7] for imaginary part of the correlation function and taking module of the received (real) and calculated imaginary part can give better understanding about the received pulse, being a smooth function with a single peak- while correlation function itself has many local maximums.

In the patent information additionaly to ideas of using of the Hilbert transform for signal envelope generation [7], also a pair of quadrature reference signal has been suggested [6,7] or delaying the input waveform by a peak-to-zero delay (PZD) interval [8], that means by 90 degrees.

For improving of the time resolution or signal-to-noise ratio so called "pulse compression" can be used, by modulating the excitation burst signal in the frequency or phase domain. Probably using of the linear chirp is a simple alternative. Simplification of the used waveforms, eg using of the rectangular (binary) signals instead of sinewaves can allow to relax the requirements to the hardware and software of the embedded structural health monitoring solutions [9].

## Measurement setup

Generation of the excitation waveform ("bursts" of sine-wave or binary pulses), as well as data acquisition and processing has been carried out by PC-based setup. PZTs (of Noliac - www.noliac.dk) – 3 pieces (of which two pieces were used in the described experiments)- are fixed to a glass fiber composite material 500x500x4 mm) by special glue (Fig. 1).

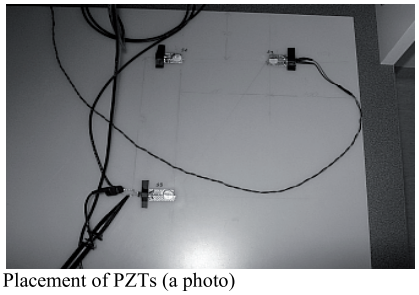

**Fig. 1.** Placement of PZTs (a photo)

For described experiments a following setup has been used. Measurement system is PC-based (with Matlab tools and interfaces) with using of National Instruments' USB-6259, a USB high-speed M-series multifunction data acquisition (DAQ) module optimized for good accuracy at fast sampling. This unit contains multiplexed analog-to-digital converter (ADC) and digital-to-analog converter (DAC), both with maximum 1.25Ms/s speed (actually 1Ms/S was used in described experiments) and 16-bit resolution. A signal conditioning analog front end is containing a power driver with Ku=3 voltage amplification and a voltage divider (1:3) to measure excitation voltage Uexc (to ±30V) is on the PZT1 circuit and a response voltage from another PZT2 (Fig. 2).

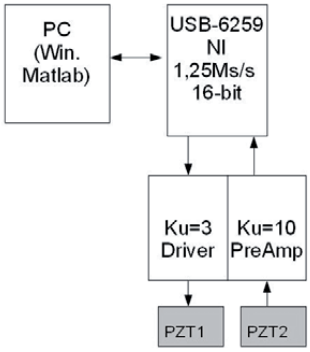


**Fig. 2.** Measurement setup (block diagram)

**Algorithms and measurement results**

In current study a burst of the sine-wave of 5 periods of 200 kHz has been generated. The following cases has been studied:

1) In one case the excitation signal has been windowed by Gaussian windows;
2) In another case no windowing (that means "rectangular window") has been used;
3) In third case a binary sequence instead of sine-wave has been for excitation and instead of fixed frequency a linear chirp (from 180 kHz to 220 kHz) has been used.

In all cases the absolute value of the *cross-correlation* with excitation signal (as expected response) has been found as a function of a time delay (or lag, in other words, in ms units). Furthermore, a *correlation with "quadrature"* version of the excitation (cosine wave, identical to used sine-wave) has been calculated and combined, in one case *as sum of absolute values*, in another case as *sum of squared values of these two ("inphase and quadrature") correlations.* Using of "quadrature correlation" component, calculated from the cosine reference wave is calculation-efficient, compared with using of Hilbert transform in general form (over received input signal, for example).

So, the following experiments has been carried out (with measured and calculated results showed on Fig. 3 till Fig. 17.

*Windowed burst of 5 sine-periods (200kHz).*

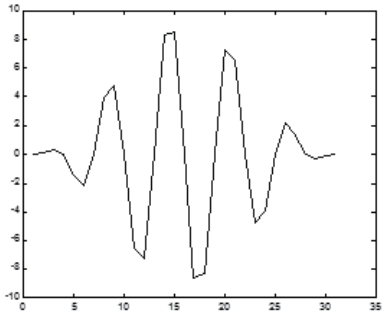

**Fig. 3.** Windowed burst of excitation *(relative amplitud vs indexes of samples)*

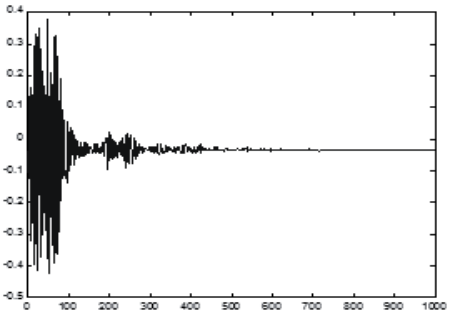

**Fig. 4.** Windowed burst of excitation- response signal *(voltage vs time in ms)*

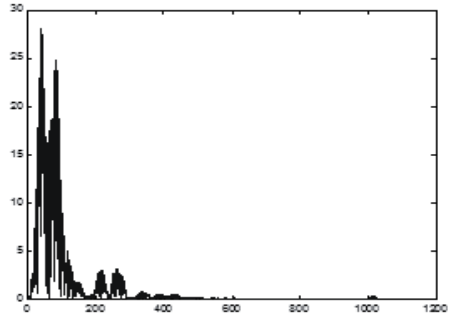

**Fig. 5.** Windowed burst of excitation- cross-correlation (absolute value) with response *signal (accumulated dotproduct vs time in ms)*

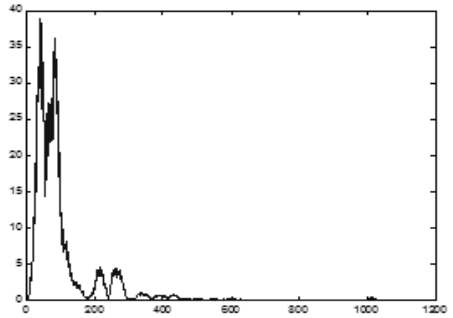

**Fig. 6.** Windowed burst of excitation- sum of cross-correlations (absolute values) with response signal *and its quadrature component*

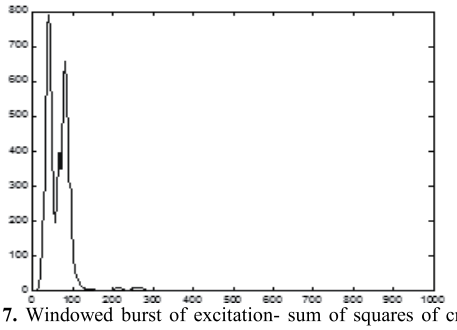

**Fig. 7.** Windowed burst of excitation- sum of squares of cross-correlation with response signal and **its quadrature component** (*time in ms)*

*Burst of 5 binary periods of 200kHz.*

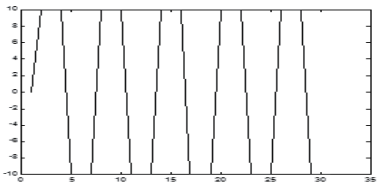

**Fig. 8.** Binary burst of excitation excitation *(relative amplitud vs indexes of samples)*

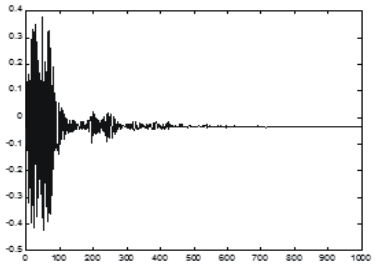

**Fig. 9.** Binary burst of excitation- response signal*(voltage vs time in ms)*

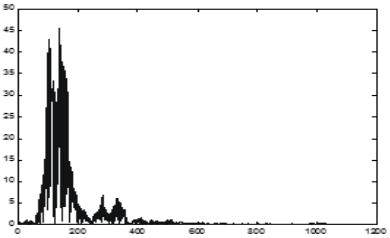

**Fig. 10.** Binary burst of excitation- cross-correlation (absolute value) with response signal *(accumulated dotproduct vs time in ms)*

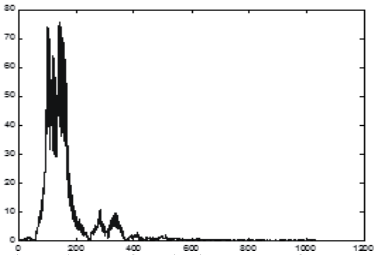

**Fig. 11.** Binary burst of excitation- sum of cross-correlations (absolute values) with response signal *and its quadrature component*

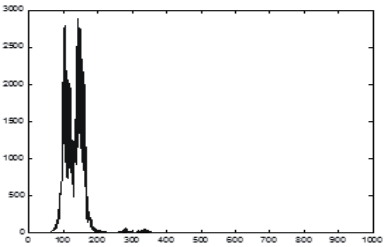

**Fig. 12.** Windowed burst of excitation- *sum of squares* of cross-correlation with response signal and *its quadrature component* (*time in ms)*

*Burst of 5 binary periods of chirp (180-220kHz).*

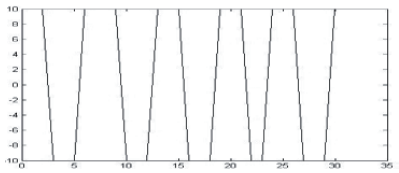

**Fig .13.** Binary burst of excitation (Chirp) *(relative amplitud vs indexes of samples)*

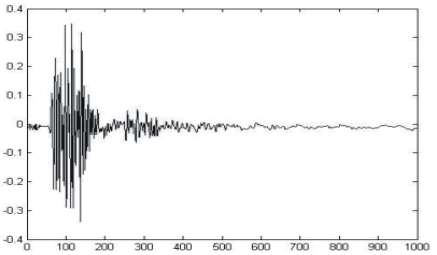

**Fig. 14.** Binary burst of excitation (chirp)- response signal *(voltage vs time in ms)*

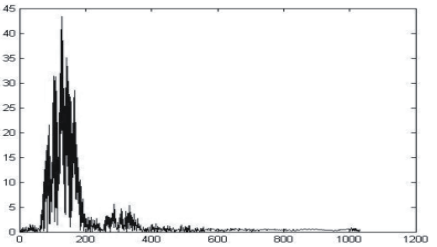

**Fig. 15.** Binary burst of excitation- cross-correlation (absolute value) with response signal *(accumulated dotproduct vs time in ms)*

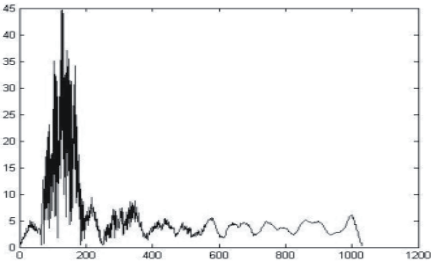

**Fig. 16.** Binary burst of excitation- sum of cross-correlations (absolute values) with response signal *and its quadrature component*

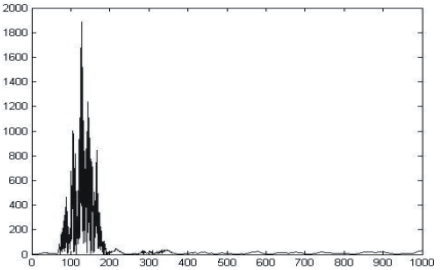

**Fig. 17.** Windowed burst of excitation – *sum of squares* of cross-correlation with response signal *and its quadrature component*

## Conclusions

While using of correlation calculation for finding of time-of-flight and parameters of the received pulse (burst), using of additional "quadrature correlation" component improve the envelope shape and is computationally more efficient, compared with widely used Hilbert transform. Alternatively to summing of in-phase and quadrature correlation components as squared *values a linear sum of absolute values of correlations can much improve the envelope,* with lower cost of algorithm realization complexity and still with good results, *especially for binary signals.* Also experiments show the efficiency of using of binary and chirp signals for excitation and as reference signals for correlation calculation.


## Acknowledgements

Current work has been supported by the EUREKA Eurostars project "Smart Embedded Sensor System (SESS)", Enterprise Estonia (support to Competence Center ELIKO). Special thanks to NOLIAC Ltd and DTU (Risoe site, Denmark), Innowacja Polska and EC Electronics (Poland). This research was also supported by the European Union through the European Regional Development Fund.


## References


1. **Ng C., Veidt M.A.** Lamb–wave–based technique for damage detection in composite laminates // Smart Mater. Struct.– 2009. – Vol. 18. – Iss. 7.
2. **Ostachowicz W., Kudelaa, P., Malinowskia P. and Wandowskia T.** Damage localisation in plate–like structures based on PZT sensors // Mechanical Systems and Signal Processing, 2009. – Vol. 23. – Iss. 6. – P.1805–1829 .
3. **Yu L., Giurgiutiu V.** Advanced signal processing for enhanced damage detection with piezoelectric wafer active sensors // Smart Structures and Systems, 2005. – Vol. 1. – No. 2. – P. 185–215.
4. **Yu L., Giurgiutiu V.** In–situ Optimized PWAS Phased Arrays for Lamb Wave Structural Health Monitoring // Journal of Mechanics of Materials and Structures, 2007. – Vol. 2. – No. 3. – P. 459–487.
5. **Yu L., Bao J., Giurgiutiu, V.** Signal processing techniques for damage detection with piezoelectric wafer active sensors and embedded ultrasonic structural radar // Smart Structures and Materials 2004: Sensors and Smart Structures Technologies for Civil, Mechanical, and Aerospace Systems (edit. Liu S.), proceedings of the SPIE, 2004. – Vol. 5391. – P.492–503.
6. **Vasile C.** Signal processing technique for ultrasonic inspection Inventor. – US Patent 4307616. – Published December 29, 1981.
7. **Seyed–Bolorforosh M., Mo L., Chim S.** Method, apparatus and applications for combining transmit wave functions to obtain synthetic waveform in ultrasonic imaging system. – US Patent 5891038. – Published April 6, 1999.
8. **Fluhler H., Nag S., Barnes M.** Method of envelope detection and image generation. – US Patent 6552677. – Published April 22, 2003.
9. **Sicard R., Goyette J., Zellouf D.** Lamb wave generation with an air–coupled piezoelectric concave array using square–wave burst excitation // NDT & E International, 2008. – Vol. 41. – Iss. 4. – P. 292–299.
10. **Bielskis A. A., Denisovas V., Drungilas D., Gricius G., Dzemydienė D.** Multi-Agent-Based Human Computer Interaction of E-Health Care System for People with Movement Disabilities // Electronics and Electrical Engineering. – Kaunas: Technologija, 2010. – No. 7(103). – P. 77–82.
11. **Vanagas G., Viržonis D., Paukštaitis V., Baranauskas D., Červiakov S.** Integrated Front End Electronics Design for Micromachined Ultrasound Transducers // Electronics and Electrical Engineering. – Kaunas: Technologija, 2010. – No. 7(103). – P. 117–120.



Received 2010 02 18



**O. Märtens, T. Saar, M. Reidla. Study of Various Excitation and Reference Signals for Pulsed Correlation-based Ultrasound Signal Processing // Electronics and Electrical Engineering. – Kaunas: Technologija, 2010. – No. 9(105). – P. 89–92.**

Ultrasound Lamb waves are used for health monitoring of composite structures. Received signals are correlated by windowed bursts of excitation signal to find time-of-flight and parameters of the received waveforms. In current paper modifications of excitations signals and reference signals are studied, emulations with using a PC-based measurement experimental setup with a composite plate and piezo-sensors are carried out. The study shows the ways of improvement of correlation-based signal processing accuracy, for finding the signal envelopes more precisely, from one side, and possible simplifications of the signal waveforms and signal processing from other side, to make the solutions more practical for implementations. Ill. 17, bibl. 11 (in English; abstracts in English and Lithuanian).

**O. Märtens, T. Saar, M. Reidla. Ultragarsinių signalų apdorojimas taikant impulsinę koreliaciją įvairaus žadinimo ir šaltinių signalams // Elektronika ir elektrotechnika. – Kaunas: Technologija, 2010. – Nr. 9(105). – P. 89–92.**

Sveikatos stebėsenai sudėtinėse sistemose taikomos ultragarsinės Lamb'o bangos. Gautieji signalai koreliuoja su žadinimo signalais. Apžvelgiami žadinimo ir pirminiai šaltinių signalai. Atlikti eksperimentiniai matavimai su kompozicine plokštele ir pjezojutikliais. Iš gautų rezultatų matyti koreliacijos sąlygotų signalų tikslumo didinimo bei signalų apdorojimo supaprastinimo būdai. Il. 17, bibl. 11 (anglų kalba; santraukos anglų ir lietuvių k.).

## Appendix II

O. Märtens and T. Saar, “Fast Impedance Spectroscopy of Piezosensors for Structural Health Monitoring,” Electronics and Electrical Engineering, Vol. 103, No. 7, pp. 31–34, 2010.

*ELECTRONICS AND ELECTRICAL ENGINEERING*
*ISSN 1392 – 1215* *2010. No. 7(103)*
*ELEKTRONIKA IR ELEKTROTECHNIKA*

*T 121* *SIGNAL TECHNOLOGY*
*SIGNALŲ TECHNOLOGIJA*

# Fast Impedance Spectroscopy of Piezosensors for Structural Health Monitoring

**O. Märtens, T. Saar, M. Min, R. Land, M. Reidla**
*Tallinn University of Technology, Department of Electronics,*
*Competence Center ELIKO, Ehitajate tee 5, 19086, Tallinn, e-mail: olev@elin.ttu.ee*

## Introduction

Electromechanical impedance measurement by electro-impedance spectroscopy (EIS) of piezoelectric transducers (based on lead zirconate titanate, PZT) is widely used in health monitoring of composite structures, primarily for near-sensor monitoring of the structure and for checking quality of sensors and bonding of sensors to the surface of the material. Reasonable frequency range for testing of structures and sensors is often determined by experimental results. In the impedance-based method, multiple frequency ranges with multiple peaks could be used. A frequency range higher than 200 kHz is found to be favorable for local sensing, while frequencies lower than 70 kHz cover larger sensing areas. Typically the frequency range of 30 kHz to up to 400 kHz is used. For higher frequencies, the wavelength of the excitation is small, and sensitive enough to detect small changes in the structures. For higher frequencies the sensing region of the PZT is limited to an area near to the PZT sensor/actuator. Typically the real part of electric impedance is more reactive to damage or changes in the structure's integrity than the imaginary part. Temperature changes, among all other ambient conditions, significantly affect the electric impedance signatures measured by a PZT [1].

Paper [2] summarizes the description of the modified electromechanical impedance model, for parametric studies for impedance-based sensor diagnostics. Paper [3] describes, how a PZT patch is surface bonded to the structure to be monitored and its corresponding electro-mechanical admittance signature is used for damage detection. Among other features and defects cracks and even multiple cracks in the material under test can be found by impedance measurements [4].

By measuring electrical impedance over certain frequency range one can make conclusions about quality of the bond. If bond between piezoelectric device and material is week then sharp resonance peaks can be seen on impedance-frequency plot. But if bond is strong then impedance curve is much smoother, peaks of resonance frequencies are lower and sometimes resonance frequencies are even shifted along frequency axis. [1, 5]

Electrical admittance Y(ω) (inverse function of the electrical impedance) of the piezoelectric transducer (PZT) is a combined function of the mechanical impedance of the PZT actuator $Z_a(\omega)$ and that of the host structure Z(ω) [6]:

$$Y(\omega) = i \cdot \omega \cdot a \left( \bar{\varepsilon}_{33}^{\ T} - \frac{Z(\omega)}{Z(\omega) + Z_a(\omega)} d_{3x}^2 \hat{Y}_{xx}^{\ E} \right). \quad (1)$$

For carrying out measurements in the research phase commercial impedance analyzer instruments (like HP4194A) could be used. Alternative is to use special impedance measurement chip-based solutions (like AD5933-1 MSPS, 12 Bit impedance converter network analyzer) [7]. Unfortunately such chips are limited by accuracy (resolution) or frequency range and can measure one frequency at a time, making the impedance measurements slow and so fast changes could not be monitored.

Also a good solution is to make special (preferably wireless) embedded measurement nodes, like [8] with dedicated analog front-end and digital signal processor (DSP).

## Measurement setup

For described experiments a following setup has been used. Measurement system is PC-based (with Matlab tools and interfaces), using of National Instruments' USB-6259, a USB high-speed M Series multifunction data acquisition (DAQ) module optimized for accuracy at fast sampling. This unit contains multiplexed analog-to-digital converter (ADC) and digital-to-analog converter (DAC), with 1,25Ms/S speed and 16-bit resolution. A signal conditioning analog front end is containing a power driver with Ku=3 voltage amplification and a voltage divider (1:3) to measure excitation voltage Uexc (to ±30V) is on the PZT circuit and shunt resistor R=70Ω for current sensing in a PZT (Iz signal) (Fig. 1). Generation of various waveforms (sine-waves and their combinations) and also data acquisition and processing, is carried out by the PC

software, according to the selected algorithms. PZTs (of Noliac - www.noliac.dk) – 3 pieces- are fixed to a glass fiber composite material 500x500x4 mm) by special glue (Fig. 2), plus fourth PZT sensor has been measured in the air.

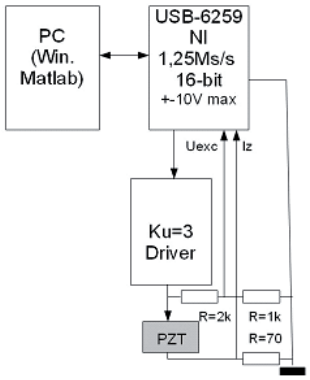


**Fig. 1.** Measurement setup (block diagram)

**Fig. 2.** Measurement setup

## General approach to tried algorithms

General idea of the algorithms is generation of sinewave(s), one frequency at a time (discrete scanning or linear chirp) or simultanous multi-frequency voltage for excitation and measurement of the voltage drop of the current on the shunt resistor and then calculation of the complex impedance by Discrete Fourier Transform (DFT), taking into account the transfer coefficients of the measurement setup and subtracting the shunt resistor real value of the total complex impedance of the measured circuit, for PZT complex impedance. In some case DFT is reasonable to implement as Fast Fourier Transform (FFT). In current setup for reference (excitation) value one analog measurement channel is used, to get synchronous samples for excitation(Uexc) and current channels (Iz).

Voltage range of ±10V of ADC and DAC has been used, to ±30 V excitation (peak-to-peak). Actually amplitudes of about 30% of the full scale has been used. Sample rate has been 1.25 Ms/s for DAC and 500 kS/s for each ADC channel in current experiments. As used USB-6259 has multiplexed input with one ADC, the (phase shift between two "synchronous" ADC channels, corresponding to half of the ADC sampling period time delay has been corrected for current frequencies. Frequency range has been about from 10-300 kHz (or more) with frequency step (and resolution) of 5 kHz. The results of the PZT (labeled as "S3") measurements are presented and described below. For reference, the impedance of PZT sensors has been measured by commercial Precision Impedance Analyzer 6500B of Wayne Kerr- look to Fig 3, a) -PZT "S3" and for comparison PZT in the air (PZT Sx) –b). Here and on next figures- highest line shows the module of the impedance, next line- real part and lowest part -the imaginary part of the measured complex impedance.

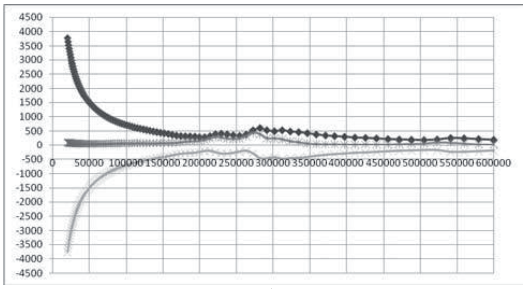

a)

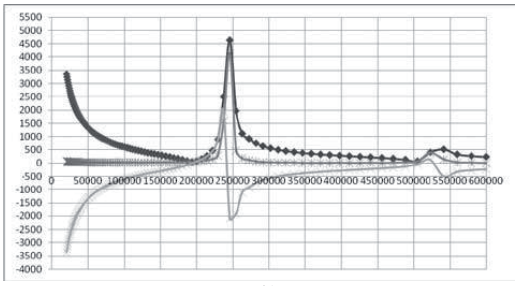

b)

**Fig. 3.** Bonded (S3): a – vs. free(Sx); b – PZT impedance

## Algorithms and measurement results

The following excitation signals and processing algorithms were tried:

*1) Frequency scanning* (one frequency at a time, 0,5s measurement per frequency, complex DFT realized as convolution or dot-product by reference (excitation frequency) sine- and cosine-waves (Fig. 4).

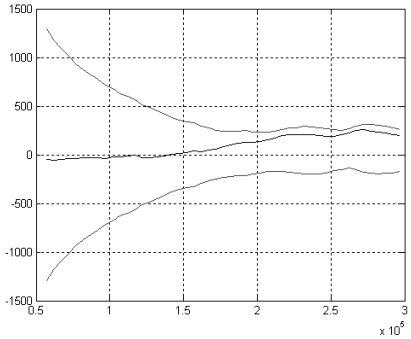

**Fig. 4.** PZT (S3) impedance for frequency scanning method

*2) Multi-frequency:* simultaneous multi-frequency excitation and DFT calculation (Fig. 5 a). Frequency values were shifted by 2 kHz from the 5 kHz grid, to have more realistic results (Fig. 5 b).

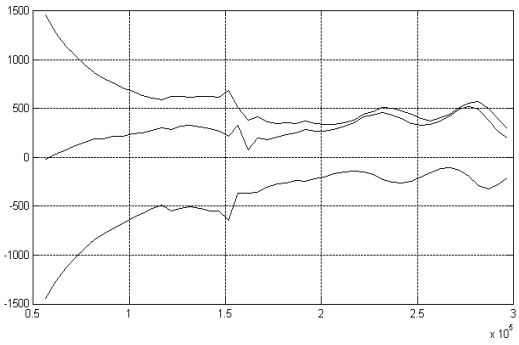


a)

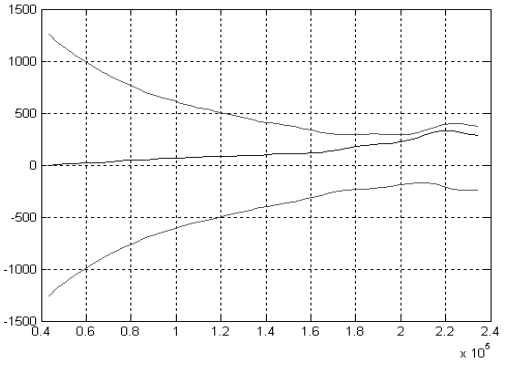


b)

**Fig. 5.** PZT (S3) impedance of simultaneous multi-frequency method (a) measured by using of 5 kHz frequency grid, in (b) the used frequencies has been shifted by 2 kHz.from the 5 kHz grid

*3) Multi-frequency excitation with FFT analysis.* Initially here the idea was to use a regular (linear) FFT frequency grid for excitation and analysis frequencies. The results had clear artifacts, probably simultaneous ultrasound waves of integer frequency ratios cause interactions and disturbances to each other. The method was modified-resolution of FFT has been 4 times increased (so to 1.25 kHz) and used excitation (and analysis) frequencies have been shifted by this 1.25 kHz discrete value ( ¼ of initial grid resolution value), giving quite reasonable results (Fig. 6). In spite of using 4 times "oversampling" of FFT this method is still computationally very efficient, compared with all other methods. Furthermore, the averaging of FFT results over sequence (as FFT is a linear transform) of time windows (frames) can be turned into accumulating of the received sequential time-buffer segments into one accumulated buffer of ("4x") FFT-size and then performing FFT only once.

*4) Chirp signal:* for chirp signal the frequency changes linearly over time period T. It can be expressed as

$$V(t) = \sin(2\pi(f_1 t + \frac{(f_2 - f_1)t^2}{2T}). \qquad (2)$$

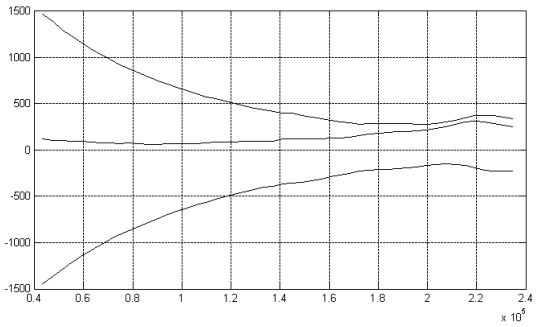


**Fig. 6.** PZT (S3) impedance obtained by the □ido f simultaneous multi-frequency method, by using 4x FFT and ¼ shift of frequency values

In general terms, ignoring specific applications and practical aspects the chirp signal clearly offers optimal features for use in dynamic process [9]. Excitation signal with frequency range 20kHz-600kHz has been generated. Pulse width from 0,8 -80 ms was tested. Longer pulse width resulted more accurate impedance plot. Figure 7 shows 80 ms chirp pulse result. In current example the impedance is calculated by using of FFTs of excitation voltage and current signals.

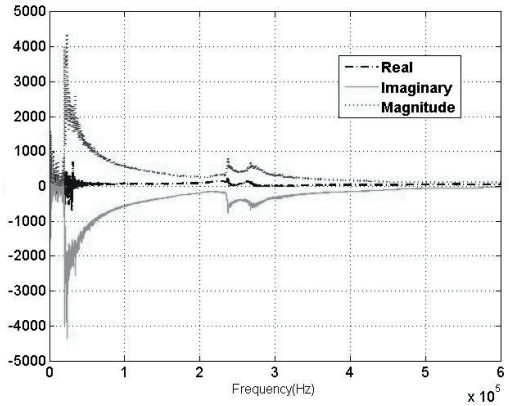


**Fig. 7.** PZT (S3) impedance obtained by the aid of a chirp (80ms) signal

Also works [10–12] offer interesting approaches for using of chirp signals for spectral impedance measurements, and can be further investigated. Trying of "signum chirp" signals to simplify the solution did not give good results in these experiments.

## Conclusions

Using of multi-frequency and chirp signals shows a great potential in using of EIS in piezo-sensor based embedded SHM solutions by making the solutions cheaper and more easily operating in real-time.

## Acknowledgements

Current work has been supported by the EUREKA

Eurostars project “Smart Embedded Sensor System (SESS)”, Enterprise Estonia (support to Competence Center ELIKO). Special thanks to NOLIAC Ltd and DTU (Risoe site, Denmark), Innowacja Polska and EC Electronics (Poland). This research was also supported by the European Union through the European Regional Development Fund.

## References

1. **Park G., Sohn H., Farrar C., Inman D.** Overview of piezoelectric impedance–based health monitoring and path forward // The Shock and Vibration Digest, 2003. – No 35(6). – P. 451–463.
2. **Park S., Park G., Yun C.–B., Farrar C.** Sensor Self–diagnosis Using a Modified Impedance Model for Active Sensing–based Structural Health Monitoring // Structural Health Monitoring 2009. – No 8. Doi:10.1177/1475921708094792.
3. **Lim Y. Y., Bhalla S., Soh C. K.** Structural identification and damage diagnosis using self–sensing piezo–impedance transducers // Smart Mater. Struct., 2006. – No 15 – P. 987–995.
4. **Park S., Ahmad S., Yun C.–B. and Roh Y.** Multiple Crack Detection of Concrete Structures Using Impedance–based Structural Health Monitoring Techniques // Experimental Mechanics, 2006. – No 46. – P. 609–618.
5. **Bhalla S., Soh C.K.** Calibration of piezo impedance transducers for strength prediction and damage assessment of concrete // Institute of physics publishing. – Smart Mater. Struct. – 2005. – No. 14. – P. 671–684.
6. **Liang, C., Sun, F.P. and Rogers, C.A**. Coupled Electro–Mechanical Analysis of Adaptive Material Systems–Determination of the Actuator Power Consumption and System Energy Transfer // Journal of Intelligent Material Systems and Structures, 1994. – No. 1. – Vol. 5. – P. 12–20.
7. **Pitchford C.W.** Impedance–Based Structural Health Monitoring of Wind Turbine Blade (Msc Thesis). – Virginia Polytechnic Institute, 2007. – 120 p.
8. **Mascarenas D., Todd M, Park G., Farrar C**. Development of an impedance–based wireless sensor node for structural health monitoring // Smart Mater. Struct. – 2007. – No. 16. – P. 2137–2145.
9. **Nahvi M., Hoyle B. S.** Electrical Impedance Spectroscopy Sensing for Industrial Processes // Sensors Journal, IEEE 2009. – No. 12. – P. 1808–1816.
10. **Paavle T., Min M., Annus P., Birjukov A., Land R., Parve T.** Wideband Object Identification with Rectangular Wave Chirp Excitation // Proc. of European Conference on Circuit Theory and Design. – Antalya, Turkey. – 2009. – P. 421–424.
11. **Darowicki K., Slepski P.** Influence of the analyzing window on electrode impedance measurement by the continuous frequency scanning method // Journal of Electroanalytical Chemistry. – Elsevier. – 2002. – No. 533. – P. 25–31.
12. **Slepski P., Darowicki K.** Optimization of impedance measurements using ‘chirp’ type perturbation signal // Measurement. – Elsevier, 2009. – Vol. 42. – No. 8. – P. 1220 –1225.

Received 2010 03 09

**O. Märtens, T. Saar, M. Min, R. Land, M. Reidla. Fast Impedance Spectroscopy of Piezosensors for Structural Health Monitoring // Electronics and Electrical Engineering. – Kaunas: Technologija, 2010. – No. 7(103). – P. 31–34.**

Electroimpedance spectroscopy (EIS) of piezoelectric transducers (PZT) is used in structural health monitoring (SHM) of composites and for checking quality of PZT and bondings. Measurements have to be precise, as small changes in real or imaginary parts of the impedance can indicate early changes in the structure or in the sensor. EIS methods, by one frequency at a time, are time and energy consuming, limiting such approach for embedded systems. Alternative faster methods of EIS are suggested here and tested in an PC-based experimental setup, with a composite plate and PZTs. Usage of simultaneous multi-frequency or wide-band excitation signals like chirps have been studied and compared. Ill. 7, bibl. 12 (in English; abstracts in English, Russian and Lithuanian).

**О. Мяртенс, Т. Саар, М. Мин, Р. Ланд, М. Рейдла. Быстрая спектроскопия импеданса пьезоэлектрических сенсоров для структурного мониторинга здоровья // Электроника и электротехника. – Каунас: Технология, 2010. – № 7(103). – С. 31–34.**

Элекроимпедансная спектроскопия (ЭИС) пьезоэлектрических сенсоров используется для мониторинга структурального здоровья композитных материалов, сенсоров и их крепления. Измерения должны быть прецизионными, так как малые изменения комплексного импеданса могут предсказать ранние изменения структуры или сенсора. Методы ЭИС, при которых измерения проводятся по одной частоте одновременно, требуют много времени и энергии, ограничивая таким образом их применение в строенных системах. Альтернативные быстрые методы ЭИС предложены и испытаны здесь. Рассмотрены методы с использованием многочастотного (мультисинус) или широкополосного (например „чирп“) сигнала возбуждения. Ил. 7, библ. 12 (на английском языке; рефераты на английском, русском и литовском яз.).

**O. Märtens, T. Saar, M. Min, R. Land, M. Reidla. Sveikatos struktūrinės stebėsenos pjezoelektrinių jutiklių apkrovos analizė // Elektronika ir elektrotechnika. – Kaunas: Technologija, 2010. – Nr. 7(103). – P. 31–34.**

Šiandieninei sveikatos stebėsenai turi būti naudojamos labai didelio tikslumo medžiagos ir įvairūs jutikliai. Šiuo atveju tikslinga naudoti pjezojutiklius. Išnagrinėti daugiadažniai ir plačiajuosčiai signalų atvaizdavimo metodai ir pasiūlyti originalūs pjezojutikliai, kurie gerokai sumažina sveikatos tyrimų trukmę ir leidžia optimizuoti sistemų struktūrą. Il. 7, bibl. 12 (anglų kalba; santraukos anglų, rusų ir lietuvių k.).

## Appendix III

T. Saar, O. Martens, M. Reidla and A. Ronk, “Chirp-based impedance spectroscopy of piezo-sensors,” in *Proceedings of the 12th Biennial Baltic Electronics Conference (BEC), 2010, 12th Biennial Baltic*, 2010, pp. 339–342.

2010 12th Biennial Baltic Electronics Conference (BEC2010)
Tallinn, Estonia, October 4-6, 2010

# Chirp-based impedance spectroscopy of piezo-sensors

T. Saar[1,2], O. Märtens[1,2], M. Reidla[1,2] , A. Ronk[1]

[1]*Department of Electronics, TUT, Ehitajate tee 5, 19086 Tallinn, Estonia, E-mail: olev@elin.ttu.ee*
[2]*Competence Centre ELIKO, Teaduspargi 6/2, Tallinn, 12618, Estonia*

**ABSTRACT: Impedance spectroscopy is widely used in various test&measurement fields and applications. In current paper a novel approach of excitation with chirp signal with simple time-domain analysis of response signal for such task is introduced and described with examples of measurement of the electro-mechanical impedance of piezo-sensors, in the frequency range of several hundred kiloherz. In one approach smoothed separately (by Savitzky-Golay filter) of excitation voltage and (current) response signals in a sliding window are found and their ratio is used for impedance module estimation, at corresponding time and frequency values. Alternative method for vector measurement of impedance spectra in time domain has also tested.**

## 1 Introduction

Impedance spectroscopy is an efficient method for health monitoring of human beings [1]. In work [2] a "signum chirp" excitation signal has been used to measure complex spectrum of impedance of biological objects in a wide range of frequencies. In this work complex FFT -and correlation-function based analysis for getting impedance has been proposed, needing significant computational effort.

Multi-frequency eddy current (induction-type) conductivity measurement of objects under test by using of complex impedance values of measurement coil(s) are also relevant for medical applications [3], as well as for testing and measuring and validation of metallic materials and constructions [4].

Impedance spectroscopy is also an efficient method for monitoring health of electrochemical objects, like batteries [5, 6]. In paper [6], a (sine-wave) chirp signal has been proposed for excitation signal, as an efficient multi-frequency signal, with following (quite sophisticated) short-time Fourier' (STFT) analysis in a sliding window.

Electromechanical impedance measurements of piezo-sensors can give relevant information for structural health monitoring of mechanical structures, for example of composite materials [7, 8].

In current paper impedance spectroscopy of piezo-sensors for structural health monitoring applications has been studied, with using of chirp excitation signal in combination with proposed novel simple time-domain analysis (without using of complex spectral analysis like FFT) is described and evaluated.

## 2 Previous work

Impedance of piezoelectric transducers (based on lead zirconate titanate, PZT) can be measured using different methods. Traditionally impedance is calculated by dividing voltage on PZT with current passing it on wide range of frequencies. Unfortunately this method has high measurement time and resource requirements. By using wide-band excitation signals, impedance can be measured by only one sweep. Fast Fourier Transform (FFT) is usually being used to transform recorded signal from time domain to frequency domain.

Work [9] describes usage of the pulsed excitation for a wideband signal and Fourier analysis (FFT) for analysis of the signal, for piezo-impedance measurements, as way to cost-efficient solution.

Work [10] describes using of piezo impedance for concrete strength prediction and damage assessment. Frequency range used was between 0-1000 KHz. A new impedance based NDE (non-destructive evaluation) for concrete has been proposed.

Work [11] has claimed, that impedance method is very sensitive to incipient damage in structure and is unaffected by changes in boundary conditions, loading and operational vibrations. It also claims piezo-impedance method is suitable for autonomous continuous systems.

Previous work [12] has also shown great potential for wide band excitation signals for impedance measurements in a wider frequency range, including for measurement of PZT sensors.

## 3 Experimental setup

Experimental test-site consisted of a PC-based (with MATLAB tools) work-place, with NI-6259 USB data

978-1-4244-7359-5/10/$26.00 ©2010 IEEE

acqusition box (16-bit max 1,25 Ms/s), with own-made analog front-end to piezo-sensors [12], 3 PZT piezosnsors (all produced by Noliac) fixed to a 80x80x4 mm glass-fibre composite plate and one sensor in the air.

## 4 Method for impedance module estimation

To save measurement time and hardware resources chirp signal was used for PZT excitation. Chirp signal changes it's frequency linearly over time period T. It can be expressed as

$$V(t) = \sin(2\pi(f_1 t + \frac{(f_2 - f_1)t^2}{2T})$$

Chirp signal used, had frequency range 20kHz-600kHz and was 80 ms long. Voltage was measured on point Vm. Current passing PZT was calculated by measuring voltage on resistor Zp and dividing it with resistance Zp (68Ω) value.

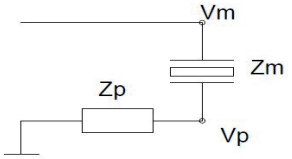


Figure 1. Measurement scheme

Both voltages Vp and Vm are noisy. For current and voltage magnitude smoothing Savitzky-Golay filter has been used. Smoothing filter was 2-nd polynomial order and frame size was 250. Savitzky-Golay filter is for wide band signal filtering, because of ability to retain signal maximum values. Regular FIR filter would smooth out all sharp resonant frequency values from signal.

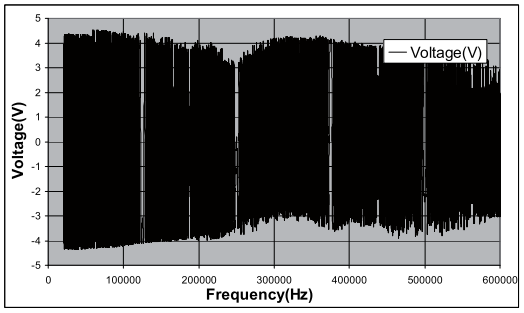


Figure 2. Measured voltage

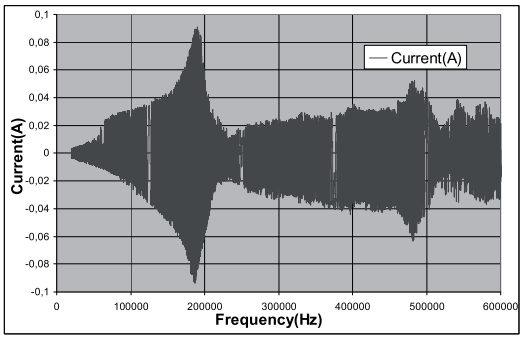


Figure 3. Calculated current

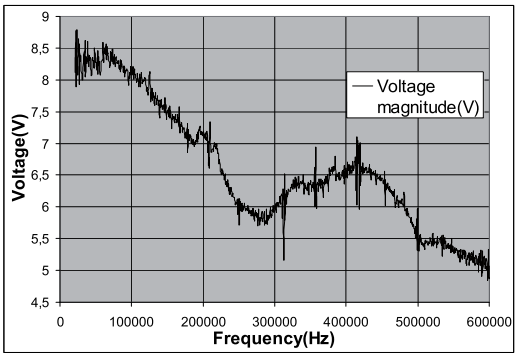


Figure 4. Calculated voltage magnitude

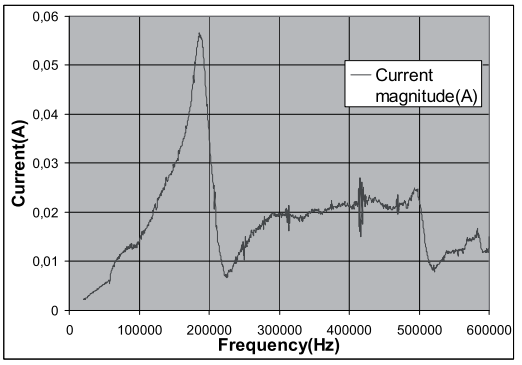


Figure 5. Calculated current magnitude

**a)Impedance magnitude measurement**

Impedance magnitude was calculated by dividing voltage magnitude with current magnitude. To asses (estimate) results accuracy, it was compared against measurements made by commercial impedance analyzer type 6500B of Wayne Kerr. Figure 6 shows both results on same plot. Chirp impedance result has much lower resonance frequencies magnitudes. Also resonance frequencies have been shifted to lower. Overall impedance magnitude shape is very similar to one made with impedance analyzer. Although impedance magnitudes are not

identical it clearly shows that chirp impedance measurement could be used for evalution of the objects under test. Differences could be explained by different excitation signal amplitude or different measurement technique as impedance analyzer measures impedance on discrete frequencies one by one.

Because voltage magnitude changes very little while measuring different PZT's, it could be used as constant vector. Based on this impedance magnitude can be calculated by only measuring current passing PZT. This lowers hardware requirements and cost of measurement system.

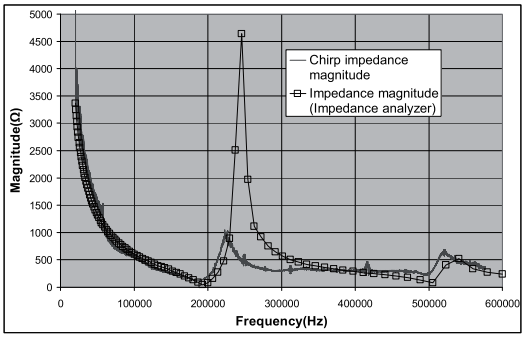


Figure 6. Calculated vs. measured impedance magnitude

**b)Bond quality indicators**

Impedance magnitude can indicate PZT and host structure bond quality. If bond between piezoelectric device and material is week then sharp resonance peaks can be seen on impedance-frequency plot. But if bond is strong then impedance curve much smoother, peaks of resonance frequencies are lower and sometimes resonance frequencies are even shifted along frequency axis. [10][11].

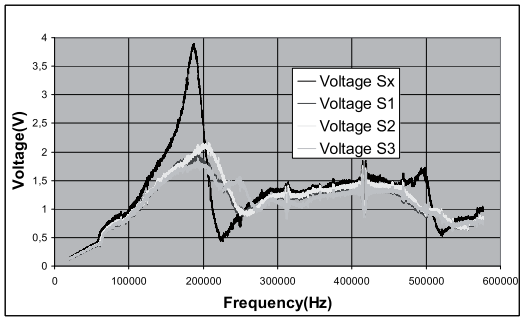


Figure 7. Resistor voltage magnitude of 3 bonded and 1 unbonded PZT

## 5 Method for impedance vector estimation

Alternative novel method for impedance spectroscopy, to get both real and imaginary part estimations of the impedance under interest, has been proposed. Possible realization of this idea has been shown on fig 8. Solution includes a generator of the (sine-based) chirp signal (1) for excitation and also as a first reference signal, second ("quadrature") reference signal (2) is generated as a cosine-based chirp signal with same (synchronous) parameters. Excitation signal is feed through DAC (3) to device under test (4), and response (current sense) signal is acquired through ADC (5) as a response signal waveform (6) buffer, which is further correlated in a sliding (eg Gaussian) window (7) (actually found convolution by "multiply and accumulate" operations ("MAC"-units 8 and 9) in the digital domain) to said first and second reference signals to get real and imaginary components of the measured (acquired) signal, in time domain (which is also, due to known chirp parameters) also result in the frequency domain.

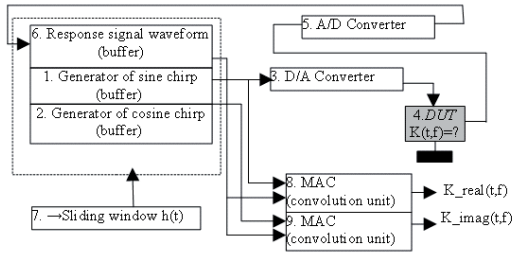


Figure 8. Proposed alternative method for vector measurement

In practical realization, by some practical reasons, two (quadrature) reference signals has been replaced by only one (sine-based) signal, which is measured also back (synchronously with response signal channel of ADC) by another channel of the ADC of data acquisition, and to get "cosine" (quadrature") result component second "imaginary" response signal waveform is generated from original ("real") signal waveform by Hilbert Transform (in Matlab). A linear chirp 5-300 kHz has been used with duration of 1 second and sampling frequency of DAC was 1,25 Ms/s and of ADC 2x 625 kHz. The length of Gaussian window for convolution was N=200 sample points and step of the correlation analysis was N2=100. The analysis results for one PZT sensor (in non-normalized units) are given on fig 9 (curves of module, real and imaginary part form up to down, in the frequency domain), showing quite reasonable impedance spectra, comparable to which was got with other methods [12].

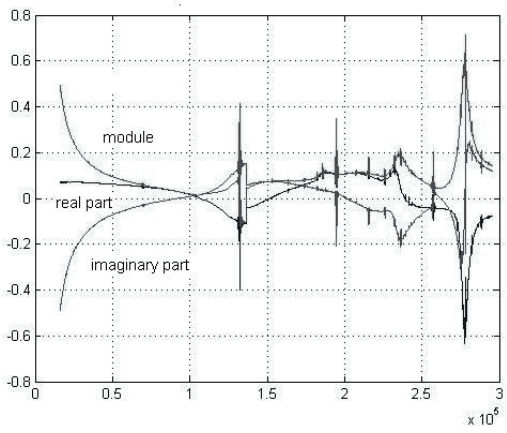


Figure 9. Measured complex impedance of a piezosensor (from up to down: module, real- and imaginary part curves)

## 6 Results and Conclusions

As can be seen from measured results linear chirp excitation signal can be effectively used to measure PZT impedance magnitude. Both impedance magnitude and resistor voltage magnitude can indicate bond quality.

Latter one needs less computational power and time. Impedance magnitude has been more widely used to measure different parameters on host structure.

Also proposed alternative of time domain processing of chirp signal with synchronous processing (convolution) of reference (excitation) against received signal is very promising approach, due to simplicity to realization, as no Fourier' or other sophisticated transforms are needed.

## 7 Acknowledgements

Current work have been supported by Enterprise Estonia (support of Competence Centre ELIKO), target financing SF0142737s06 (Estonian Science Foundation) and by the European Union through the European Regional Development Fund, but also by the EUREKA Eurostars project “Smart Embedded Sensor System (SESS)”. Special thanks also to NOLIAC Ltd, for providing the sensors for testing and all nice colleagues (dr Raul Land, prof Mart Min and others).

## References

[1] S. Grimnes, Ų.G. Martinsen. Bioimpedance and Bioelectricity Basics. Academic Press,London -San Diego, 2000.

[2] T. Paavle, M. Min, P. Annus, A. Birjukov, R. Land and T. Parve, “Wideband Object Identification with Rectangular Wave Chirp Excitation” In Proc. of European Conference on Circuit Theory and Design (Antalya, Turkey, August 23-27, pp. 421 – 424, ECCTD'09. – IEEE 2009,

[3] P. Brunner, R. Merwa, A. Missner, J. Rosell, K Hollaus and H. Scharfetter, “Reconstruction of the shape of conductivity spectra using differential and multifrequency MIT”, Physiological Measurement, Vol. 27, No. 5, pp. 237-248, May 2006.

[4] W. Yin, A.J. Peytona, "Thickness measurement of non-magnetic plates using multi-frequency eddy current sensors", NDT & E International, Vol. 40, Issue 1, pp. 43-48, January 2007.

[5] “Electrochemical Impedance Spectroscopy for Battery Research and Development, ”Technical Report 31, Solarton Analytical, *http://www.solartronanalytical.com/downloads/technotes/technote31.pdf*

[6] K. Darowicki, P. Slepski, “Influence of the analyzing window on electrode impedance measurement by the continuous frequency scanning method.”, Journal of Electroanalytical Chemistry, ( Elsevier Science B.V.). Vol. 533, Issues 1-2 (20. September), pp. 25-31, 2002

[7] G. Park, H. Sohn, C. Farrar, D. Inman, “Overview of piezoelectric impedance-based health monitoring and path forward”, The Shock and Vibration Digest, No. 35 (6), pp. 451-463, 2003.

[8] Y.Y. Lim, S. Bhalla, C.K. Soh, “Structural identification and damage diagnosis using self-sensing piezo-impedance transducers”, Smart Mater. Struct., No. 15, pp. 987-995, 2006.

[9] G. K. Lewis Jr., G.K. Lewis Sr. and W. Olbricht, "Cost-effective broad-band electrical impedance spectroscopy measurement circuit and signal analysis for piezo-materials and ultrasound transducers", Measurement Science and Technology (IOPscience), Vol. 19, No. 10, 2008

[10] C. K. Soh and S. Bhalla, “Calibration of piezo-impedance transducers for strength prediction and damage assessment of concrete”. In Proc. Measurement Science Technology. 14, No. 4, pp. 7, 2008.

[11] G. Park and D. J. Inman, “Structural health monitoring using piezoelectric impedance measurements”. In Proc. Phil Trans R Soc A. 365, No. 1851, pp. 373-392, 2007.

[12] O. Märtens, T. Saar, M. Reidla, M. Min and R. Land, "Fast impedance spectroscopy of piezosensors for structural health monitoring". To be published in Electronics and Electrical Engineering. 28, No. 10 , 2010.

## Appendix IV

T. Saar, “Robust Piezo Impedance Magnitude Measurement Method,” *Electronics and Electrical Engineering*, Vol. 113, No. 7, pp. 107–110, July 2011.

ELECTRONICS AND ELECTRICAL ENGINEERING
ISSN 1392 – 1215 2011. No. 7(113)
ELEKTRONIKA IR ELEKTROTECHNIKA

T 121 SIGNAL TECHNOLOGY
SIGNALŲ TECHNOLOGIJA

# Robust Piezo Impedance Magnitude Measurement Method

**T. Saar**
*Competence Center ELIKO,*
*Department of Electronics, Tallinn University of Technology,*
*Ehitajate tee 5, 19086, Tallinn, Estonia, phone: +372 52 37 269, e-mail: saar.t6nis@gmail.com*

## Introduction

In SHM (structural health monitoring) applications PZT (lead zirconate titanate) impedance measurement is widely used for condition monitoring. PZT E/M (electro-mechanical) impedance can indicate defects on PZT host structure in early stage. Condition of the host structure can be derived from changes on PZT EMI spectrum. E/M impedance provides non-invasive measurement method, while response of the host structure is not modified by the sensor [1].

Electrical admittance Y(ω) of the piezoelectric transducer (PZT) is a combined function of the mechanical impedance of the PZT actuator $Z_a(\omega)$ and that of the host structure Z(ω) [2]

$$Y(\omega) = i\omega a\left( \bar{\varepsilon}_{33}^{\ T} - \frac{Z(\omega)}{Z(\omega)+Z_a(\omega)} d_{3x}^2 \hat{Y}_{xx}^{\ E} \right), \quad (1)$$

When comparing high-frequency local impedance against low-frequency global impedance, then high-frequency local impedance is more sensitive to damage in its initial stage. Because of this, E/M impedance method is more effective in SHM application than other more conventional methods [3].

Purpose of this research was to find the cheapest and most minimal setup needed for impedance magnitude measurement to find alternative to bulky and expensive industrial impedance analyzers or USB data acquisition boxes. Goal was to use simple off-the-shelf components and to keep design as simple as possible. Also avoiding computationally hard tasks like Fourier transform, would help save processing power and lower overall cost. Measurement time is critical factor. For example load changes on host structure (bridges, walls, windmills blades etc) can cause false measurement results. To minimize this measurement time should be as short as possible.

## Previous works

[3] proposed low-cost impedance analyzer based on DAQ card. 10 MHz sample rate and 8 bit dynamic range was used for signal sampling. Digitally synthesized signals were used for active SHM. Results of linear chirp and frequency swept signal were compared by simulations and experiments. E/M impedance results were compared to HP4194A commercial impedance analyzer. Firstly free piezo was measured. After that an aluminum test panel with artificial damage (disbond, cracks and corrosion) was used. New impedance analyzer was proposed for aluminum disbond detection.

Work [4] described procedures for determination of frequency ranges where the PZT transducers are more sensitive for damage detection. Usually most sensitive frequency ranges are determined empirically. In this case tests were carried out on specimens with different sizes and good correlation between experimental and theoretical results was found.

In paper [5] results of using PZT transducers on surface of concrete were compared against embedded transducers. Comparison was made under different conditions, in different locations and extents. Results showed that embedded PZT transducers were more effective for identifying cracks in large-sized concrete structures.

[6] used E/M admittance signatures to model structural impedance. It described multiple –degrees-of-freedom system consisting of a number of one-degree-of-freedom elements with mass, spring and damper components. To solve unknown dynamic system, genetic algorithms were used. Genetic algorithms minimized an objective function. Effects of earthquake were simulated on two-storey concrete frame. Base vibrations hat simulate earthquake were applied to concrete frame. E/M admittance signatures were measured. Using genetic algorithm, the changes of the structural parameters were derived and analyzed. The results demonstrated that the appearance of damage leads to increase in damping and decrease in stiffness and mass at the driven point. Also results demonstrated that, created model was more sensitive to severe damage.

Paper [7] proposed "efficient and inexpensive methodology for electrical impedance measurement". System consisted of National Instruments USB-6211 data

acquisition box and a PC. Software was created using LabVIEW development tools. Results were compared against HP 4192A impedance analyzer.

In paper [8] a novel approach of excitation with chirp signal with simple time-domain analysis of response signal for such task was introduced and described with examples of measurement of the electro-mechanical impedance of piezosensors, in the frequency range of several hundred kilohertz. In one approach smoothed separately (by Savitzky-Golay filter) of excitation voltage and (current) response signals in a sliding window were found and their ratio was used for impedance module estimation, at corresponding time and frequency values. Alternative method for vector measurement of impedance spectra in time domain was also tested.

In papers [9, 10] interface for impedance spectroscopy measurements of piezo-sensors was developed, for a digital signal processor of Delfino series of Texas Instruments. DAC of the interface was based on a 16-bit PWM with extra 8-bit part of "high resolution" (of picoseconds), with external simple (3-rd order) analog filter. Internal 12-bit ADC is converting at rates of up to 10 MS/s with 2 simultaneous sample-and-holds. With few extra components, high-performance analog interface was" improvised" (developed and investigated) with a frequency range 10 kHz -400 kHz about 0,1% of the full scale resolution and repeatability of measurements.

## Method

Proposed setup uses 4 main components microcontroller unit (MCU), waveform generator, amplifier and analog front end. Aim was to use as low cost and few parts as possible. Figure 1 describes method principle layout.

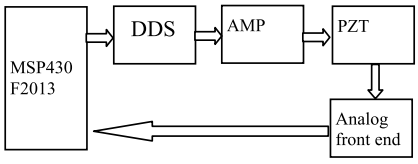


**Fig. 1.** Principle layout

Texas Instruments MSP430F2013 was chosen for MCU. MSP430F2013 is optimized for extended battery life in mobile measurement applications. It has five different power saving modes. Switch between low-power mode and operational-power mode takes less than 1µs. Architecture is based on 16 bit RISC CPU. Efficient code use is achieved by use of 16 bit registers and constant generators. MCU has built-in 16 bit timer and 10 I/O pins. It also has integrated 16 bit sigma/delta A/D converter and built-in communication capability using synchronous protocols (SPI and I2C). Proposed method SPI was used for waveform generator pre-programming and internal 16 bit A/D converter for signal sampling.

Analog Devices AD5932 waveform generator was used for excitation signal generation. The AD5932 is a pre-programmable waveform generator. Start frequency, frequency step, number of steps and time delay between frequencies are all pre-programmed. Generator uses internal logic to increment (or decrement) frequencies automatically step-by-step. Alternatively frequencies can be incremented on-by-one by toggling control pin. Programming is done over SPI interface using 16 bit words. Signal generation is started by only toggling control bin on generator. This saves MCU or DSP processing resources for other purposes and enables to use cheaper processing units. Signal changes frequencies phase-continuously, which enables easily to determine phase shifts. After finishing frequency sweep generator continues to generate last frequency until reset is done. AD5932 uses only 6.7 mA which enables to use it on mobile or low-power applications. In current solution use of AD5932 combined with MSP430F3013 enables to lower overall power consumption.

For excitation signal amplification simple OP-amp based wide-band amplifier was used. Excitation signal voltage was between +15 and -15 V.

Analog front end consists of full period rectifier and first order low pass filter. Rectifier design was based on LM318 operational amplifiers and diodes. Rectifier was designed and simulated using Texas Instruments TINA software package. Schematics was simulated on frequencies between 20-600 kHz. Fig. 2 and Fig. 3 describe analog front end schematics and simulation results.

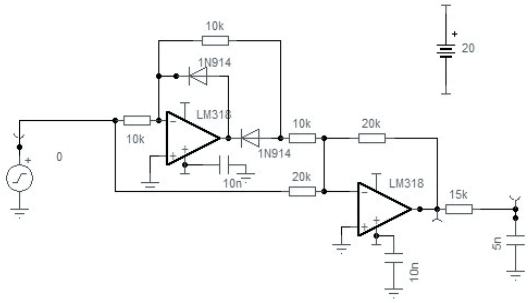


**Fig. 2.** Full period rectifier with low pass filter

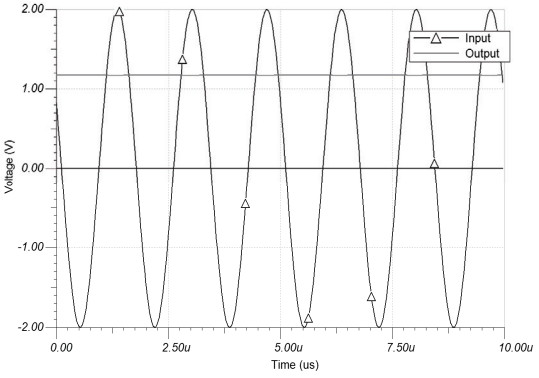


**Fig. 3.** Ti TINA simulation results at 600 kHz

Based on previous work [8] linear chirp signal was used for excitation

$$V(t) = \sin(2\pi(f_1 t + \frac{(f_2 - f_1)t^2}{2T}) . \quad (2)$$

Excitation signal had frequency range 20kHz-600kHz and was 100 ms long. Impedance magnitude was calculated by dividing voltage magnitude with current magnitude. Because voltage (Vm Fig. 4) magnitude changes very little while measuring different PZT's, it could be used as constant vector. Based on this impedance magnitude can be calculated by only measuring current passing PZT. This lowers hardware requirements and cost of measurement system. It enables to use single analog input on MCU. Current was calculated by measuring voltage (Vp) on resistor (Zp on Fig. 4).

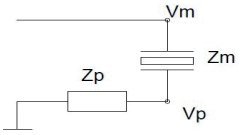


**Fig. 4.** Measurement scheme

Proposed method was tested using Ni USB-6529 DAQ, signal generator and assembled analog front end. 10 kHz sampling rate was used for signal sampling. Recorded signal was decimated to preserve memory. Results were recorded using Matlab based software.

## Results

Measured results were compared against measurements made by made by commercial impedance analyzer type 6500B of Wayne Kerr. Piezos in two cases were measured. Firstly piezo was free in the air, secondly piezo was glued on 500x500 mm fiberglass plate.

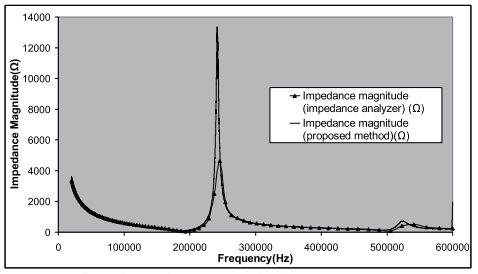


**Fig. 5.** Free piezo impedance magnitude

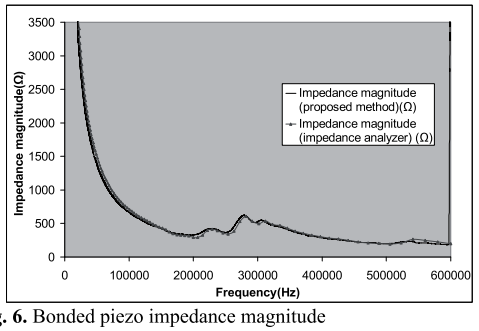


**Fig. 6.** Bonded piezo impedance magnitude

Measured results (Fig. 5 and 6) were very similar to measurements made using commercial impedance analyzer. Only by measuring free piezo, resonance frequency impedance values were much higher compared against commercial impedance analyzer. This effect can be caused by higher excitation signal voltage.

Overall cost of simulated hardware was around 50 Euros, without power supplies. Total power consumption of proposed system was below 3,5W. Most of the power was consumed by excitation amplifier. Low power consumption enables system to be used in wireless configuration. Because maximum power is only needed during 100ms bursts, system could spend extended periods of time in standby mode on battery power.

## Conclusions

Proposed method has been studied and simulated. Also experimental results were measured. Method has high measurement speed, low price and low energy consumption compared against conventional methods. This makes it suitable for real-time on-site SHM application. Use of analog front end enables to use very low cost DSP or MCU. This makes it especially useful for application where great number of impedance spectrum measurement nodes are needed.

## Future work

Future work should focus on impedance spectroscopy on even more extended frequency range. In some applications frequencies up to 2MHz are required. Also analog front end for impedance phase measurement should be developed. Depending on specific application impedance magnitude, phase or both are needed.

## Acknowledgements

Current work have been supported by Estonian Information Technology Foundation, Grant ETF8905 of Estonian Science Foundation, Enterprise Estonia (support of Competence Centre ELIKO), target financing SF0142737s06 (Estonian Science Foundation) and by the European Union through the European Regional Development Fund, but also by the EUREKA Eurostars project "Smart Embedded Sensor System (SESS)". Special thanks also to NOLIAC Ltd, for providing the sensors for testing. Special thanks to colleagues dr. Olev Märtens and Marko Reidla.

## References

1. **Giurgiutiu V., Zagrai A. N.** Embedded Self–Sensing Piezoelectric Active Sensors for Online Structural Identification // ASME Journal of Vibration and Acoustics, 2002. – Vol. 124. – P. 116–125.
2. **Park G., Sohn H., Farrar C., Inman D.** Overview of piezoelectric impedance–based health monitoring and path forward // The Shock and Vibration Digest, 2003. – No 35(6). – P. 451–463.

3. **Xu B., Giurgiutiu V.** A Low–Cost and Field Portable Electromechanical (E/M) Impedance Analyzer for Active Structural Health Monitoring // Proceeding of the 5th International Workshop on Structural Health Monitoring, 2005. – P. 634–643.
4. **Baptista F. G., Filho J. V.** Optimal Frequency Range Selection for PZT Transducers in Impedance–Based SHM Systems // Sensors Journal, IEEE, 2010. – Vol. 10. – P. 1297 – 1303.
5. **Jing Y., Hongping Z, Minshui H.** Numerical study of structure health monitoring using surface–bonded and embedded PZT transducers // International Conference on Mechanic Automation and Control Engineering (MACE'2010), 2010. – P. 895–898.
6. **Hu Y. H., Yang, Y. W., Zhang L., Lu Y.** Identification of structural parameters based on PZT impedance using genetic algorithms // Evolutionary Computation, 2007, CEC 2007, IEEE Congress, 2007. – P. 4170–4177.
7. **Baptista F. G., Filho J. V.** A New Impedance Measurement System for PZT–Based Structural Health Monitoring // Instrumentation and Measurement, IEEE Transactions, 2009. – Vol. 58 – P. 3602–3608.
8. **Saar T., Martens O., Reidla M., Ronk A.** Chirp–based impedance spectroscopy of piezo–sensors // Proceedings of the 12th Biennal Baltic Electronics Conference, 2010. – P. 339–342.
9. **Märtens O., Reidla M., Saar T.** Simple DSP interface for impedance spectrscopy of piezo–sensors // Proceedings of the 12th Biennal Baltic Electronics Conference, 2010. – P. 343–344.
10. **Anton J., Saar T.** Three–Dimensional Cell Counting based on Two Dimensional Cross–Section Images // Electronics and Electrical Engineering. – Kaunas: Technologija, 2011. – No. 6(112). – P. 89–94.

Received 2011 02 15

**T. Saar. Robust Piezo Impedance Magnitude Measurement Method // Electronics and Electrical Engineering. – Kaunas: Technologija, 2011. – No. 7(113). – P. 107–110.**

Piezo impedance spectroscopy is widely used in structural health monitoring (SHM) applications. Purpose of the research was to find most robust and cheap method for impedance magnitude measurement. Proposed system consists of analog front end (AFE), signal synthesizer and microcontroller unit. AFE enables to use low sampling rate, while using high frequency excitation signal. Proposed system uses chirp excitation signal in 20kHz- 600kHz frequency range. Results were compared against measurements made with commercial impedance analyzer. Results show great potential for this method in SHM applications. Ill. 6, bibl. 10 (in English; abstracts in English and Lithuanian).

**T. Saar. Pjezoelemento impedanso vertės matavimo metodas // Elektronika ir elektrotechnika. – Kaunas: Technologija, 2011. – Nr. 7(113). – P. 107–110.**

Pjezo impedanso spektroskopija plačiai taikoma struktūrinei sveikatos stebėsenai. Siekiama rasti patikimą ir pigų metodą impedanso vertei nustatyti. Siūlomoji sistema sudaryta iš analoginės dalies, sintezatoriaus ir mikrovaldiklio. Sistemos matavimo rezultatai buvo palyginti su komerciniais matuokliais atlikto matavimo rezultatais. Gauti daug žadantys rezultatai. Il. 6, bibl. 10 (anglų kalba; santraukos anglų ir lietuvių k.).

## Appendix V

O. Märtens, M. Reidla and T. Saar, “Simple DSP interface for impedance spectroscopy of piezo-sensors, in *Proceedings of the 12th Biennal Electronics Conference (BEC), 2010, 12th Biennial Baltic*, Tallinn, 2010, pp. 343–348.

# Simple DSP interface for impedance spectroscopy of piezo-sensors

O. Märtens[1,2], *IEEE member*, M. Reidla[1,2], T.Saar[1,2]

[1]*Department of Electronics, TUT, Ehitajate tee 5, 19086 Tallinn, Estonia, E-mail: olev@elin.ttu.ee*
[2]*Competence Centre ELIKO, Teaduspargi 6/2, Tallinn, 12618, Estonia*

**ABSTRACT: An interface for impedance spectroscopy measurements of piezo-sensors has been developed, for a digital signal processor of Delfino series of Texas Instruments. DAC of the interface is based on a 16-bit PWM with extra 8-bit part of "high resolution" (of picoseconds), with external simple (3-rd order) analog filter. Internal 12-bit ADC is converting at rates of up to 10 MS/s with 2 simultaneous sample-and-holds. So, with few extra components, high-performance analog interface has been "improvised" (developed and investigated) with a frequency range 10 kHz -400 kHz about 0,1% of the full scale resolution and repeatability of measurements.**

## 1. Introduction

Impedance spectroscopy is used in many applications-bio-impedance measurements, electro-chemistry- battery health estimations etc. Impedance spectra of piezo-sensors allow to estimate the quality of structures around the sensors [1] and see the early changes. Typically the frequency range of up to some hundred (eg 400) kHz is under interest [2].

In low-cost low-power solutions programmable DSP could be an efficient platform for such measurement devices. One practical challenge in realizing such impedance measurement solution in required frequency range and accuracies, is developing of the measurement interface to the analog sensors.

Furthermore, even specialised impedance measurement chips have limited specifications. For example, impedance analyzer chip AD5933 has a limited bandwidth of 100 kHz [3].

Modern control-oriented and general-purpose low-cost digital signal processor (DSP) [4] chips include multiple channels of 16-bit pulse-width modulators (PWM) with high resolution 8-bit part with possibility to adjust the PWM in fractions of the digital clock ("micro-steps"). Such PWM work at clock frequencies of 100 MHz or more and can be used as precise digital-to-analog converters (DAC). Such DSP chips also include multichannel (multiplexed) analog-to-digital converter (ADC), of up to 12-bits resolution, working at conversion rate of up to 10 MHz or more and having sometimes 2 simultaneous sample-and-holds. So, combining these resources together, with few extra components, high-performance digital-to-analog and analog-to-digital conversion is possible.

DSP (Delfino series of Texas Instruments with floating point hardware support) has, additionally to PWM outputs and ADC inputs also direct memory access (DMA) controller, making the generation of waveforms and acquiring of the analog data more smooth and flexible, in real-time.

## 2. Solution in brief

Developed solution is described by a block-diagram (Fig. 1). Hardware part of the solution consists of the DAC, based on th internal (of DSP) High-resolution enhanced PWM (HR-EPWM) with external 3-rd order active analog low-pass filter to smooth the signal, output driver-amplifier (capable of driving of the capacitive loads of piezo-sensors), device under test PZT1 (e.g. a PZT -Lead zirconate titanate) sensor, shunt resitor RB for current measurement and analog input conditioning unit U2 (for shifting of the analog voltage to unipolar for internal ADC and optional amplification). Additionally another (secondary) sensor PZT2 could be connected to the interface via IC2 amplifier for "pitch-catch" or "pitch-echo" type measurements, eg by using of Lamb waves for structural health monitoring (SHM) of materials and structures [5].

Both ADC and PWM had sampling frequency of 2 MHz, in tested configurations (so providing an oversampling feature of multiple times) and were connected to internal DMA of DSP channels so reducing significantly the software load from data-acquisition tasks.

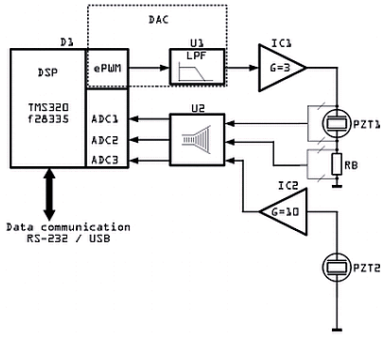


Figure 1. Block diagram of the proposed hardware interface

978-1-4244-7359-5/10/$26.00 ©2010 IEEE

## 3. Analog filter of PWM signal

Analog filter for converting of HR-EPWM signal into analog (eg sinusoidal) signal has been realised as a 3-rd order active filter, according to Fig 2, being optimal for current solution and requirements. Simulated frequency response is given on Fig. 3. Actual results are similar to predicted ones.

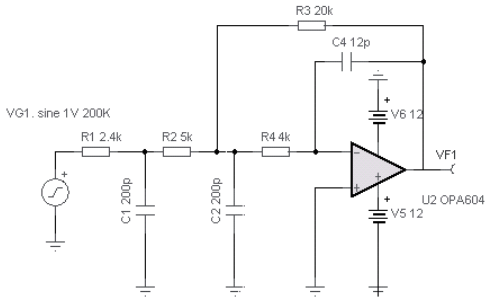


Figure 2.Circuit diagram of an PWM filter

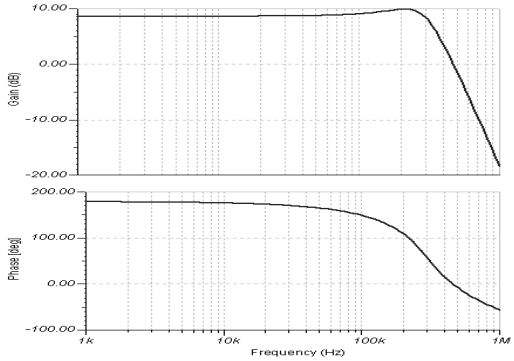


Figure 3.Frequency response of an PWM filter

## 4. Results

So, with few extra components, high-performance analog interface have been developed and investigated with a frequency range 10 kHz -400 kHz about 0,1% of the full scale resolution and repeatability of measurements. Plot of an real-life acquired DSP signals are given on Fig. 4 (higher plot is measured response signal on resistor RB (current sense) and lower graph is measured back excitation signal). Used signal is an chirp signal, sinewave with frequency sweep of 50 to 300 kHz, with N=1000 points with display of first 300 points. Code Composer Studio tools (of Texas Instruments) has been used for developing and debugging of the DSP system in real-time.

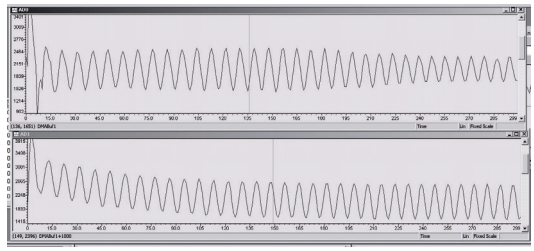

Figure 4. Plot of the actually acquired data

## 5. Conclusions and discussion

Using of modern DSPs allow, additionally to direct signal processing tasks implement efficiently analog data acquisition tasks, alternatively to ”classical” separate ADC and DAC solutions, having complex interfaces and circuitries. Progress in development of DSP peripherals improve further the situation.

## 6. Acknowledgements

Current work have been supported by Enterprise Estonia (support of Competence Centre ELIKO), target financing SF0142737s06 (Estonian Science Foundation) and by the European Union through the European Regional Development Fund., but also by the EUREKA Eurostars project “Smart Embedded Sensor System (SESS)”. Special thanks also to NOLIAC Ltd, for providing the sensors for testing and all nice colleagues (dr Raul Land, prof Mart Min and others).

## References

[1] G. Park, H.Sohn, C. Farrar, D. Inman, “Overview of piezoelectric impedance-based health monitoring and path forward”. The Shock and Vibration Digest, No. 35 (6), pp. 451-463, 2003.

[2] Y.Y. Lim, S. Bhalla, C.K. Soh, “Structural identification and damage diagnosis using self-sensing piezo-impedance transducers”, Smart Mater. Struct., No. 15, pp. 987-995, 2006.

[3] Application Note AD5933 (Rev.0): 1 MSPS, 12-Bit Impedance Converter, Analog Devices 2005.

[4] “TMS320F28335, TMS320F28334, TMS320F2833, TMS320F28235, TMS320F28234, TMS320F28232 Digital Signal Controllers (DSCs)”, Data Manual, Texas Instruments, SPRS439H, June 2007–Revised March 2010

[5] W. Ostachowicz, P. Kudelaa, P.Malinowskia and T.Wandowskia, “Damage localisation in plate-like structures based on PZT sensors”, Mechanical Systems and Signal Processing. Vol. 23, Issue 6 (Special Issue: Inverse Problems), pp.1805-1829, 2009.

## Appendix VI

O. Märtens, T. Saar and M. Reidla, “TMS320F28335-Based Piezosensor Monitor-Node,” in *EDERC2010 European DSP in Education and Research Conference Proceedings*, Nice, 2010, pp. 62–65.

# TMS320F28335-BASED PIEZOSENSOR MONITOR-NODE

*Olev Märtens[1,2], Tõnis Saar[1,2], and Marko Reidla[1,2]*

[1]Departement of electronics, Tallinn University of Technology,
Ehitajate str 5, Tallinn, 19086, Estonia

[2]Competence Centre Eliko
Teaduspargi 6/2, Tallinn, 12618, Estonia

phone: (+372) 6202167, fax: (+372) 6202151, email: olev@elin.ttu.ee
web: www.elin.ttu.ee, www.eliko.ee

**ABSTRACT**

*TMS320F28335 (real-time digital signal processor of Delfino-family) is an ideal platform for developing of ultrasound (in the frequency range of up to 1 MHz) "almost-single-chip" piezosensor based measuring devices. Preliminary prototype of measurement sensor node, capable of measuring impedance spectra of the piezosensor, but also of sending and catching of the ultrasound measurement signal bursts for monitoring of the structure under test, has been developed and tested. Using of internal flash-memory of the DSP, enhanced high-resolution PWM and internal multichannel ADC allows to make very efficient (in form size, cost and power consumption) solution, as demonstrated.*

## 1. INTRODUCTION

### *1.1. Applications of the impedance spectroscopy*

Impedance spectroscopy is widely used in bio-impedance measurements for medical purposes, but also for various industrial condition monitoring applications[1]. Both-contact, as well as eddy-current (with help of measurement coils) based measurement setups could be used for such applications. Also battery health estimation [2] is an important usage field of impedance spectra measurements. Impedance spectra of piezosensors allow to estimate the quality of mechanical structures around the sensors [3] and see the early changes there. Typically the frequency range of up to some hundred (eg 400) kHz is under interest [4].

### *1.2. Introduction to the solution*

In current development a preliminary digital-signal-processor(DSP)-based solution (demonstrator and development platform) has been developed for a monitor-node with piezosensor(s). Needed frequency range for ultrasound monitoring is up to 400 kHz (better if with reserve up to 1 MHz).

One measurement setup, required to be implemented, is an impedance measurement configuration of the piezosensor (that means, the voltage and current of the same piezosensor are needed to be measured, directly or indirectly, in the measurement circuit network). Alternative (second) setup needed- is a configuration, where one piezosensor is transmitting bursts of the excitation signal (eg 5 windowed sinewave periods of ultrasound- eg with frequency of 200 kHz) signal and the second sensor of a measurement node is receiving a signal (what can be a direct signal form the transmitting sensor, but also reflections from the edges of the structure under test). Also in this case the excitation frequency have to be software defined (and also chirp or other wider-spectrum signals could be used).

TMS320F28335 [5] (real-time digital signal processor with controller features of Delfino-family) has been chosen as a core of the solution. Additional important features of this DSP are on-board DMA-controller, high-resolution enhanced PWM (HR-EPWM), 12-bit multichannel (incl dual sample/hold circuit) 12-bit ADC, internal flash memory of the program, etc. Useful could be also built-in floating point arithmetic of the processor.

TMS320F28335 control card and corresponding experimenter's kit [6] has been used for the first prototyping.

### *1.3. Benefits and motivation of DSP-based solutions*

For low-cost low-power measurement devices programmable DSP could be an efficient -digital and programmable and real-time platform. But one practical challenge in realizing such measurement solution in required frequency range and accuracies, is developing of the measurement interface to analog sensors.

Furthermore, even specialized impedance measurement chips have very limited specifications. For example, impedance analyzer chip AD5933 has a limited bandwidth of 100 kHz [7] only, making such solution not applicable for a wide range of solutions, including ultra-sound condition monitoring.

Modern control-oriented and general-purpose low-cost DSPs, like TMS320F28335 chips include multiple channels of 16-bit pulse-width modulators (HR-EPWM) with high resolution 8-bit part with possibility to adjust the PWM in fractions of the digital clock ("micro-steps"). Such PWM works at clock frequencies of 100 MHz or more and can be used as precise digital-to-analog converters (DAC). Such DSP chips also include multichannel (multiplexed) analog-

to-digital converter (ADC), of up to 12-bits resolution, working at conversion rate of up to 10 MHz or more and having 2 simultaneous sample-and-holds. So, combining these resources together, with few extra components, high-performance digital-to-analog and analog-to-digital conversion is possible.

DSP Delfino series of Texas Instruments with floating point hardware arithmetic has, additionally to PWM outputs and ADC inputs also direct memory access (DMA) controller, making the generation of waveforms and acquiring of the analog data more smooth, efficient and flexible, in real-time.

## 2. HARDWARE

### 2.1 Overview

Developed solution (DSP-and core part) is described by a block-diagram (Fig. 1). Hardware part of the solution consists of a DAC, based on the internal high-resolution HR-EPWM with external 3-rd order active analog low-pass filter to smooth the signal, output driver-amplifier (capable of driving of capacitive loads of piezosensors) U1 (OPA552, max +-30V power supply, GBW=12MHz), device under test PZT1 (eg lead zirconate titanate) sensor, shunt resitor RB for current measurement and analog input conditioning unit U2 (for shifting of the analog voltage to unipolar for internal ADC and optional amplification). Additionally another (secondary) sensor PZT2 could be connected to the interface via IC2 amplifier (OPA604) for "pitch-catch" or "pitch-echo" type measurements, eg by using of Lamb waves for structural health monitoring (SHM) of materials and structures [9].

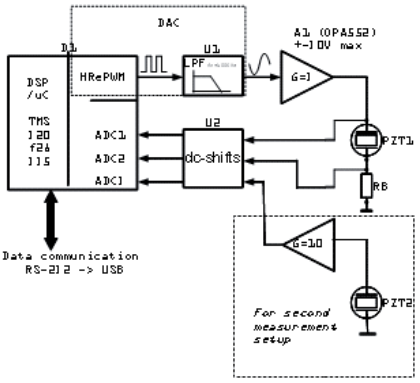


*Figure 1. Block diagram of the proposed hardware interface*

Both ADC and PWM had sampling frequency of 2 MHz, in tested configurations (so providing an oversampling feature of multiple times) and were connected to internal DMA of DSP channels, so reducing significantly the software load from data-acquisition tasks. Also generation of sinewaves with PWM sampling rate of 6 MHz and with PWM-filter with fc=1MHz has been verified

Photo of the developed first preliminary prototype in testing environment is given on fig.2

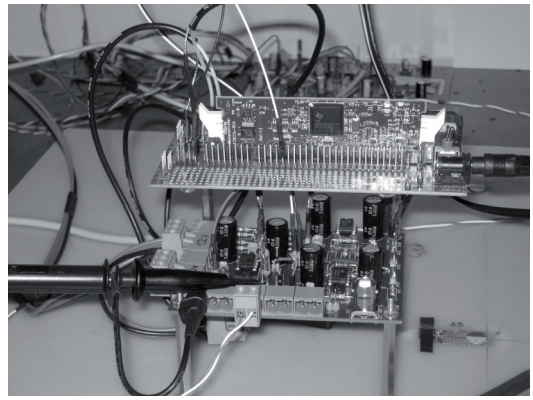

*Figure 2. Photo of the prototype and testsite*

### 2.2 Analog filter of the PWM signal

Analog filter for converting of HR-EPWM signal into analog (eg sinusoidal) signal has been realized as a 3-rd order active filter [10], in two versions, with fc= 400 kHz and fc=1 MHz, according to Fig 2 (component values for 1MHz case), being optimal for current solution and requirements. Simulated frequency response for fc=1 MHz case is given on Fig. 3. Actual results are similar to predicted ones. Current simulations have been done with help of SPICE-Based Analog Simulation Program TINA-TI [11].

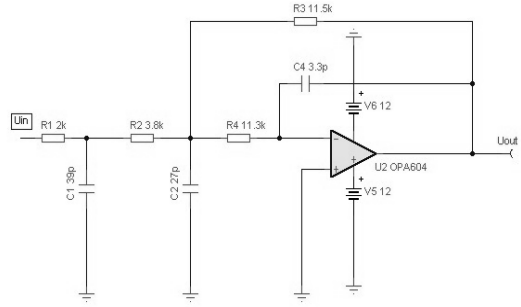


*Figure 3. Circuit diagram of an PWM-output filter (fc=1MHz)*

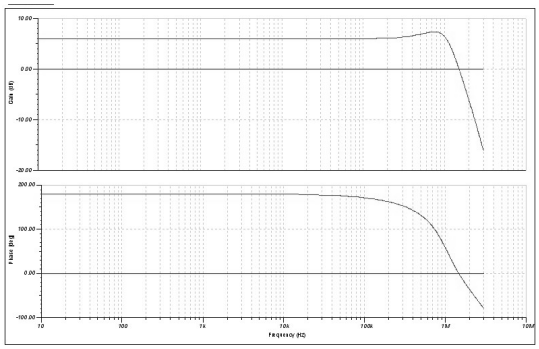

Figure 4.Frequency response of an fc=1MHz PWM-output filter

### 2.3 Output driver of piezosensors

Circuit diagram of the output driver is given on the fig 5 (a PZT sensor is described here as a capacitor) and a frequency diagram of the circuit is given on the fig 6.

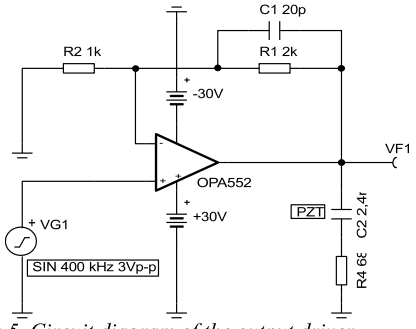


*Figure 5. Circuit diagram of the output driver*

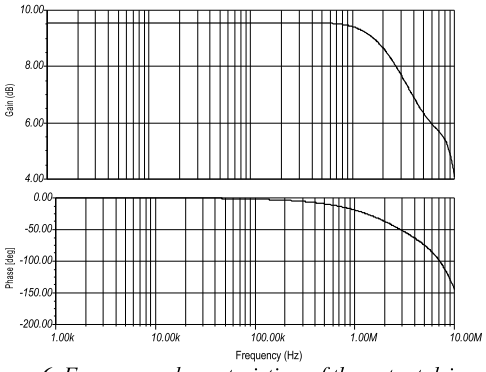


*Figure 6. Frequency characteristics of the output driver*

## 3. SOFTWARE

Code Composer Studio (CCS) tools (of Texas Instruments) has been used for developing and debugging of the DSP system in real-time. Source code has been developed in C/C++. Software is generating (via look-up-tables, initially calculated by software and HR-EPWM) required sinewaves (with fixed frequency or chirp-like signals, with varying frequency), with modulating amplitude window to make the signal bursts smoother. Also processing of the received signal, by founding real and imaginary parts of the complex impedance or transfer functions, realized by corresponding convolutions with base sine- and cosine waves, are implemented in the DSP-software.

## 4. EVALUATION AND TESTING

Evaluation and testing of the prototype shows, that the results correspond to theoretical considerations and simulations.

Generation of sinewaves have been successfully tested in two configurations, with sampling (refresh) frequency of PWM of 2 MHz (PWM filter fc= 400 kHz, frequencies 10kHz to 400 kHz) and at sampling (refresh) frequency of PWM of 6 MHz (PWM filter fc=1 MHz, frequencies 10kHz to 1 MHz). .

Tests and evaluation of the (complex) impedance measurements, and also “pitch and catch” measurements have been performed at sampling frequency fs= 2 MHz case.

Example plot (fragment) of CCS of an real-life acquired DSP signals is given on Fig. 7 (higher plot is measured response signal on resistor RB (current sense) and lower graph is measured back excitation signal). Used signal is an chirp signal, sinewave with frequency sweep of 50 to 300 kHz, with N=1000 points with display of first 300 points.

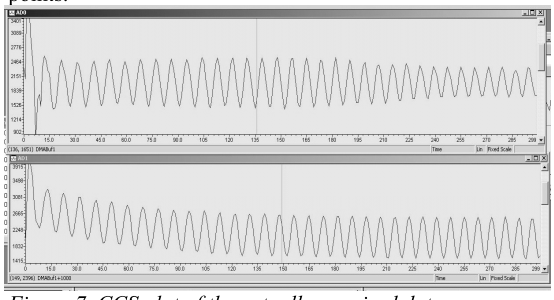

*Figure 7. CCS plot of the actually acquired data*

Examples of the acquired modules of the complex impedance spectra of the piezosensor is given on the fig. 8 (sensor in the air) and 9 (sensor fixed to a composite plate under condition monitoring). Results show reasonable correspondence of the curves with the alternatively measured results by a commercial Precision Impedance Analyzer 6500B of Wayne Kerr (fig 10, for the sensor in the air).

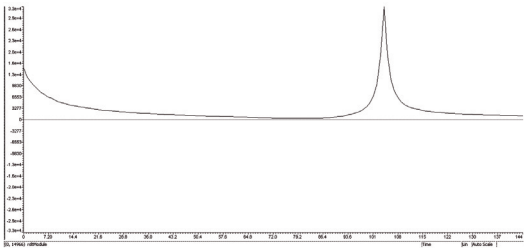

Figure 8. DSP-acquired impedance spectrum (-300kHz)-sensor in the air

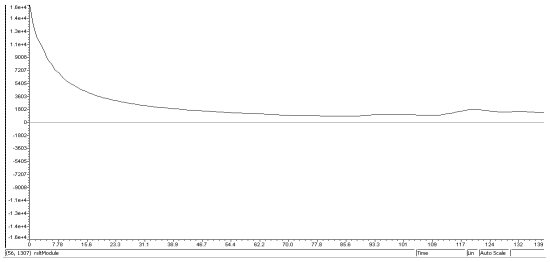

*Figure 9. DSP-acquired impedance spectrum (-300kHz)-sensor fixed to a composite board*

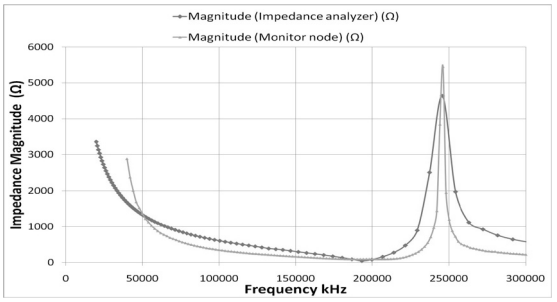


Figure 10. Comparison of the sensor-in-the-air impedance module spectra measurements

## 5. RESULTS

So, with DSP and few extra components, a relatively high-performance piezosensor-monitoring have been developed and investigated for a frequency range 10 kHz- 400 kHz (with possibility to extend the frequency range up to 1 MHz) and with about 0,1% of the full scale resolution and repeatability of measurements.

## 6. CONCLUSIONS AND DISCUSSION

Using of modern DSPs allow, additionally to direct signal processing tasks implement efficiently analog data acquisition tasks, alternatively to classical separate ADC and DAC solutions, having complex interfaces and circuits. So efficient, low-cost low-power sensor measurement nodes could be implemented.

## 7. ACKNOWLEDGEMENTS

Current work have been supported by Enterprise Estonia (support of Competence Centre ELIKO), target financing SF0142737s06 (Estonian Science Foundation) and by the European Union through the European Regional Development Fund, but also by the EUREKA Eurostars project “Smart Embedded Sensor System (SESS)”. Special thanks also to NOLIAC Ltd, for providing the sensors for testing and all nice colleagues (dr Raul Land, prof Mart Min and others) and finally to Texas Instruments, European University program.

## REFERENCES

[1] *Electrical Impedance Tomography, Methods, History and Applications* (Edited by David S. Holder), Taylor & Francis 2004, 456 p.

[2] U. Troltzsch, O. Kanoun and H.- R. Trankler, “Characterizing aging effects of lithium ion batteries by impedance spectroscopy”, *Electrochimica Acta,* Volume 51, Issues 8-9, *Electrochemical Impedance Spectroscopy* - Selection of papers from the 6th International Symposium (EIS 2004) 16-21 May 2004, Cocoa Beach, FL, USA, 20 January 2006, Pages 1664-1672.

[3] G. Park, H.Sohn, C. Farrar, D. Inman, “Overview of piezoelectric impedance-based health monitoring and path forward”, *The Shock and Vibration Digest,* No. 35 (6), pp. 451-463, 2003.

[4] Y.Y. Lim, S. Bhalla, C.K. Soh, “Structural identification and damage diagnosis using self-sensing piezo-impedance transducers”, *Smart Mater. Struct.*, No. 15, pp. 987-995, 2006.

[5] *TMS320F28335, TMS320F28334, TMS320F28332, TMS320F28235, TMS320F28234, TMS320F28232, Digital Signal Controllers (DSCs)*, Texas Instrument, Data Manual. Literature Number: SPRS439H June 2007–Revised March 2010.

[6] *TMS320C2000™ Experimenter Kit Overview*. Texas Instruments, Quick Start Guide, SPRUFR5D–June 2008–Revised August 2009.

[7]*1 MSPS, 12-Bit Impedance Converter*, Analog Devices, Application Note AD5933 (Rev.B), February 2010.

[8] *TMS320F28335, TMS320F28334, TMS320F2833, TMS320F28235, TMS320F28234, TMS320F28232 Digital Signal Controllers (DSCs)*, Data Manual, Texas Instruments, SPRS439H, June 2007–Revised March 2010

[9] W.Ostachowicz, P.Kudelaa, P.Malinowskia and T.Wandowskia, “Damage localisation in plate-like structures based on PZT sensors”, *Mechanical Systems and Signal Processing*. Vol. 23, Issue 6 (Special Issue: Inverse Problems), pp.1805-1829, 2009.

[10] Jim Karki, *Active Low-Pass Filter Design*, Texas Instruments, Application Report, SLOA049A - October 2000.

[11] *Getting Started with TINA-TI™*. Texas Instruments , Quick Start Guide SBOU052A–August 2007–Revised August 2008

## Appendix VII

O. Märtens, M. Min, R. Land, P. Annus, T. Saar and M. Reidla, “Method and device for frequency response measurement,” US Patent Application, US2012/0007583, 2012.

US 20120007583A1

(19) United States

(12) Patent Application Publication

(10) Pub. No.: US 2012/0007583 A1

(43) Pub. Date: Jan. 12, 2012

Märtens et al.

(54) METHOD AND DEVICE FOR FREQUENCY RESPONSE MEASUREMENT

(75) Inventors: **Olev Märtens**, Tallinn (EE); **Mart Min**, Tallinn (EE); **Raul Land**, Tallinn (EE); **Paul Annus**, Tallinn (EE); **Tõnis Saar**, Tallinn (EE); **Marko Reidla**, Tartumaa (EE)

(73) Assignees: **OU ELIKO Tehnoloogia Arenduskeskus**, Tallinn (EE); **TALLINN UNIVERSITY OF TECHNOLOGY**, Tallinn (EE)

(21) Appl. No.: **13/177,961**

(22) Filed: **Jul. 7, 2011**

(30) **Foreign Application Priority Data**

Jul. 7, 2010 (EE) ..... P201000060

**Publication Classification**

(51) **Int. Cl.**
*G01R 23/02* (2006.01)

(52) **U.S. Cl.** ..... **324/76.39**

(57) **ABSTRACT**

A method is provided for measuring a frequency response of an object, the method involving: generating an excitation signal having relatively fast changing frequency, defined by a time-domain function; generating at least one reference signal, having a waveform corresponding to the excitation signal; introducing the excitation signal into the object, receiving a response signal from the object; analyzing said response signal in a signal analyzer by correlating the response signal with at least one reference signal during a relatively short sliding time-domain window.

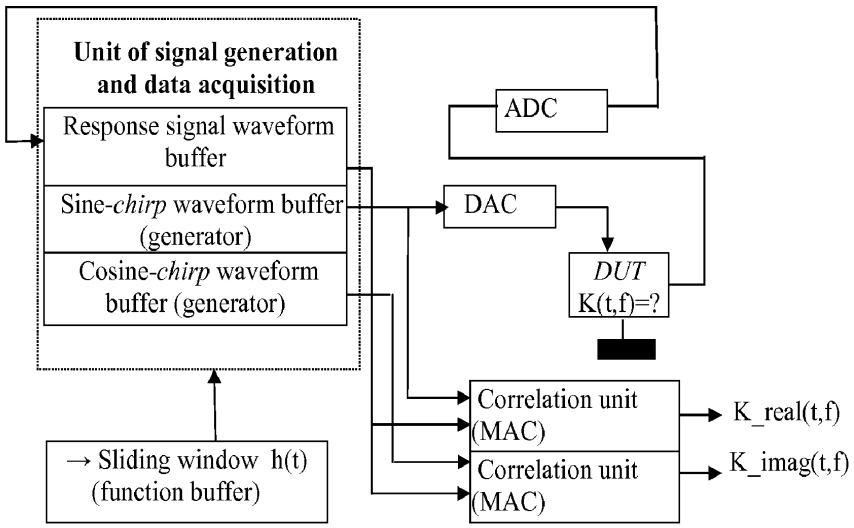

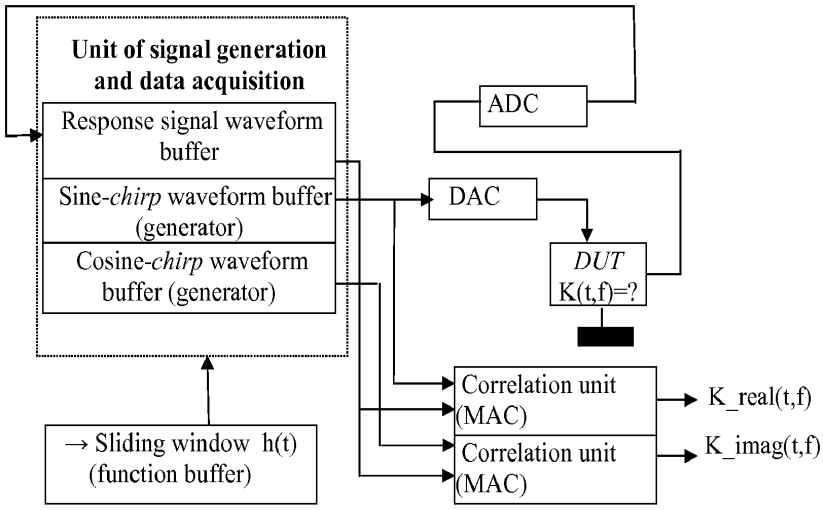
Unit of signal generation and data acquisition
Response signal waveform buffer
Sine-chirp waveform buffer (generator)
Cosine-chirp waveform buffer (generator)
ADC
DAC
DUT K(t,f)=?
Correlation unit (MAC)
Correlation unit (MAC)
K_real(t,f)
K_imag(t,f)
→ Sliding window h(t) (function buffer)

FIG 1

# METHOD AND DEVICE FOR FREQUENCY RESPONSE MEASUREMENT

## BACKGROUND OF THE INVENTION

**[0001]** 1. Technical field

**[0002]** The invention relates to measurement techniques, particularly to the field of measurement of the frequency response. For example, included in this field are electrical network and vector-impedance analyzers which measure the transfer coefficient as a function of the frequency. The invention can be used in bio-impedance measurement devices for medical diagnosis, in testers of electrical and electronics circuits, in analyzers of electrochemical elements for their condition monitoring, for investigating of materials by their electrical properties (e.g., conductivity) and also for many other applications.

**[0003]** 2. Background art

**[0004]** Solutions are known, where the transfer coefficient of the circuit is measured by applying an excitation signal (e.g., of sinusoidal waveform) to the measured circuit and by multiplying and accumulating of the response signal waveform to this excitation signal, or in other words, by correlating (which is a practical equivalent to mathematical convolution) of these signals, and carried out, in digital implementation, by multiply-and-accumulate (MAC) unit. Also second, quadrature (90 degrees shifted, from excitation signal) reference signal for second correlation (quadrature result component) could be used (U.S. Pat. No. 7,428,683). Correlation calculation can often include also normalization of the result, taking into account average levels and amplitudes (intensities) of the signals.

**[0005]** Such solution is also described in the paper, "FPGA-Based Analog Functional Measurements for Adaptive Control in Mixed-Signal Systems", JIE QIN et al, August 2007, for BIST, the device consisting of numerically controlled oscillators, digital-to-analog converter and analog-to-digital converter and adjusted for applying excitation signal to an object (e.g., circuit under test and reading back the response signal from the object, and numerical multiplier and accumulator to analyze the properties of the object under test. The disadvantage of such solutions is that the result is calculated by correlation of the reference and response signals as one integral value over the full measurement cycle and therefore such measurement is not showing the transfer coefficient separately for individual frequencies (that means, frequency response) and secondly, such integral measurement is not reflecting correctly and in real-time dynamical, changing in time circuit or object.

**[0006]** For measurement of the frequency response, including dynamic (fast changing in time) circuits and objects, the technical solutions are known, where wideband, e.g., chirp excitation signal are used, and the response signal is analyzed in relatively short sliding time-domain-window by frequency analysis, e.g., by short-time Fourier' transform (STFT) or by wavelet analysis, as described in U.S. Pat. No. 6,885,960 and U.S. Pat. No. 5,797,840.

**[0007]** The closest solution known in the art is described in the paper "Influence of the analyzing window on electrode impedance measurement by the continuous frequency scanning method", K. Darowicki, P. Slepski, Journal of Electroanalytical Chemistry, Vol 533, Issues 1-2, 20 Sep. 2002, pp 25-31. In this solution a linear chirp signal is generated for an excitation signal. For dynamical time and frequency domain analysis, a combined time-frequency analysis in the form of short-time Fourier transform (STFT) is used, in which Fast Fourier Transform (FFT) is used in a relatively short-time sliding window, while this window could be weighted by the Gauss window function.

**[0008]** The disadvantage of this solution is the complexity of combined time-frequency analysis of the response signal, as a very sophisticated full spectral Fourier analysis is carried out in every short-time window, demanding a huge processing power and much computing time for calculations. This limits significantly the usage of such solutions for real-time monitoring of the objects and circuits, because and for limited by computational power of processors, which in its turn is limited by cost and available power.

**[0009]** Thus, there is a need for new improved method and device for frequency response measurements

## Disclosure of the Invention

**[0010]** Objective of the invention is to simplify the measurement of the frequency response, what in turn allows to use cheaper, simpler electronic devices with lower power consumption. Another objective is improved accuracy of frequency response measurements in time or frequency domain.

**[0011]** The objective of the invention is achieved by the invented method, comprising generating an excitation signal having relatively fast changing frequency, defined by a time-domain function, generating at least one reference signal having waveform corresponding to said excitation signal, introducing said excitation signal into the object, receiving a response signal from said object, analyzing said response signal in a signal analyzer by correlating said response signal with said at least one reference signal during a relatively short sliding time-domain window.

**[0012]** The relatively short time window can be further divided into several independent sliding sub-windows. The analysis could be performed digitally in one implemented correlation of the excitation signal and a reference signal, which could be the excitation signal itself It is reasonable to use a second, quadrature channel to determine the second (quadrature, imaginary) component of the response signal, e.g., the first and second reference signals, generated as sine and cosine wave chirp signals, respectively.

**[0013]** Alternative is to use Hilbert Transform to get the quadrature (imaginary) reference waveform from the first reference waveform.

**[0014]** As excitation signals, the linear, logarithmic or exponential chirp signals can be used for linear, logarithmic or exponential representation of the frequency response correspondingly. Also arbitrarily changing frequency could be used in some applications, e.g., for measurement of very specific frequency response shapes, where specific frequencies under interest are known (e.g., for eddy current measurement and validation of electrical properties of metals and metal products such as coins, when often discrete frequencies (e.g., 120, 240 and 480 kHz) are used for measurement). Furthermore, by adaptive changing the frequency dependency function of the excitation signal, or parameters of the analysis window, it is possible to classify the object under test with minimum computational and signal processing needs and achieve so the maximal processing speed, making so the proposed solution also preferable to monitor the objects with fast changing parameters.

**[0015]** Also, as typically measurements are carried out periodically, it is possible, according to the current measurement results (e.g., depending on the measured values and

dispersion of the results in specific frequency regions), to improve the measurement accuracy and decrease the fluctuations (e.g., caused by noise) of the measurements, by adaptively changing the amplitude of the excitation signal and the length of analysis window for specific frequency regions or values.

**[0016]** By shape of the waveform both sine waves and non sine waves (e.g., square waves) can be used. Preferably, the beginning and ending of the short time-window are selected at zero-crossing time-instants of the excitation signal. Preferably the time-window duration is adjusted according to the running frequency of the signal, thus e.g., using for lower frequencies a longer time-window.

**[0017]** Alternative to usage of the two quadrature against each other reference waveforms, is to use only one, the first reference waveform, corresponding to the excitation signal waveform, by transforming the received response signal by Hilbert transform, to the complex response signal containing both direct (real) and imaginary parts and then performing the complex correlation with the first reference signals, getting a complex transfer functions for time instants and related frequency values, according to the sliding of the time domain window.

## BRIEF DESCRIPTION OF THE DRAWINGS

**[0018]** The essence of the invention is described in FIG. **1**, as a block-diagram for an example of the implementation of the invention.

**[0019]** Example of carrying out the invention

**[0020]** One embodiment of the invention shown on FIG. **1** comprises a unit of signal generation and data acquisition **1** for generating of the excitation signal, comprising a sine chirp waveform buffer (or generator) **2** and a cosine chirp waveform buffer (or generator) **3** (or other signals with relatively fast changing frequency). Waveform generation buffers are to be initialized with arrays of values, corresponding to the waveform, at the initialization of the whole system. In the generated waveform, the instance values of the frequency have to change relatively fast. The output of the sine chirp waveform buffer is connected, through digital-analog converter **5** (and an additional driver, if needed) into an device to be tested (DUT) **6** with unknown time variant transfer function K (t, f). It can be appreciated that instead of device, any other object with can be tested such as electrical or electronics circuits, biological objects (e.g., in bio-impedance measurements for medical diagnosis), electrochemical elements, and materials). The response signal is acquired from the object through analog-digital converter (ADC) **7** (if needed, after amplification and conditioning, not shown) into a response signal waveform buffer **4** and is further processed in a correlation unit **9** for inphase component K_real(t, f), using sine chirp as reference signal, and in a correlation unit **10** for quadrature component K_imag(t, f), using cosine chirp as reference signal. Multiply-and-accumulate (MAC) units can be used as correlation units **9** and **10** in processing signals in digital form.

**[0021]** Further, a relatively short time-domain sliding window, e.g., weighted by Gauss function window, which could be initialized into array of values h(t) into a sliding window h(t) buffer **8**, is applied for analysis of the response signal. In the scope and with weights of the window the response signal is convolved by the reference sine and cosine wave chirps to calculate the real and imaginary parts of the response signal. As the excitation signal value is known, the transfer function of the circuit (object) under test can be calculated from this result, for the time instance (and thus, for a specific frequency). Further, a parameter of the object under investigation, e.g., unknown impedance part of the circuit can be calculated. The mentioned short-time window is sliding synchronously in all the mentioned waveform buffers: sine and cosine wave reference buffers and response signal buffer. So the value of transfer coefficient is defined just for corresponding to the sliding window position (time and frequency values) position.

**[0022]** Preferably chirp-signals are used, where the frequency of the signal is changing linearly or logarithmically in time, giving so linear or logarithmic frequency response function. Of course, other time dependences of the frequencies can be used, depending on the application and on which frequency-domain resolution is currently needed.

**[0023]** Instead the sine and cosine waveform signals in some applications non-sinusoidal waveforms, e.g., square wave signals, can be used. Such signals are easier to generate and simpler to use for correlation calculation.

**[0024]** Measurement could be performed in steps, by using adaptively at every step the results of the previous step for defining the parameters of the excitation signal or the analysis window.

**[0025]** Corresponding adaptive parameters of the excitation signal or of the analysis window can be defined for minimizing the effect of noise and measurement errors.

**[0026]** Corresponding adaptive parameters of the excitation signal or of the analysis window can be defined to identify an object, e.g., as 1 euro coin, 2 euro coin, or to distinguish real coin from forged coin, or to classify the measured object, e.g., by "pass" or "not pass", e.g., in a production process.

**[0027]** Of course, the mentioned waveforms of cosine and sine wave signals could be generated, and the response signal waveform processed, without buffers by using known analog-to-digital signal processing techniques.

**[0028]** Analog-to-digital and digital-to-analog converters are needed for the digital implementation of the solution (e.g., when using a digital signal processor). In analog solution, these converters are not needed and in correlation calculation the accumulation of multiplication results is changed by integration of the multiplication results.

**[0029]** The length of the time-domain sliding window can be implemented as dynamically and adaptively variable, being for lower frequencies longer. Preferably the beginning and ending of the sliding time-domain window are synchronized by zero-crossings of the excitation signal, so decreasing the spectral leakage of analysis, as integer number of periods of the signal is included in the analysis window.

**[0030]** The sliding time-domain window can consist of several sub-windows. For example, when the frequency dependence of time has the same instant value of frequency at various time instances, e.g., if the same excitation signal (burst) includes positive and negative chirp signal sequences. As the same frequency is at both positive and negative parts of the chirp, the analysis window can consist of one sub-window from the positive and the other from the negative part of the chirp.

**1**. A method for measuring a frequency response of an object, the method comprising:

generating an excitation signal having relatively fast changing frequency, defined by a time-domain function;

generating at least one reference signal, having a waveform corresponding to said excitation signal;

introducing said excitation signal into the object,

receiving a response signal from said object;

analyzing said response signal in a signal analyzer by correlating said response signal with said at least one reference signal during a relatively short sliding time-domain window.

**2**. The method as in claim **1**, wherein said relatively short sliding time-domain window is divided into several time-domain sub-windows.

**3**. The method as in claim **1**, wherein the length of said relatively short sliding time-domain window is variable and determined by running frequency value.

**4**. The method as in claim **1**, wherein the beginning and the end of said relatively short sliding time-domain window are chosen at zero-crossings of said excitation signal.

**5**. The method as in claim **1**, wherein said excitation signal is generated as a sinusoidal wave.

**6**. The method as in claim **1**, wherein the excitation signal is generated as non-sinusoidal wave.

**7**. The method as in claim **6**, wherein said excitation signal is a square wave signal.

**8**. The method as in claim **1**, wherein the excitation signal is generated as a chirp signal.

**9**. The method as in claim **8**, wherein said chirp signal is a linear chirp signal.

**10**. The method as in claim **8**, wherein said chirp signal is a nonlinear chirp signal.

**11**. The method as in claim **10**, wherein said nonlinear chirp signal is selected from the group consisting logarithmic, exponential and arbitrarily formulated chirp signal.

**12**. The method as in claim **1**, comprising analyzing said response signal in at least two consecutive steps, while using adaptively results of an earlier step for determining the parameters of said excitation signal or at least one analysis window for a subsequent step.

**13**. The method as in claim **12**, wherein in said previous step the parameters of the excitation signal or of at least of one analysis window for the subsequent step are defined to minimize the effect of noise or measurement inaccuracy.

**14**. The method as in claim **12**, wherein in said previous step the parameters of said excitation signal or of at least one analysis window for the subsequent step are defined to classify said object.

**15**. The method as in claim **1**, wherein said reference signals are convolved in complex arithmetic in said short time-domain window by said response signal for calculation of the real and imaginary parts of the response signal, to be used for calculation of the real and imaginary parts of the object's transfer coefficient as a function of the frequency.

**16**. The method as in claim **1**, wherein a first reference waveform corresponding to said excitation signal, is used to determine real and imaginary parts of a transfer coefficient by correlating it in the short-time window by complex representation of said response signal, given by Hilbert Transform of the acquired response signal.

**17**. A device for measuring of the frequency response of an object, comprising:

a unit of signal generation and data acquisition for generating an excitation signal with a fast changing frequency to be introduced into said object and

a response-signal analyzer adapted to receive a response signal from said object,

said response-signal analyzer working in a short time window, wherein the analyzer comprises a first unit adapted to generate a first reference waveform that is in phase with the excitation signal, and a second unit adapted to generate a second reference waveform that is in quadrature with the excitation signal,

wherein the waveforms of the first and second excitation signals are defined by said excitation signal waveform, and means for correlating said response waveform with the first reference waveform and with the second reference waveform in a short time-domain window.

* * * * *

## Appendix VIII

O. Märtens, M. Min, R. Land, P. Annus, T. Saar and M. Reidla, „Meetod ja seade sageduskarakteristiku mõõtmiseks,” Estonian patent EE 05616 B1, 2012.

EE 05616 B1

(19) EESTI VABARIIK
PATENDIAMET

(11) **EE 05616 B1**

(51) Int.Cl.
*G01N 27/00 (2012.01)*
*G01R 31/00 (2012.01)*
*G06F 11/00 (2012.01)*
*G06F 17/00 (2012.01)*

# (12) PATENDIKIRJELDUS

(21) Patenditaotluse number: **P201000060**

(22) Patenditaotluse esitamise kuupäev: **07.07.2010**

(24) Patendi kehtivuse alguse kuupäev: **07.07.2010**

(43) Patenditaotluse avaldamise kuupäev: **15.02.2012**

(45) Patendikirjelduse avaldamise kuupäev: **17.12.2012**

(73) Patendiomanikud:

**Tallinna Tehnikaülikool**
**Ehitajate tee 5, 19086 Tallinn, EE**

**OÜ ELIKO Tehnoloogia Arenduskeskus**
**Teaduspargi 6/2, 12618 Tallinn, EE**

(72) Leiutise autorid:

**Olev Märtens**
**Sügislase 20/1, 11913 Tallinn, EE**

**Mart Min**
**Kuklase 3-4, 13424 Tallinn, EE**

**Raul Land**
**Akadeemia tee 7A-17, 12611 Tallinn, EE**

**Paul Annus**
**Harju 5-12, 10146 Tallinn, EE**

**Tõnis Saar**
**Lageda tee 9-6, Viimsi vald,**
**74020 Harju maakond, EE**

**Marko Reidla**
**Vahesaare talu, Konguta vald,**
**61215 Tartu maakond, EE**

(74) Patendiomaniku ühine esindaja:

**Tallinna Tehnikaülikool**

## (54) Meetod ja seade sageduskarakteristiku mõõtmiseks

(57) Meetod ja seade sageduskarakteristiku mõõtmiseks kuuluvad mõõtetehnika valdkonda. Meetodi käigus genereeritakse ajas etteantud funktsiooni alusel muutuva sagedusega ergutussignaal ning vastussignaali analüüsitakse suhteliselt lühikeses libisevas ajavalla-aknas, kasutades perioodilisi tugilainekujusid. Vastussignaali analüüs teostatakse ajavallas. Analüüsil võidakse kasutada esimest ja teist tugilainekuju, mis on omavahel ortogonaalsed ja on vastavuses ergutussignaaliga, ning mainitud tugikujude korrutamist vastuvõetud signaaliga ja akumuleerimist, et saada vastavalt vastuvõetud signaali reaal- ja imaginaarosad eri ajahetkedel (ja vastavatel sagedustel) mõõdetava objekti kompleksne ülekandefunktsioon arvutamiseks. Seade sageduskarakteristiku mõõtmiseks sisaldab ajast sõltuva sagedusega ergutussignaali generaatorit ning suhteliselt lühikeses ajavalla-aknas ajavallas toimivat vastussignaali analüsaatorit.

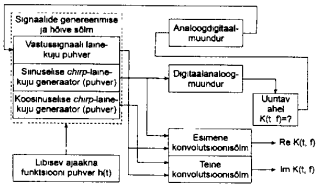


(57) Method and device for frequency response measurement, including generation of a excitation signal (like sinewave) with time-depending frequency (eg *chirp* signal) and time-domain (in a short-time sliding window) analyzing of the response signal. Said analyzing can include first and second reference waveforms, being "orthogonal" to each other and corresponding to the excitation signal (eg sine- and cosine- based chirps respectivley), and multiplication of said reference waveforms to the received signal and accumulation in said short window to get real and imaginary parts of the response signal, for calculating the complex transfer function for various time instants (and so for corresponding frequencies).

# MEETOD JA SEADE SAGEDUSKARAKTERISTIKU MÕÕTMISEKS

## Tehnikavaldkond

Leiutis kuulub mõõtetehnika, täpsemalt sageduskarakteristikute mõõtmise valdkonda. Antud valdkonda kuuluvad ka elektriahelate analüsaatorid ning vektorimpedantsi mõõtjad, mis määravad samuti elektriliste ülekandekarakteristikute sõltuvuse sagedusest. Leiutist saab kasutada meditsiinidiagnostikas elektrilistes bioimpedantsi mõõtjates, elektri- ja elektroonikaskeemide testrites, elektrokeemiliste elementide analüsaatorites näiteks patareide seisukorra hindamiseks elementide sisetakistuse spektri abil ning materjalide omaduste uurimiseks ja kontrollimiseks nende elektriliste omaduste kaudu.

## Tehnika tase

Tuntud on lahendused, kus skeemi või ahela ülekannet mõõdetakse, näiteks siinuselise vahelduvsignaaliga ergutamise tulemusena tekkinud vastussignaali korrutamise ja akumuleerimise teel mainitud ergutussignaaliga, st ergutus- ja vastussignaalide konvolutsiooniga. Analoogiliselt võidakse kasutada samuti kvadratuurset, ergutussignaali suhtes 90° faasis nihutatud teist tugisignaali teise konvolutsiooni (kvadratuurkomponendi) leidmiseks (US7428683B2).

Artiklis „FPGA-Based Analog Functional Measurements for Adaptive Control in Mixed-Signal Systems“, Jie Qin et al, IEEE Transactions on Industrial Electronics, Vol 54 (4), August 2007, kirjeldatakse analoogilist BIST lahendust, mis sisaldab numbriliselt juhitava sagedusega ostsillaatoreid, digitaal-analoog- ja analoog-digitaal muundureid uuritavale objektile ergutussignaali andmiseks ja vastussignaali tagasilugemiseks ning numbriliste signaalide korrutit ja akumulaatorit uuritava objekti (ahela) omaduste analüüsiks.

Taoliste lahenduste puuduseks on see, et tulemus saadakse tugisignaali ja mõõdetava vastussignaali konvolutsiooni tulemusel integraalsena üle terve mõõtetsükli, mis esiteks ei näita mõõdetava ahela või objekti ülekannet eri sagedustel eraldi ehk sageduskäiku ja teiseks ei kajasta taoline integraalne mõõtmine õigesti ja reaalajaliselt dünaamilist ehk ajas muutuvat ahelat või objekti.

Sageduskarakteristikute mõõtmiseks ning ajas dünaamiliste ahelate ja objektide mõõtmiseks on tuntud tehnilised lahendused, kus kasutatakse laiaribalist ergutussignaali ehk nn *chirp*-signaale ja vastussignaalide osas lühiajalisi, suhteliselt lühikeses ajas libisevas aknas sageduslikke teisendusi, näiteks lühiajalist Fourier' teisendust või lainekestega analüüsi (US6885960B2 ja US5797840A).

Leiutisele kõige lähedasemat ja tehnilise tulemuse poolest kõige sarnasemat lahendust kirjeldatakse artiklis „Influence of the analyzing window on electrode impedance measurement by the continuous frequency scanning method", K. Darowicki, P. Slepski, Journal of Electroanalytical Chemistry, Vol 533, Issues 1-2, 20 Sept 2002, pp 25-31.

Selles lahenduses genereeritakse ergutussignaalina *chirp*-signaal, mille puhul ergutava siinussignaali sagedus muutub ajas lineaarselt. Vastuvõetud signaali dünaamiliseks analüüsiks ajas ja sageduse järgi kasutatakse kombineeritud aeg-sagedus analüüsi lühiajalise Fourier' teisendusega, mis kujutab endast tüüpiliselt kiiret Fourier' teisendust suhteliselt lühikeses ajas libisevas aknas, mis omakorda on kaalutud näiteks Gaussi aknafunktsiooniga.

Antud lahenduse puuduseks on vastuvõetud signaali analüüsi osa kombineeritud aeg-sagedus teisenduste keerukus, kuna igas lühikeses ajavalla aknas teostatakse töömahuka Fourier' teisendusega spektraalanalüüs, mis nõuab suurt arvutusressurssi ja palju arvutusaega. See piirab oluliselt antud lahenduse kasutamist reaalajas kiiresti muutuvate objektide jälgimisel ja piiratud arvutusvõimsusega protsessorite puhul, mida omakorda piiravad lahenduse hind ja saadaolev toiteenergia.

**Leiutise olemus**

Leiutise eesmärgiks on lihtsustada sageduskarakteristikute mõõtmist, mis omakorda võimaldab kasutada odavamat, lihtsamat ja väiksema voolutarbega ning miniatuursemat elektroonikalahendust ja tõsta sageduskarakteristikute mõõtmise ajalist või sageduslikku eraldusvõimet ning täpsust.

Leiutise eesmärk saavutatakse võrreldes tuntud lahendusega, kus genereeritakse ajas etteantud funktsiooni alusel muutuva sagedusega ergutussignaal ning teostatakse vastussignaali analüüs suhteliselt lühikeses libisevas ajavalla aknas, kasutades

perioodilisi tugisignaale, sellega et vastussignaali analüüs teostatakse ajavallas ning mainitud perioodiline tugilainekuju või perioodilised lainekujud on vastavuses ergutussignaali kujuga ajavallas.

Kogupikkuselt suhteliselt lühike ajavalla aken võib omakorda koosneda mitmest sõltumatult libisevast alamaknast. Analüüs võib ühel juhul toimuda esimese tugisignaali, milleks võib olla ergutussignaal ja vastussignaali ajavallas toimuva konvolutsioonina digitaalse töötluse puhul. Sealjuures on mõistlik kasutada tulemuse kvadratuurse teise komponendi määramiseks teist paralleelset kanalit, kus teise tugisignaalina kasutatakse kvadratuurset varianti ergutussignaalist, näiteks siinuselise ja koosinuselise *chirp*-signaali kasutamine vastavalt esimese ja teise tugisignaalina. Alternatiiviks on ka Hilbert'i funktsiooni kasutamine kvadratuurse tugisignaali saamiseks esimesest tugisignaalist. Ergutussignaalidena on otstarbekas kasutada lineaarset või logaritmilist *chirp*-signaali. Ergutus- ja tugisignaali kujuna on mõistlik kasutada siinuselisi või mittesiinuselisi näiteks meandersignaale. Sealjuures on eelistatud teatud juhtudel libiseva ajavalla akna alguse ja lõpu valimine ergutussignaali nullist läbimineku hetkedel. Mõistlik võib-olla ka mainitud akna pikkuse adaptiivne muutmine sõltuvalt ergutussignaali hetkesagedusest, näiteks madalate sageduse jooksvate väärtuste juures kasutada suhteliselt pikemat ajaakent.

Alternatiiviks kahe kvadratuurse tugisignaali kasutamisele on ainult ühe tugisignaali kasutamine, mis on vastavuses ergutussignaaliga, muutes seejuures vastuvõetud vastussignaali Hilbert'i teisenduse abil kompleksekskes otse- ja kvadratuurkomponenti sisaldavaks signaaliks ja siis teostades konvolutsiooni esimese tugisignaaliga, saades kompleksse ülekandefunktsiooni antud ajahetkedel ja vastavatel sagedustel vastavalt lühikese ajavalla akna libisemisele.

**Jooniste loetelu**

Fig 1 kujutab leiutise teostamise näite plokkskeemi.

**Leiutise teostamise näide**

Pakutud lahendus sisaldab signaalide genereerimise ja hõive sõlme, mis omakorda sisaldab siinuselise ja koosinuselise *chirp*-lainekuju või muu suhteliselt kiiresti muutuva

sagedusega generaatoreid ehk lainekujude puhvreid. Vastavad lainekujud on digitaalses variandis mõistlik initsialiseerimisel genereerida puhvritesse ettearvutatud muutujate massiividena. Samuti sisaldab signaalide genereerimise ja hõive sõlm vastussignaali lainekuju puhvri. Sealjuures peab lainekujude generaatorite abil tekitatav sageduse hetkväärtus olema ajas suhteliselt kiiresti muutuv funktsioon. Mõistlik on kasutada *chirp*-signaali kujusid, kus sagedus muutub ajas lineaarselt või logaritmiliselt, et saada vastavalt lineaarne või logaritmiline sageduskäik ajas. Loomulikult on konkreetsete rakenduste juures mõistlik kasutada muid sagedussõltuvusi ajas, sõltuvalt sellest, millises sageduspiirkonnas on millist eraldusvõimet vaja. Siinuselise *chirp*-lainekuju generaatori signaal ergutab digitaalanaloogmuunduri ja vajadusel lisadraiveri kaudu uuritavat ahelat, mille sageduskarakteristikut K(t, f) mõõdetakse. Uuritavast ahelast tulev vastussignaal (vajadusel pärast analoogvõimendamist ja muud konditsioneerimist, mida pole kujutatud) kogutakse läbi analoogdigitaalmuunduri vastussignaali lainekuju puhvrisse. Edasi kasutatakse ajas suhteliselt lühikest ajas libisevat akent, näiteks Gaussi kaalufunktsiooniga, mis võib olla initsialiseeritud väärtuste massiivina libiseva ajaakna funktsiooni h(t) puhvrisse. Selle akna ulatuses ja vastava kaaluga konvolueeritakse esimeses ja teises konvolutsioonisõlmes vastussignaali siinuselise ja koosinuselise *chirp*-lainekuju generaatori (puhvri) signaalidega vastussignaali reaal- ja imaginaarosa määramiseks. Teades uuritava ahela ergutussignaali suurust, saab sellest arvutada mõõdetava objekti ülekandefunktsiooni antud punktis. Omakorda saab sellest arvutada uuritava objekti väärtuse, nt elektriahela tundmatu impedantsi. Mainitud libisev aken libiseb sünkroonselt siinuselise ja koosinuselise *chirp*-lainekuju ning vastussignaali lainekuju puhvrites. Seega määratakse ülekandefunktsioon antud ajahetkele vastavale libiseva akna asukohale vastaval siinuselise *chirp*-lainekuju generaatori signaali sagedusel.

Siinus- ja koosinussignaalide asemel on mõnes rakenduses otstarbekas kasutada ka mittesiinuselisi lainekujusid, näiteks meandersignaale, mida on lihtsam genereerida ja lihtsam kasutada konvolutsioonide arvutamisel.

Mõistlik võib olla ka teostada mõõtmist etapiviisiliselt, kasutades igal etapil adaptiivselt eelmise etapi tulemusi nii ergutussignaali parameetrite kui analüüsi akna parameetrite arvutamisel.

Sealjuures võib olla mõistlik, et vastavad ergutussignaali või analüüsi aja-akna ja aja-akende adaptiivsed parameetrid arvutatakse müra või mõõtevigade minimiseerimiseks.

Sealjuures võib olla mõistlik, et ergutussignaali või analüüsi aja-akna ja aja-akende parameetrid arvutatakse mõõdetava objekti klassifitseerimiseks, näiteks „vastav" või „mittevastav" etteantud normile.

Loomulikult võib antud lainekujusid, näiteks siinus- ja koosinussignaale mõnel juhul genereerida ja vastussignaali töödelda ka ilma vahepuhvriteta tuntud analoog- või digitaaltehnikaid kasutades, ilma et lahenduse tööpõhimõte sellest muutuks.

Analoogdigitaalmuundur ja digitaalanaloogmuundur on vajalikud antud lahenduses, kui antud leiutis teostatakse digitaalsel kujul, näiteks digitaalse signaaliprotsessori baasil. Analooglahendust kasutades ei ole mainitud muundurid ja muundamised vajalikud ning konvolutsioonis asendub korrutiste akumuleerimine nende integreerimisega.

Libiseva ajavalla akna pikkus on otstarbekas teha dünaamiliselt muutuvana ja adaptiivsena, kusjuures madalamate hetksageduste väärtuste juures omades suuremat pikkust.

Samuti on otstarbekas sünkroniseerida mainitud libiseva ajavalla akna algus ja lõpp ergutussignaali nullist läbiminekuhetkedega, tagades sellega väiksemad spektrilekked, kuna analüüsitavasse aknasse mahub siis alati signaali täisarv perioode.

Ajavallas libisev aken võib igal antud ajahetkel koosneda ka mitmest alamaknast. See on otstarbekas, kui sageduse funktsioon ajast omab sama sageduse väärtust mitmel erineval ajahetkel, nt ühes ergutussignaali paketis on järjest positiivne ja negatiivne *chirp*-signaal. Kuna sellisel juhul esineb iga hetksagedus kaks korda, siis omab mõtet kasutada vastavate analüüsiaegade osas liitakent, mis koosneb vastavatest alamakendest.

## PATENDINÕUDLUS

1. Meetod sageduskarakteristiku mõõtmiseks, mille käigus genereeritakse ajas etteantud funktsiooni alusel suhteliselt kiirelt muutuva sagedusega ergutussignaal ning teostatakse vastussignaali analüüs suhteliselt lühikeses libisevas ajavalla aknas, kasutades perioodilisi tugisignaale, **mis erineb** selle poolest, et vastussignaali analüüs teostatakse vastussignaali analüsaatoris, konvolutsiooni arvutamise seadmes, kasutades konvolutsiooni tugisignaalidena vastavaid kiirelt muutuva sagedusega ergutussignaalidest tuletatud signaale.

2. Meetod vastavalt nõudluse punktile 1, **mis erineb** selle poolest, et ajavallas libisev aken jaotatakse mitmeks ajas libisevaks alamaknaks.

3. Meetod vastavalt nõudluse punktile 1, **mis erineb** selle poolest, et ajavallas libisev aken teostatakse muutuva pikkusega, sõltuvalt ergutussignaali jooksvast sagedusest.

4. Meetod vastavalt nõudluse punktile 1, **mis erineb** selle poolest, et ajavalla akna algus ja lõpp seotakse ergutussignaali nullist läbimineku hetkedega.

5. Meetod vastavalt nõudluse punktile 1, **mis erineb** selle poolest, et ergutussignaal genereeritakse siinuselisena.

6. Meetod vastavalt nõudluse punktile 1, **mis erineb** selle poolest, et ergutussignaal genereeritakse meandersignaalina või mittesiinuselise signaalina.

7. Meetod vastavalt nõudluse punktile 1, **mis erineb** selle poolest, et ergutussignaal genereeritakse lineaarse või logaritmilise *chirp*-signaalina.

8. Meetod vastavalt nõudluse punktile 1, **mis erineb** selle poolest, et analüüs teostatakse etapiviisiliselt, kasutades igal etapil adaptiivselt eelmise etapi tulemusi ergutussignaali parameetrite või analüüsi akna parameetrite arvutamisel.

9. Meetod vastavalt nõudluse punktile 8, **mis erineb** selle poolest, et vastavad ergutusignaali või analüüsi aja-akna ja aja-akende adaptiivsed parameetrid arvutatakse müra või mõõtevigade minimiseerimiseks.

10. Meetod vastavalt nõudluse punktile 1, **mis erineb** selle poolest, et vastavad ergutusignaali või analüüsi aja-akna ja aja-akende parameetrid arvutatakse mõõdetava objekti klassifitseerimiseks.

11. Meetod vastavalt nõudluse punktile 1, **mis erineb** selle poolest, et tugisignaalid konvolueeritakse kompleksel lühikeses ajavalla aknas vastussignaaliga vastuvõetud signaali reaal- ja imaginaarosa määramiseks ning sellest omakorda arvutatakse vastava mõõdetava objekti ülekandeteguri reaal- ja imaginaarosade väärtused funktsioonina sagedusest.

12. Meetod vastavalt nõudluse punktile 1, **mis erineb** selle poolest, et analüüsiks kasutatakse tugisignaali esimest lainekuju, mis on vastavuses ergutussignaaliga ning mida mõõdetava objekti ülekandeteguri reaal- ja imaginaarosa väärtuste arvutamiseks funktsioonina sagedusest konvolueeritakse lühikeses ajaaknas Hilbert'i teisenduse abil arvutatud vastussignaali komplekse esitusega.

13. Seade sageduskarakteristiku mõõtmiseks, mis sisaldab ajast sõltuva suhteliselt kiirelt muutuva sagedusega ergutussignaali lainekuju genereerimise sõlme ning suhteliselt lühikeses ajavalla aknas toimivat vastussignaali analüsaatorit, **mis erineb** selle poolest, et vastussignaali analüsaator sisaldab kahte kvadratuurset tugisignaali lainekujude genereerimise sõlme, mille signaalid on määratud ergutussignaali kujuga ajas ning vahendeid vastussignaali lainekuju konvolutsiooniks lühikeses libisevas ajavalla aknas tugisignaali nii esimese kui ka teise lainekujuga.

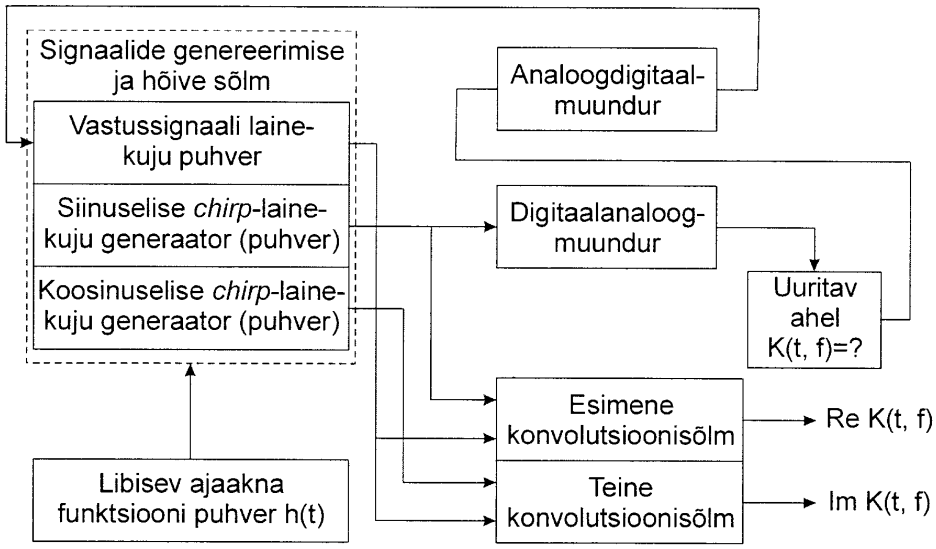
Signaalide genereerimise ja hõive sõlm
Vastussignaali laine-kuju puhver
Siinuselise *chirp*-laine-kuju generaator (puhver)
Koosinuselise *chirp*-laine-kuju generaator (puhver)
Analoogdigitaal-muundur
Digitaalanaloog-muundur
Uuritav ahel K(t, f)=?
Esimene konvolutsioonisõlm
Teine konvolutsioonisõlm
Re K(t, f)
Im K(t, f)
Libisev ajaakna funktsiooni puhver h(t)

FIG 1

# CURRICULUM VITAE

1. Personal data

| | |
|---|---|
| Name | Tõnis Saar |
| Date and place of birth | 27.04.1982, Tallinn, Estonia |
| E-mail | Tonis.Saar@outlook.com |

2. Education

| Educational institution | Graduation year | Education (field of study/degree) |
|---|---|---|
| Tallinn Technical Gymnasium | 2001 | Secondary education |
| Tallinn University of Technology | 2007 | Electronics and biomedical engineering/B.Sc. |
| Tallinn University of Technology | 2008 | Electronics engineering/M.Sc. |

3. Language competence / skills (fluent, average, basic skills)

| Language | Level |
|---|---|
| Estonian | High |
| English | High |
| German | Medium |
| Finnish | Basic |

4. Professional employment

| Period | Organization | Position |
|---|---|---|
| 2001–2010 | OÜ MiTe Engineering | Design Engineer |
| 2009– present | Competence Center ELIKO | Contracted Research Engineer |
| 2010– present | STACC (The Software Technology and Applications Competence Centre) | Research Engineer |

5. Research activity, including honours and thesis supervised

Research topics: electromechanical impedance, structural health monitoring, PZT, electrical impedance, signal processing, image processing

Research projects: Electronic components and subsystems for mission critical embedded systems (SF0142737s06 SF 01.01.06 - 31.12.11), Energy efficient electronic systems (SF0140061s12 SF 01.01.12 - 31.12.14), Highly Efficient Road Surface Measurement and Control System (FP7-SME 01.08.12-31.07.14), Metrology for competitive competence (B04 HTM 01.05.11 - 31.12.13), Research of the adaptively oversampled and modulated conversion and processing algorithms of signals (ETF8905 ETF 01.01.11 - 31.12.13)

# ELULOOKIRJELDUS

1. Isikuandmed


| | |
|---|---|
| Ees- ja perekonnanimi | Tõnis Saar |
| Sünniaeg ja -koht | 27.04.1982 Tallinn, Eesti |
| Kodakondsus | Eesti |
| E-posti aadress | Tonis.Saar@outlook.com |


2. Hariduskäik

| Õppeasutus (nimetus lõpetamise ajal) | Lõpetamise aeg | Haridus (eriala/kraad) |
|---|---|---|
| Tallinna Tehnikagümnaasium | 2001 | Keskharidus |
| Tallinna Tehnikaülikool | 2007 | Elektroonika ja biomeditsiinitehnika/bakalaureus |
| Tallinna Tehnikaülikool | 2008 | Elektroonika/magister |

3. Keelteoskus (alg-, kesk- või kõrgtase)

| Keel | Tase |
|---|---|
| Eesti | Kõrgtase |
| Inglise | Kõrgtase |
| Saksa | Kesktase |
| Soome | Algtase |

4. Teenistuskäik

| Töötamise aeg | Tööandja nimetus | Ametikoht |
|---|---|---|
| 2001–2010 | OÜ MiTe Engineering | insener |
| 2009– | ELIKO TAK | teadur |
| 2010– | STACC (The Software Technology and Applications Competence Centre) | teadur |

5. Teadustegevus, sh tunnustused ja juhendatud lõputööd

Uurimisvaldkonnad: Elektromehhaaniline impedants, elektriline impedants, PZT, signaalitöötlus, pilditöötlus

Teadus- arendusprojektid: Adaptiivselt ülevõendatud ja moduleeritud signaalide muundamise ja töötlemise algoritmide uurimine (ETF8905 ETF 01.01.11 - 31.12.13), Energiasäästlikud elektroonikasüsteemid (SF0140061s12 SF 01.01.12 - 31.12.14), Innovative, Highly Efficient Road Surface Measurement and Control System (VFP567 välisleping, FP7-SME 01.08.12 - 31.07.14), Metroloogia kaasaegsetes tehnoloogiates (B04 HTM baasfinantseerimine 01.05.11 - 31.12.13), Missioonikriitiliste sardsüsteemide elektroonsed komponendid ja alamsüsteemid (SF0142737s06 SF 01.01.06 - 31.12.11)

# DISSERTATIONS DEFENDED AT TALLINN UNIVERSITY OF TECHNOLOGY ON *INFORMATICS AND SYSTEM ENGINEERING*

1. **Lea Elmik**. Informational Modelling of a Communication Office. 1992.
2. **Kalle Tammemäe**. Control Intensive Digital System Synthesis. 1997.
3. **Eerik Lossmann**. Complex Signal Classification Algorithms, Based on the Third-Order Statistical Models. 1999.
4. **Kaido Kikkas**. Using the Internet in Rehabilitation of People with Mobility Impairments – Case Studies and Views from Estonia. 1999.
5. **Nazmun Nahar**. Global Electronic Commerce Process: Business-to-Business. 1999.
6. **Jevgeni Riipulk**. Microwave Radiometry for Medical Applications. 2000.
7. **Alar Kuusik**. Compact Smart Home Systems: Design and Verification of Cost Effective Hardware Solutions. 2001.
8. **Jaan Raik**. Hierarchical Test Generation for Digital Circuits Represented by Decision Diagrams. 2001.
9. **Andri Riid**. Transparent Fuzzy Systems: Model and Control. 2002.
10. **Marina Brik**. Investigation and Development of Test Generation Methods for Control Part of Digital Systems. 2002.
11. **Raul Land**. Synchronous Approximation and Processing of Sampled Data Signals. 2002.
12. **Ants Ronk**. An Extended Block-Adaptive Fourier Analyser for Analysis and Reproduction of Periodic Components of Band-Limited Discrete-Time Signals. 2002.
13. **Toivo Paavle**. System Level Modeling of the Phase Locked Loops: Behavioral Analysis and Parameterization. 2003.
14. **Irina Astrova**. On Integration of Object-Oriented Applications with Relational Databases. 2003.
15. **Kuldar Taveter**. A Multi-Perspective Methodology for Agent-Oriented Business Modelling and Simulation. 2004.
16. **Taivo Kangilaski**. Eesti Energia käiduhaldussüsteem. 2004.
17. **Artur Jutman**. Selected Issues of Modeling, Verification and Testing of Digital Systems. 2004.
18. **Ander Tenno**. Simulation and Estimation of Electro-Chemical Processes in Maintenance-Free Batteries with Fixed Electrolyte. 2004.
19. **Oleg Korolkov**. Formation of Diffusion Welded Al Contacts to Semiconductor Silicon. 2004.
20. **Risto Vaarandi**. Tools and Techniques for Event Log Analysis. 2005.
21. **Marko Koort**. Transmitter Power Control in Wireless Communication Systems. 2005.

22. **Raul Savimaa**. Modelling Emergent Behaviour of Organizations. Time-Aware, UML and Agent Based Approach. 2005.
23. **Raido Kurel**. Investigation of Electrical Characteristics of SiC Based Complementary JBS Structures. 2005.
24. **Rainer Taniloo**. Ökonoomsete negatiivse diferentsiaaltakistusega astmete ja elementide disainimine ja optimeerimine. 2005.
25. **Pauli Lallo.** Adaptive Secure Data Transmission Method for OSI Level I. 2005.
26. **Deniss Kumlander**. Some Practical Algorithms to Solve the Maximum Clique Problem. 2005.
27. **Tarmo Veskioja**. Stable Marriage Problem and College Admission. 2005.
28. **Elena Fomina**. Low Power Finite State Machine Synthesis. 2005.
29. **Eero Ivask**. Digital Test in WEB-Based Environment 2006.
30. **Виктор Войтович**. Разработка технологий выращивания из жидкой фазы эпитаксиальных структур арсенида галлия с высоковольтным p-n переходом и изготовления диодов на их основе. 2006.
31. **Tanel Alumäe**. Methods for Estonian Large Vocabulary Speech Recognition. 2006.
32. **Erki Eessaar**. Relational and Object-Relational Database Management Systems as Platforms for Managing Softwareengineering Artefacts. 2006.
33. **Rauno Gordon**. Modelling of Cardiac Dynamics and Intracardiac Bio-impedance. 2007.
34. **Madis Listak**. A Task-Oriented Design of a Biologically Inspired Underwater Robot. 2007.
35. **Elmet Orasson**. Hybrid Built-in Self-Test. Methods and Tools for Analysis and Optimization of BIST. 2007.
36. **Eduard Petlenkov**. Neural Networks Based Identification and Control of Nonlinear Systems: ANARX Model Based Approach. 2007.
37. **Toomas Kirt**. Concept Formation in Exploratory Data Analysis: Case Studies of Linguistic and Banking Data. 2007.
38. **Juhan-Peep Ernits**. Two State Space Reduction Techniques for Explicit State Model Checking. 2007.
39. **Innar Liiv**. Pattern Discovery Using Seriation and Matrix Reordering: A Unified View, Extensions and an Application to Inventory Management. 2008.
40. **Andrei Pokatilov**. Development of National Standard for Voltage Unit Based on Solid-State References. 2008.
41. **Karin Lindroos**. Mapping Social Structures by Formal Non-Linear Information Processing Methods: Case Studies of Estonian Islands Environments. 2008.
42. **Maksim Jenihhin**. Simulation-Based Hardware Verification with High-Level Decision Diagrams. 2008.
43. **Ando Saabas**. Logics for Low-Level Code and Proof-Preserving Program Transformations. 2008.

44. **Ilja Tšahhirov**. Security Protocols Analysis in the Computational Model – Dependency Flow Graphs-Based Approach. 2008.
45. **Toomas Ruuben**. Wideband Digital Beamforming in Sonar Systems. 2009.
46. **Sergei Devadze**. Fault Simulation of Digital Systems. 2009.
47. **Andrei Krivošei**. Model Based Method for Adaptive Decomposition of the Thoracic Bio-Impedance Variations into Cardiac and Respiratory Components. 2009.
48. **Vineeth Govind**. DfT-Based External Test and Diagnosis of Mesh-like Networks on Chips. 2009.
49. **Andres Kull**. Model-Based Testing of Reactive Systems. 2009.
50. **Ants Torim**. Formal Concepts in the Theory of Monotone Systems. 2009.
51. **Erika Matsak**. Discovering Logical Constructs from Estonian Children Language. 2009.
52. **Paul Annus**. Multichannel Bioimpedance Spectroscopy: Instrumentation Methods and Design Principles. 2009.
53. **Maris Tõnso**. Computer Algebra Tools for Modelling, Analysis and Synthesis for Nonlinear Control Systems. 2010.
54. **Aivo Jürgenson**. Efficient Semantics of Parallel and Serial Models of Attack Trees. 2010.
55. **Erkki Joasoon**. The Tactile Feedback Device for Multi-Touch User Interfaces. 2010.
56. **Jürgo-Sören Preden**. Enhancing Situation – Awareness Cognition and Reasoning of Ad-Hoc Network Agents. 2010.
57. **Pavel Grigorenko**. Higher-Order Attribute Semantics of Flat Languages. 2010.
58. **Anna Rannaste**. Hierarcical Test Pattern Generation and Untestability Identification Techniques for Synchronous Sequential Circuits. 2010.
59. **Sergei Strik**. Battery Charging and Full-Featured Battery Charger Integrated Circuit for Portable Applications. 2011.
60. **Rain Ottis**. A Systematic Approach to Offensive Volunteer Cyber Militia. 2011.
61. **Natalja Sleptšuk**. Investigation of the Intermediate Layer in the Metal-Silicon Carbide Contact Obtained by Diffusion Welding. 2011.
62. **Martin Jaanus**. The Interactive Learning Environment for Mobile Laboratories. 2011.
63. **Argo Kasemaa**. Analog Front End Components for Bio-Impedance Measurement: Current Source Design and Implementation. 2011.
64. **Kenneth Geers**. Strategic Cyber Security: Evaluating Nation-State Cyber Attack Mitigation Strategies. 2011.
65. **Riina Maigre**. Composition of Web Services on Large Service Models. 2011.
66. **Helena Kruus**. Optimization of Built-in Self-Test in Digital Systems. 2011.
67. **Gunnar Piho**. Archetypes Based Techniques for Development of Domains, Requirements and Sofware. 2011.

68. **Juri Gavšin**. Intrinsic Robot Safety Through Reversibility of Actions. 2011.
69. **Dmitri Mihhailov**. Hardware Implementation of Recursive Sorting Algorithms Using Tree-like Structures and HFSM Models. 2012.
70. **Anton Tšertov**. System Modeling for Processor-Centric Test Automation. 2012.
71. **Sergei Kostin**. Self-Diagnosis in Digital Systems. 2012.
72. **Mihkel Tagel**. System-Level Design of Timing-Sensitive Network-on-Chip Based Dependable Systems. 2012.
73. **Juri Belikov**. Polynomial Methods for Nonlinear Control Systems. 2012.
74. **Kristina Vassiljeva**. Restricted Connectivity Neural Networks based Identification for Control. 2012.
75. **Tarmo Robal**. Towards Adaptive Web – Analysing and Recommending Web Users` Behaviour. 2012.
76. **Anton Karputkin**. Formal Verification and Error Correction on High-Level Decision Diagrams. 2012.
77. **Vadim Kimlaychuk**. Simulations in Multi-Agent Communication System. 2012.
78. **Taavi Viilukas**. Constraints Solving Based Hierarchical Test Generation for Synchronous Sequential Circuits. 2012.
79. **Marko Kääramees**. A Symbolic Approach to Model-based Online Testing. 2012.
80. **Enar Reilent**. Whiteboard Architecture for the Multi-agent Sensor Systems. 2012.
81. **Jaan Ojarand**. Wideband Excitation Signals for Fast Impedance Spectroscopy of Biological Objects. 2012.
82. **Igor Aleksejev**. FPGA-based Embedded Virtual Instrumentation. 2013.